# PERFORMANCE OF THE NANOSILICA FILLED NEAT EPOXY AND CARBON FIBER FILAMENT WOUND COMPOSITES

A THESIS SUBMITTED TO
THE GRADUATE SCHOOL OF NATURAL AND APPLIED SCIENCES
OF
MIDDLE EAST TECHNICAL UNIVERSITY

BY

ERDAL SAPANCI

IN PARTIAL FULFILLMENT OF THE REQUIREMENTS
FOR
THE DEGREE OF MASTER OF SCIENCE
IN
POLYMER SCIENCE AND TECHNOLOGY

OCTOBER 2019

Approval of the thesis:

# PERFORMANCE OF THE NANOSILICA FILLED NEAT EPOXY AND CARBON FIBER FILAMENT WOUND COMPOSITES

submitted by **ERDAL SAPANCI** in partial fulfillment of the requirements for the degree of **Master of Science in Polymer Science and Technology Department, Middle East Technical University** by,

Prof. Dr. Halil Kalıpçılar
Dean, Graduate School of **Natural and Applied Sciences**

Prof. Dr. Necati Özkan
Head of Department, **Polymer Science and Technology**

Prof. Dr. Necati Özkan
Supervisor, **Polymer Science and Technology, METU**

**Examining Committee Members:**

Prof. Dr. Cevdet Kaynak
Metallurgical and Materials Engineering, METU

Prof. Dr. Necati Özkan
Polymer Science and Technology, METU

Prof. Dr. Göknur Bayram
Chemical Engineering, METU

Assoc. Prof. Dr. İrem Erel Göktepe
Chemistry, METU

Dr. Cemal Merih Şengönül
Manufacturing Engineering, Atılım University

Date: 14.10.2019

**I hereby declare that all information in this document has been obtained and presented in accordance with academic rules and ethical conduct. I also declare that, as required by these rules and conduct, I have fully cited and referenced all material and results that are not original to this work.**

Name, Surname: Erdal Sapancı

Signature:

# ABSTRACT

## PERFORMANCE OF THE NANOSILICA FILLED NEAT EPOXY AND CARBON FIBER FILAMENT WOUND COMPOSITES

Sapancı, Erdal
Master of Science, Polymer Science and Technology
Supervisor: Prof. Dr. Necati Özkan

October 2019, 103 pages

The main aim of this thesis was to investigate influences of nanosilica particle addition to epoxy resin matrices (systems) on the thermal and mechanical properties of carbon fiber reinforced epoxy-nanosilica composites. Nanosilica particles were used for increasing the matrix dependant mechanical properties of conventional composite materials with easy dispersion processes in matrix. In the first part of the thesis, nanosilica filled epoxy composites were prepared using both a probe type ultrasonic processor and manuel mixing. Viscosities of the nanosilica filled epoxy resins were determined to understand the gelling time and wetting behaviour of those resins and to select the processing parameters for the filament winding process. The nanosilica filled epoxy composites with different weight ratios of nanosilicas were prepared, and then the mechanical, thermal, and morphological characterizations of the cured specimens were carried out. The best result in terms of tensile strength for those composites was obtained when 0.5 wt% nanosilica was added. The addition of nanosilica did not influence the elastic modulus of those composites considerably.

In the second part of the thesis, the aim was to investigate the effects of nanosilica on the properties of carbon fiber reinforced epoxy composites. Test coupons for mechanical tests were prepared from the flat plates manufactured using a filament winding process. The glass transition temperatures of the nanosilica filled carbon fiber reinforced epoxy composites were measured using a Dynamic Mechanical Analyser (DMA). The addition of silica particles did not change the glass transition temperatures of the composites. The Scanning Electron Microscope (SEM) analyses were performed to understand damage mechanisms of the nanosilica filled carbon fiber reinforced epoxy composites.

Mode I interlaminar fracture toughness energy, $G_{IC}$, of the nanosilica filled carbon fiber reinforced epoxy composite containing 2.0 wt% nanosilica was increased 104% compared to the control sample (i.e. no nanosilica added sample). Mode II interlaminar fracture toughness energy, $G_{IIC}$, of the carbon fiber reinforced containing 0.5 wt% nanosilica was increased about 21% compared to the control sample. The tensile strength of the carbon reinforced composites were increased 13.5% increase with addition of 0.5 wt% nanosilica in epoxy.

Keywords: Nanosilica, Epoxy, Filament Winding, Mode I Fracture Toughness, Mode II Fracture Toughness

# ÖZ

## NANOSİLİKA DOLGULU EPOKSİ VE KARBON ELYAF TAKVİYELİ FİLAMAN SARGI İLE ÜRETİLMİŞ KOMPOZİTLERİN PERFORMANSI

Sapancı, Erdal
Yüksek Lisans, Polimer Bilim ve Teknolojisi
Tez Danışmanı: Prof. Dr. Necati Özkan

Ekim 2019, 103 sayfa

Bu çalışmanın amacı epoksi reçine içerisinde ağırlıkça farklı oranlarda kullanılan nanosilikanın, karbon elyaf takviyeli kompozitlerin termal ve mekanik özelliklerinde oluşan etkisini araştırmaktır. Nanosilika geleneksel kompozitlerin matris dominant özelliklerinin iyileştirilmesi için, matris içerisinde kolayca dağılımı sağlanabilen nanokatkılardır. Tezin ilk bölümünde nanosilika dolgulu epoksi kompozitler, daldırma tipi ultrasonik ve elle karıştırma yöntemleri kullanılarak hazırlanmıştır. Filaman sarım prosesinde nanosilika dolgulu epoksi kompozitlerin, jelleşme süresi ve elyaf ıslatma davranışını anlaşılabilmesi için viskoziteleri belirlenmiştir. Kompozitler, farklı nanosilika ağırlık oranlarında hazırlanmış ve kürleşme sonrası mekanik, termal ve mikroskobik karakterizasyon testleri gerçekleştirilmiştir. Çekme mukavemetindeki ağırlıkça %0,5 nanosilikanın kullanıldığı nanokompozitlerde %13,5 ile en yüksek artış elde edilmiş, çekme modülünde ise katkısız reçinelere göre bir değişim gözlemlenmemiştir.

Tezin ikinci bölümünde, epoksi reçine içerisinde farklı ağırlıkça oranlarda nanosilika dolgusunun karbon elyafı ile güçlendirilmiş epoksi kompozitlerdeki mekanik ve termal özelliklere olan etkileri incelenmiştir. Elyaf takviyeli test kuponları, filaman sarım tekniğiyle kompozit haline getirilmiş ve düz plakadan kesilerek üretilmiştir. Karbon elyaf takviyeli nanokompozitlerin camsı geçiş sıcaklığı, Dinamik Mekanik

Analiz Cihazı (DMA) ile ölçülmüştür. Nanosilika partikül dolgusu ile hazırlanan numunelerin cam geçiş sıcaklığı değerinde kayda değer bir değişim elde edilmemiştir. Taramalı Elektron Mikroskobu (SEM) analizi karbon elyaf takviyeli kompozitlerin hasar mekanizmalarını incelemek ve katkısız referans kuponlar ile karşılaştırmak için gerçekleştirilmiştir.

Karbon elyaf takviyeli kompozitlerin mod I katlararası kırılma tokluğu enerjisi ($G_{IC}$) değerinde ağırlıkça %2 nanosilika partikül dolgusu ile yaklaşık %104; mod II katlar arası kırılma tokluğu enerjisi ($G_{IIC}$) değerinde ise ağırlıkça %0,5 nanosilika dolgusu ile yaklaşık %21 artış sağlanmıştır. Çekme dayanımı değerlerinde ağırlıkça %0,5 nanosilika dolgusu ile %13,5 olarak artış elde edilmiştir.

Anahtar Kelimeler: Nanosilika, Epoksi, Filaman Sargı, Mod I Kırılma Tokluğu, Mod II Kırılma Tokluğu

To my father..

# ACKNOWLEDGEMENTS

First of all I would like to express my thankfulness to my supervisor Prof. Dr. Necati Özkan for his valuable criticism, guidance, insight and efforts at each stage of this thesis.

I would also like to send my special thanks to Dr. Gökçe Dara and Fatih Güner for their support. I especially grateful to Dr. Sıla Güngör precious discussions, comments and helps during the progress of this study.

I would like to thank the Composite Parts Production, Physical and Metallurgical Test Laboratories and Multi-Functional Material Technologies & Material Characterization Units of Roketsan; Ms. Begüm Beril İncecik, Mrs. Gözde Sarıtaş, Mr. Hasan Dinç, Mr. Mehmet Pehlivan, Mr. Ali Kaplan, Mr. Özkan Demirbilek, Mr. Duran Ülsü, Mr. Muammer Özkorul, Mr. Hakan Karayel, Mr. Ender Sarıkan and Mr. Hakkı Sarıyağ. I would also like to thank other colleagues at Roketsan for their support during studies of this thesis.

I would like to gratefully acknowledge financial support of thesis provided by SAYP project which is conducted with Presidency of Defence Industries of Turkey, METU and Roketsan Missiles Industries Corporation agreement. I am also grateful to the Roketsan, Department of Technology and Academic Network Management; Dr. Oğuz Menekşe, Mr. Onur Bozkuş and Mrs. Didem Tamtunalı Çelik for their supports.

Last but not the least, I would like to express my deepest thankfulness to my family especially to Gamze Uysal Sapancı for their endless love and support. This dissertation would certainly be not possible without her support.

# TABLE OF CONTENTS

CHAPTERS

APPENDICES

# LIST OF TABLES

TABLES

## LIST OF FIGURES

FIGURES

# LIST OF ABBREVIATIONS

ABBREVIATONS

CFRP : Carbon Fiber Reinforced Polymer

CNT : Carbon Nano Tubes

COV : Coefficient of Variation

DMA : Dynamic Mechanical Analyser

DSC : Differential Scanning Calorimeter

EDX : Energy Dispersive X-Ray

FRPCM : Fiber Reinforced Polymer Composite Materials

GFRPCM : Glass Fiber Reinforced Polymer Composite Materials

rpm : Revolution per minute

RTM : Resin Transfer Molding

min. : Minute

n-silica : Nano Silica

SEM : Scanning Electron Microscope

TEM : Transmission Electron Microscope

VARIM : Vacuum Assisted Resin Infusion Molding

VARTM : Vacuum Assisted Resin Transfer Molding

vol. .: Volume

wt : Weight

# LIST OF SYMBOLS

SYMBOLS

$G_{IC}$ : Mode I interlaminar fracture toughness energy

$G_{IIC}$ : Mode II interlaminar fracture toughness energy

$V_f$ : Volume fraction

$T_g$ : Glass transition temperature

# CHAPTER 1

# INTRODUCTION

In this chapter, definition and description of polymeric composite materials, nanomaterials and their manufacturing with characterization techniques are presented. First of all conventional polymeric composite materials will be defined and then their constituents such as fibers and matrix will be explained. Subsequently, nanomaterials and their usages for preparing nanocomposites will be mentioned and the properties of nanocomposites will be compared with these of conventional polymeric composites. Both conventional polymeric composites and polymeric nanocomposite processing techniques will be described. Characterization techniques used for structural evaluation of composite materials will be given. Finally, some recent examples from the literature on fiber reinforced polymeric nanocomposite materials will be represented.

## 1.1. Polymer Composite Materials

Composites materials are composed of two or more constituents. Composites materials show very high strength/weight ratios compared to metallic materials and this property makes polymeric composite materials preferred in most of industrial applications such energy, automotive, marine, civil, aerospace and defense. Various types of materials (fibers, nanoparticles) are used as reinforcement additives in different polymer matrices in order to obtain polymeric composite materials with improved mechanical properties.

### 1.1.1. Fiber Reinforced Polymer Composite Materials (FRPCM)

Fiber reinforced polymers are composed of mainly two constituents: fibers and matrix materials. Fibers carry most of the load and provide strength and stiffness especially at fiber directions in the composites. Most widely used fiber materials are glass, carbon and aramid fibers with unique properties such as, density, strength and cost. According to design of FRPCMs and matrix compatibility, different fiber materials are chosen for different applications.

Two groups of matrix materials (thermoplastic and thermoset polymers) are used for FRPCMs. Thermoset resins are converted from liquid to solid material by a curing process. Most widely used thermoset matrix materials used for FRPCMs are polyesters, epoxies, vinyl esters and polyurethanes. Thermoplastics are melted, formed to intended shape, and subsequently cooled in order to obtain an engineering shape and for thermoplastic materials this melting and cooling cycles can be repeated many times due to the linear chain structure of thermoplastics. Thermoplastics are generally preferred at industry due to the low cost of raw materials, fast processing, and reshaping property. The matrix materials in FPRPCMs transfer the load between fibers, hold fibers together, and protect the composite structure from environmental effects.

### 1.1.2. Polymer Nanocomposite Materials

Polymer nanocomposites or nano-filled polymers are polymer matrices containing organic or inorganic fillers with a homogeneous nanoscale distribution (normally from 1 to 100 nm in at least one dimension) and they are prepared by physical blending or chemical polymerizing technologies [1]. Nanomaterials are mostly classified according to their dimensions as one-dimensional (1D), two-dimensional (2D), and three-dimensional (3D) nanomaterials. Polymer nanocomposites have better properties than the composites prepared using particulate additives due to the high surface area of nanoparticles. As a result, small amounts of nano additives are used in polymer nanocomposites. Nano additives are generally used for getting additional properties or improving existing properties such as electrical, mechanical, magnetic, thermal, physical, optical or barrier. Polymer nanocomposites mostly have better performance compared to the conventional polymeric composite materials [2].

Manufacturing stages of polymer nanocomposites, especially the dispersion of the nano additives in the polymer matrix, are very critical for getting improved material properties. Various dispersion techniques are used in order to disperse the nano additives in polymer matrices. Polymer nanocomposites can be manufactured by solution, in situ polymerization, melt mixing, sol-gel method, electrospin, and template techniques. The design approach of nanocomposites are given in Figure 1.1. The nanofillers, matrix and their processing parameters are playing key role in design of them.

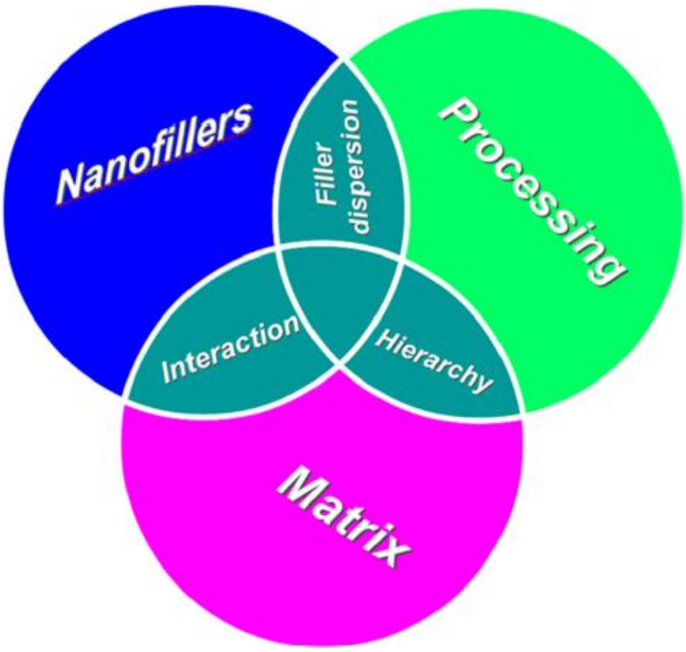

**Figure 1.1** Design approach of nanocomposites [3].

## 1.2. Nano Materials Used in Polymer Nanocomposite Materials

Various types of nanomaterials can be used in different polymer matrices. Dimensional classification of nanomaterials are shown in Figure 1.2.

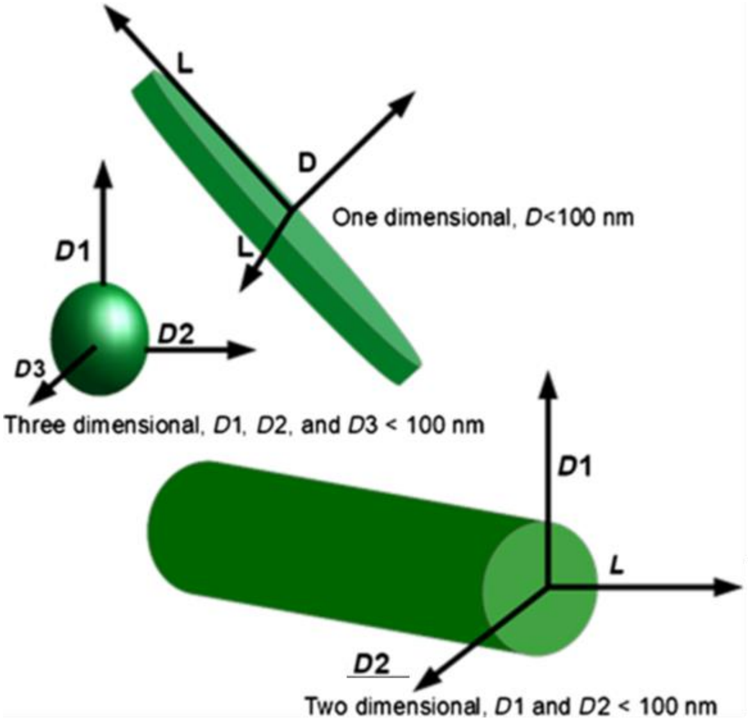

**Figure 1.2** Classification of nanomaterials according to their dimensions [3].

### 1.2.1. One-dimensional Nanomaterials Used in Polymer Composites

One-dimensional nanomaterials have one of their dimensions at nanoscale (less than 100 nm) such as sheets. Most widely used one-dimensional nanomaterials are layered silicates, graphene nanoplatelets in polymer matrices. One-dimensional nanomaterials are generally used for improving different properties in polymeric composites such as electrical conductivity, antimicrobial activity, and optical property.

### 1.2.2. Two-dimensional Nanomaterials Used in Polymer Composites

Nanotubes and nanofibers are two-dimensional nanomaterials and their two dimensions are less than 100 nm. Carbon nanotubes (CNT) are most widely used nano additives in this class and their dispersion in polymeric structures are very difficult due to Van der Waals forces and π-π stacking between layers of CNT. For dealing with this problem the addition of functional groups to surface of nanomaterials generally preferred for getting better dispersion in polymer matrices. By small amount of two-dimensional nanomaterials and with a successful dispersion of these additives in polymer matrices, it is possible to obtain better performance of composite materials.

### 1.2.3. Three-dimensional Nanomaterials Used in Polymer Composites

Three-dimensional nanomaterials have all three dimensions at nanoscale and most of them have sphere like geometry or cubical shapes. Nanosilica, nanoalumina, nanotitanium oxide are examples of three-dimensional nanofillers. 3D nanofillers are very important in the formulation of polymer nanocomposites because of their inherent properties [3].

## 1.3. Conventional Composite Manufacturing Techniques

Composite manufacturing routes are aimed to manufacture near net shape or net shape parts without need for machining or trimming. In composite manufacturing routes since composite materials have anisotropic properties, it is necessary to design reinforcement type, material orientation, layer configuration, and resin system. According to design and material configuration requirements, possible manufacturing techniques are evaluated. When selecting composite manufacturing techniques parameters like overall size, thickness, cross-sectional shape, and hollow or solid geometry requirements are determinative. Also production rate, degree of automation, post processes such as machining, cost of equipment, mold, labor, energy and mold materials are also taken into consideration for economic reasons. Some of most widely used and high quality manufacturing routes which are generally used for defense, aerospace and space applications are explained below.

### 1.3.1. Filament Winding

Filament winding is a process for fabricating a composite structure in which continuous reinforcements (filaments, wire, yarn, tape, or other), previously impregnated during winding, are placed over a rotating form or mandrel in a prescribed way to meet certain stress conditions [4]. It is generally preferred for manufacturing tubular, cylindrical and spherical geometry parts with using mandrel as tool for giving shape and winding on it.

Filament winding is automated technique and the deposition of fibers on a mandrel can be controlled by a computer. By controlling axis of the filament winding machine, fibers feed from fiber creels to tensioner and after passing from guides fibers reach to resin bath and impregnated there in a controlled manner and then fiber band positioned on a rotating mandrel as designed angle as shown in Figure 1.3. After that, it is cured in a rotating oven according to curing cycle of the resin system.

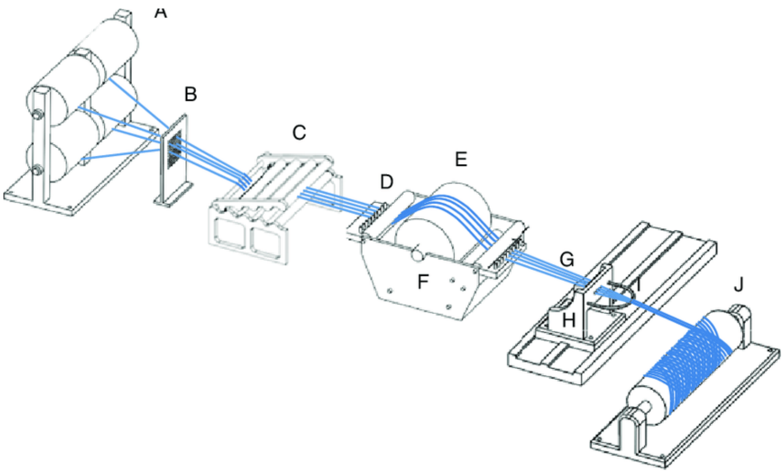

**Figure 1.3** Schematic illustration of the conventional wet-filament winding process. The key components are coded as follows: (A) fiber creels; (B) fiber guide; (C) tensioning systems; (D) guide pins; (E) drum-impregnator with a doctor-blade; (F) resin bath; (G) impregnated fibre bundles; (H) traversing carriage; (I) D-eye; and (J) rotating mandrel [5].

Filament winding process is finalized with mandrel removal and trimming if it is necessary. By using a number of spindles as shown in Figure 1.4, it is possible to manufacture more than one product simultaneously, as a result, production rate is increased and the cost of production is decreased.

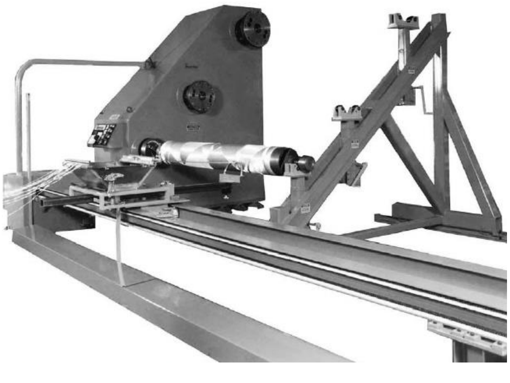

**Figure 1.4** McClean Anderson brand three-spindle filament winding machine [6].

Filament winding process can be regarded as a low cost composite manufacturing technique. During the manufacturing process, fiber tension, resin wetting amount, and layer configuration (pattern, angle, thickness) parameters are critical for final product properties.

Different types of mandrel materials are used as tooling in filament winding process. It can be water soluble, plaster, segmented-collapsible or metallic. The mandrel provides the internal geometry of part.

Filament winding can be used to manufacture motor cases, pressure vessels (Figure 1.5), launcher tubes for defence industry and various types of pipes (water, petroleum liquids and gases) for civil industry.

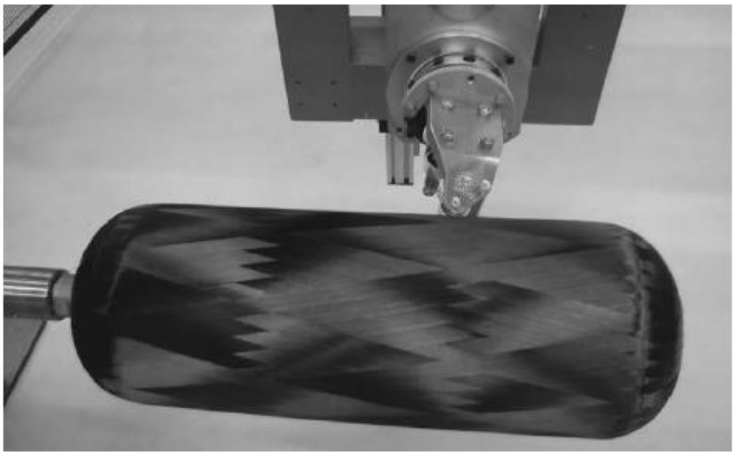

**Figure 1.5** Filament winding a pressure vessel with carbon fiber [6].

### 1.3.2. Resin Transfer Molding

Resin transfer molding (RTM) is a technique based on the injection of a liquid polymer through fibers placed in a closed mold. It is generally used for high performance composites with good surface finishes at both surfaces and preferred for complex shaped parts.

In RTM process, metallic tools are generally used and a dry preform of reinforcement materials is inserted into the mould. Subsequently, the mould is closed and then vacuum is applied to the inside of mould. The resin is pumped into the mould cavity in a controlled manner and then it is heated for curing. After the curing, the mold is opened and the part is removed from the mold.

The tools for the RTM process are expensive but they are differentiated from other techniques since good surface finishes are obtained by RTM. This process method is generally used for manufacturing aerospace parts with limited tolerances and automotive parts with good surface finish requirements.

### 1.3.3. Prepreg Molding

Fabric pre-impregnated with a resin system is referred to as prepreg material. They have already coated or wetted with the resin, thus it is not necessary to apply additional resin for manufacturing a composite part. They are generally cured under heat and pressure such as autoclave or hot press. With using prepreg materials in the processes, high fiber content with good wetting can be achieved with low void content. Disadvantage of this technique is low room temperature shelf life of prepreg materials, high cost of prepreg material and autoclaves. Prepreg moldings can be used for manufacturing aircraft structural components, formula one racing cars (Figure 1.6), and sporting goods.

**Figure 1.6** Autaclave molded Lola Formula 1 car chasis upper half [4].

### 1.4. Dispersion Techniques of Nanomaterials for Thermoset Matrix Materials

Dispersion of nanomaterials in polymer matrices is very critical and challenge for polymer nanocomposite manufacturing. Homogeneous distribution and alignment of nanomaterials in matrix materials are the main aim of dispersion processes. Different types of forces are applied during dispersion processes since nanomaterials tend to agglomerate due to the dominance of van der Walls forces for small particles.

Polymer nanocomposite performance depends on the polymer-nanomaterials interaction and all advantages of nanomaterials in matrix highly depend on the dispersion process.

#### 1.4.1. Ultrasonic Methods

The ultrasonication is most widely used method for dispersing and preventing agglomeration. When ultrasonication is applied to particulate systems, different types of mechanical and chemical effects can be realized due to cavitations formed in the mixture during the ultrasonication. By setting different levels of ultrasonic amplitude, different types of forces can be created in the dispersion such as compression and shear. The higher amplitudes result in more effective creation of cavitation [8]. There are two types of ultrasonic devices: bath and probe ultrasonic processers. Probe type ultrasonic processers apply higher energies to particulate dispersions compared to bath type processers. The bath type ultrasonic processers are mostly preferred due to their low cost and gentle mixing for low volume particulate systems. Most important parameters of ultrasonication are amplitude, temperature, viscosity of particulate system, and particulate concentration. For a probe type ultrasonic processer (Figure 1.7), the position of the probe (dip height and distance to the wall of container) in the particulate mixture is critical.

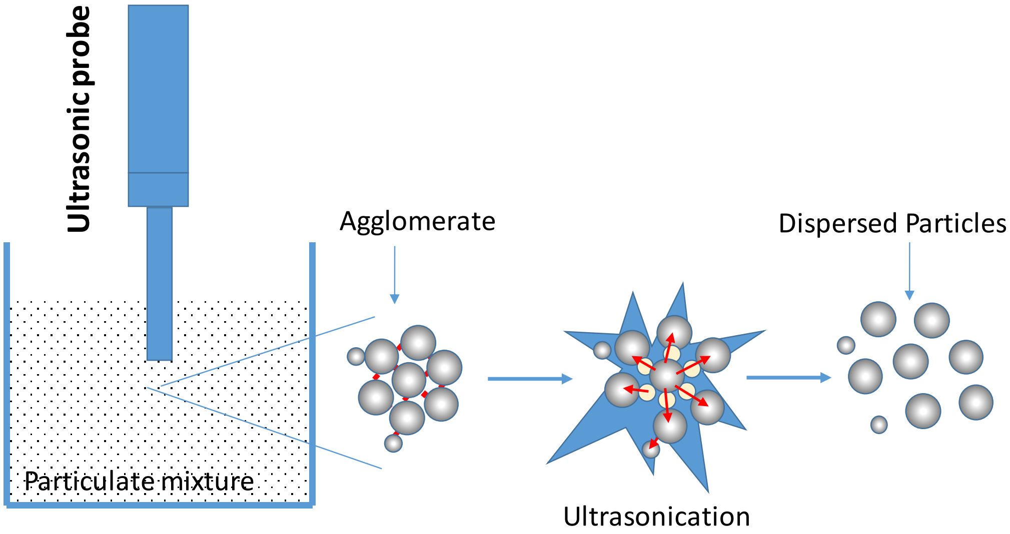

**Figure 1.7** Schematic illustration of an ultrasonic probe and dispersion of agglomerates by cavitation forces.

### 1.4.2. Three Roll Mixers

In three roll mixers, the particulate mixture is placed between the rolls. First of all, it is placed between the feed and centre rolls as shown in Figure 1.8. The particulate mixture is moved from one roll to another by adhesion. High shear forces are created between rollers and homogeneous dispersion of particles is obtained. The roller diameters, space between rollers, rollers speeds and number of passes are critical parameters for three roll mixers and the picture of which is given in Figure 1.9.

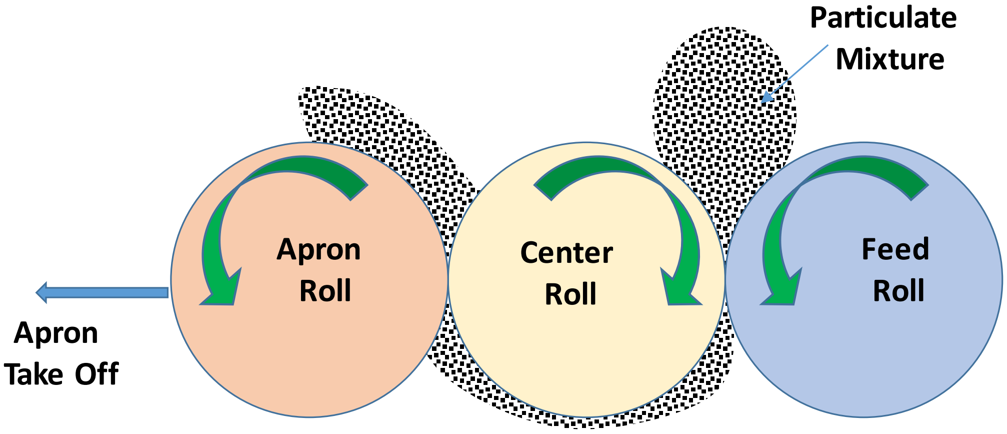

**Figure 1.8** Schematic shown of the three roll mixers (redrawn from [8]).

**Figure 1.9** Three roll mixer device.

### 1.5. Characterization Tests of Composite Materials

Characterization tests for composite materials are continuously developing since new materials and processes are being developed and new approaches are investigated according to final requirements of composite parts. Most of the characterization tests have been done at specimen level; therefore, the preparations of appropriate specimens are critical for composite part designs, analyses, and validation processes. There are some standard test methods for physical, thermal, and physical characterization of composites. Most of the standard methods were published by American Society for Testing and Materials (ASTM) and The International Organization for Standardization (ISO).

#### 1.5.1. Physical Characterization Tests

The measurements of density, volume fractions of fibers and voids are investigated as physical characterization tests. These properties depend on the materials and processes selected and affect thermal and mechanical properties of composites. Density tests have done by Archimedes Principle according to ASTM D792 [10]. The volume or weight fraction of composite can be calculated by matrix digestion approach according to ASTM D3171 [11] or resin burn off method according to ASTM D2584 [12]. After removing matrix by burning or matrix digestion, fibers are weighted and the volume (or weight) fraction of fibers in the composite is calculated. If the volatiles left in the resin are not removed properly and the pressure applied during the curing of composite materials is not sufficient, unwanted voids may form in the inside of composite materials. The void content is measured according to ASTM D2734 [13]. For void content calculation, it is necessary to measure density of composite, resin and fiber with weight fractions of resin and fiber in the composite.

### 1.5.2. Thermal Characterization Tests

Thermal tests are considered to be critical for polymer composite materials since at least one of the component of the composite (matrix) is a polymeric material. Thermal properties of polymeric matrix (glass transition and decomposition temperatures) can be evaluated and they can be used as design parameters for polymer composites. Glass transition measurements are carried out using Differential Scanning Calorimeter (DSC) and Dynamic Mechanical Analyser (DMA) for resin systems and composite materials. ASTM E1356 [14] is used for assigning of glass transition temperature of polymers by DSC and ASTM D7028 [15] is used for glass transition temperature of polymer matrix composites by DMA. The dimensions of composite materials change as a function of temperature. The dimensional changes are very important for the final application of composite structures. The coefficient of thermal expansion is calculated for composites and their dimensional dependence to temperature is measured by Thermo Mechanical Analysis (TMA) and generally ASTM E831 [16] method is used for this purpose.

### 1.5.3. Mechanical Characterization Tests

To characterize mechanical properties of composite materials, various types of test methods with different loadings can be used. Tensile, compressive, shear and torsion tests are most widely used for evaluating mechanical properties of composites. For each test method, instrument requirements, test speeds, recommended test specimen geometries, failure types and their acceptance/rejection criteria were defined in the standard methods. ASTM D3039 is used for investigation of fiber direction properties and evaluating damage mechanisms of the tested coupons [17].

The test procedures, which are used for macro and micro-composites, can also be used for nanocomposites. Nano-sized additives are expected to improve fracture toughness and delamination resistance of fiber reinforced composites when they are dispersed properly in the matrix. Mode I interlaminar fracture toughness energy test under tensile loading is measured according to ASTM D5528 [18] or EN 6033 [19]. Mode II interlaminar fracture toughness energy test under shear loading is evaluated according to ASTM D7905 [20] or EN 6034 [21].

### 1.6. Structural Evaluation of Composite Materials

The usage of composite materials is increasing day by day due to their high specific strength compared with other engineering materials. In many industries, composite materials are characterized initially at test coupon levels, and then prototype manufacturing stages are followed. According to design requirements, the test results obtained using test coupons are used for Finite Element Analysis (FEA) at the desired geometry. In design stages of projects, studies based on the scaled models are generally preferred due to low cost and rapid results when compared with full scale prototypes. Full scale structural behaviour might be stiffness, strength, coefficient of thermal expansion, vibration frequency or failure mechanism [22].

In most application of composite materials, static strength and failure modes of material and process configuration for composite materials are tested and evaluated at coupon level. In industry, generally “building block” approach are followed for composite materials which is given in Figure 1.10. This approach applied for conventional and advanced composite structures within qualification program of projects.

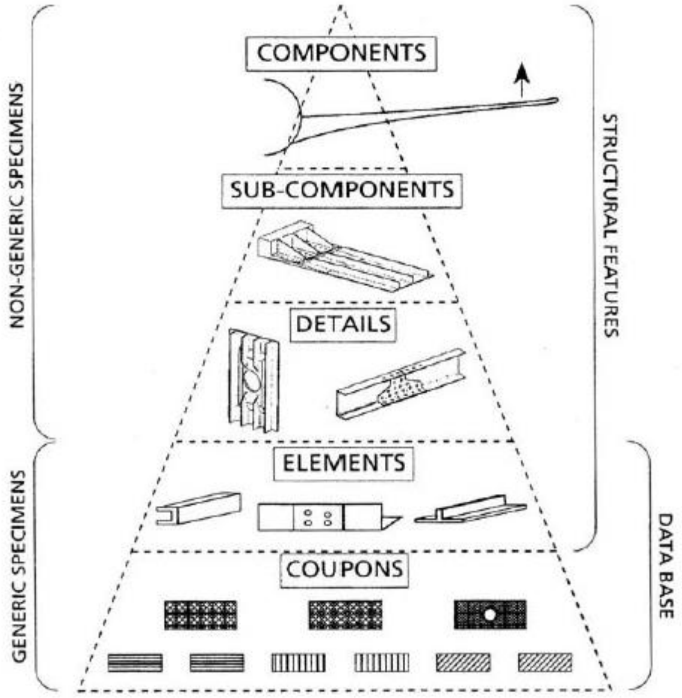

**Figure 1.10** Schematic diagram of building block tests for a fixed wing [23].

## 1.7. Latest and Selected Studies

There are many studies on literature about homogeneous dispersion of nanomaterials in thermoset matrix and their application in fiber reinforced composites. In those studies nanomaterial content, compatibility of nanomaterials with matrix and nanomaterial filled resin systems, and their processing with different conventional composite processing approaches were studied. The advantages and disadvantages of using nanomaterials in composite materials are presented with characterization test results.

Conradi et *al.* [24] studied nanosilicas with particle sizes of 130 and 30 nm and 0.5% by volume in epoxy resin systems and three point bending and tensile tests were done using manufactured test coupons with fracture surface analyses. Epoxy compatible surfactant material was used in order to disperse nanosilicas effectively in the resin matrix. Initially, the particles are added to the epoxy resin, and the mixture was subjected to a dispersion process (ultrasonication) for 20-30 minutes at 40 °C, and then a suitable resin hardener was added to the mixture and mixing was carried out by hand. After degassing process of 10-15 minutes, the mixture was poured into a mold for preparing test coupons, subsequently more degassing was done, and finally the mixture was cured using a suitable curing procedure. Maximum tensile strength and modulus values were obtained when the nanosilicas with a particle size of 130 nm were used. However maximum fracture toughness and impact energy values were obtained when the nanosilicas with a particle size of 30 nm were used. SEM analysis was carried on the fracture surfaces of hand broken test specimens. The fracture surfaces of nanosilica added specimens show fish skin like appearance which can be related to the brittleness of the nanosilica filled specimens.

Thunhorst *et al.* [25] used nanosilica particles with an average particle size of 81 nm and those particles were dispersed in an epoxy resin system, subsequently that nanosilica added resin system and carbon fibers was used in a filament winding process. The resin mixtures containing 30, 20, 10 wt% of nanoparticles were prepared. The maximum increment at hardness, tensile modulus and fracture toughness was obtained with 30 wt% nanosilica addition to epoxy in this study.

Type-3 pressure vessels were manufactured using those nanosilica filled epoxy resin and carbon fibers and then the burst pressure tests were done. The average burst pressure values of those pressure vessels increase with the increasing of nanosilica content and the maximum burst pressure value was measured as 46.74 MPa with 32.5 wt% nanosilica dispersion in epoxy. This study led to the development of 3M™ Matrix Resins 4831, 4832 and 4833 which are commercial resin systems for filament winding applications [25].

Yu *et al.* [26] used different types of silanes to modify the surfaces of nanosilica particles so that the bonding between epoxy resin matrices nanosilica particles can be improved. They examined the microstructure and properties of surface modified nanosilica-epoxy composites. In their study, ɣ-aminopropyl-triethoxysilane, ɣ-glycidoxpropyltrimethoxysilane and ɣ-methacryloxpropyltrimethoxysilane were applied onto nanosilica particles with an average particle size of 50 nm. The silane coatings were applied to the nanosilica surfaces with some chemical and thermal processes. Epoxy matrix nanocomposites reinforced by three different types of surface modified nanosilica particles with 4 wt% mass fractions were fabricated by physical blending using a high shear laboratory-mixing and ultrasonic devices. Test specimens of nanosilica-epoxy composites were characterized by mechanical, thermal, chemical and microstructural tests. Increase on glass transition temperature, flexural strength and modulus was observed for the nanosilica-epoxy composites prepared using ɣ-glycidoxpropyltrimethoxysilane bonding agent on nanosilica particles. Those results suggest that strong chemical bonds were achieved between nanosilica particles and silanes. The TEM pictures of nanosilica-epoxy composites shown that good dispersions of silica particles were obtained with the help of silanes.

Panse *et al.* [27] used spherical silica nanoparticles with an average size of 14 nm to prepare epoxy composites using unidirectional glass and carbon fibers through the resin film infusion. The nanosilica particles with different loading rates (0.2 wt%, 0.4 wt% and 0.8 wt%) in the epoxy matrices were dispersed by means of ultrasonication. Compressive strength of hybrid carbon fiber reinforced composite showed a 35% increase in comparison to its control batches, whereas there was a 30% increase for GFRPCM, both at a nanosilica loading fraction of 0.2 wt%. Tensile, compressive and interlaminar shear properties of hybrid composites in transverse direction to the reinforcement remained unchanged.

Zhu *et al.* [28] used different surface functional silanes to modify the surfaces of carbon nanotubes and carbon nanofibers. Those modified nanotubes and nanofibers were dispersed in an epoxy resin and subsequently those epoxy resins containing surface modified nano-additives were used for S2 type glass reinforced filament winding process. Two different filament winding approaches were selected in their study. One of the approaches was usage of modified matrix in all process of filament winding. The other one was the usage of modified matrix between layers of filament winding with brushing. The composites produced using the modified resin systems had better fracture toughness properties and showed better delamination resistance with brushig approach [27].

Han *et al.* [29] studied two different types of nanosilicas in an epoxy resin system. The nanosilica particles commercial names were RNS-A and RNS-E with average particle sizes of 20 nm and 10 nm, respectively. The nanosilica particles were dispersed in the molten resin by stirring at 3000 rpm for 20 minutes. High-fracture toughness values can be achieved with a small amount of nanosilica loading. The dispersion of nanosilica particles in the epoxy matrix was not efficient since some particle clusters of different sizes was observed as shown in the images of SEM. There were mostly isolated particle clusters with sizes larger than 10 microns. Author commented that plastic deformation of the epoxy around particle clusters and crack deflection through the clusters may be the dominant toughening mechanisms for those composites. Although the nanosilica particle clusters are not in nanoscale, they consist of numerous nanosized particles. The epoxy resin indeed can penetrate into the clusters and wet the nanoparticles, as shown in the SEM images.

Demirci *et al.* [30] used silica nanoparticles in an epoxy resin and basalt fibers as continuous fibers for the filament winding process. The delamination strength of the silica reinforced epoxy resin system was characterized using Split Disc Test. For the silica epoxy resin system 4 wt% nanosilica particles with an average diameter of 15 nm were used. The nanosilica particles were dispersed in the epoxy resin by stirring for 10 minutes and ultrasonicating for 15 minutes. Mode I fracture toughness values of the composites containing silica particles were increased 43%-50% compared to the neat resin composites.

Hsieh *et al.* [31] investigated the influences of nanosilica particle addition for different resin systems. The amine cured epoxyresin system was used in this study. Epoxy and hardener was mixed in stoichiometric ratio as supplied by the manufacturer. 10 wt%

and 20 wt% nanosilica particles were added to the mixture of epoxy and hardener. Fracture toughness and energy and modulus values of silica nanoparticle added epoxy system were higher than those of the neat epoxy resin system. Glass transition temperatures of the resin systems were similar.

Chen *et al.* [32] used nanosilica particles in an epoxy resin system and investigated the influences of nanosilica particle loading on the thermal and mechanical properties of the nano silica–epoxy composite. First, nanosilica particles with an average particle size of 12 nm were mixed in methyl ethyl ketone (MEK) to obtain a silica suspension. Subsequently, silica suspension was dispersed in the epoxy using an ultrasonic probe on for 12 seconds and off for 48 seconds and followed by magnetic stirring for 3 hours. MEK was evaporated from the mixture at 75 $^{o}$C and 1 torr in vacuum furnace and then the hardener of epoxy resin was added to the dispersed mixture. The nanocomposite mixture was poured to a dog bone shaped silicone mold and cured in an oven. A TEM image of the dried nanosilica particles and the dispersed nanoparticles with different loadings in the cured epoxy are given in this study. At TEM analyses, the average particle size of nanosilica particles was measured around 12 nm as reported by the manufacturer. The TEM images suggest that good dispersions of the nanosilica at different loading rates were obtained. As stated in this study, when the nanosilica particles were dispersed in the epoxy system, the tensile modulus and fracture toughness of the composite were increased.

## 1.8. Aim of the Thesis

When compared with other nanomaterials, nanosilica particles have advantage of low cost and high strength properties in thermoset matrix composites with adaptation of them to conventional composites with easy dispersion processes. In thermoset matrix fiber reinforced composites, epoxy resins are most widely used resin systems especially for structural applications since they have good adhesion properties to fiber reinforcement materials and environmental resistance with high mechanical strength.

The main aim of this thesis is to investigate the influences of nanosilica particle addition on the mechanical properties of carbon fiber reinforced epoxy composites. We also aim to develop an easy dispersion technique for nanosilica particles and adapt this easy method to an industrial filament winding process. By reinforcing the epoxy matrix with silica particles, we expect to increase the fracture toughness energy of the carbon fiber reinforced epoxy composites which is not sufficient for the conventional composite materials.

# CHAPTER 2

# EXPERIMENTAL STUDIES

## 2.1. Materials Used

### 2.1.1. Matrix Material

Bisphenol-A based epoxide was used to prepare epoxy resin (brand name: KL 790-Part A, Duratek) matrix materials used in this study. An amine hardener (brand name: KL 790-Part B, Duratek) was used as the curing agent. The curing agent was added to the epoxy resin with a ratio of 45:55 by weight. The properties of resin systems which are provided by the manufacturer is given in Table 2.1, Table 2.2, and Table 2.3. The reported mechanical and thermal properties obtained after the resin system was subjected to 4 hours 95 ˚C + 4 hours 125 ˚C curing cycle.

**Table 2.1** General properties of the epoxy resin system (mixture of Part A and Part B) provided from resin system manufacturer.

| **Density of Mixture at 20 ˚C, EN ISO 2811-1** | **Viscosity of Mixture at 25 ˚C, DIN 53229** | **Pot Life of Mixture at 120 ˚C for 200 gram, DIN 16945** | **Water Absorption, at 24 hours, DIN 53495** |
|---|---|---|---|
| 1.1-1.20 g/cm$^3$ | 700-1100 mPas | 50-80 minutes | 0.25-0.35 |

**Table 2.2** Mechanical properties of the epoxy resin system provided from resin system manufacturer.

| **Tensile Strength, DIN 53504** | **Tensile Strain, DIN 53504** | **Tensile Modulus, DIN 53504** | **Hardness, Shore D** |
|---|---|---|---|
| 90-100 MPa | 3-4 % | 3000-3200 MPa | 80-90 |

**Table 2.3** Thermal properties of the epoxy resin system provided from resin system manufacturer.

| Heat Deflection Temperature (HDT), ISO 75-2 | Decomposition Temperature, VSM 77113 | Linear Thermal Expansion Coefficient, DIN 53572 |
|---|---|---|
| 115-130 °C | 350 °C | $60\ 10^{-6}$/K |

## 2.1.2. Continuous Carbon Fiber Reinforcement

As a carbon fiber A49 brand, which is manufactured by DOWAKSA, Turkey, was used as a continuous fiber reinforcement material in this study. The carbon fiber has an epoxy sizing agent on its surface. The properties of the fibers provided by the manufacturer are given in Table 2.4.

**Table 2.4** The properties of carbon fiber properties provided from carbon fiber reinforcement manufacturer.

| Properties | Value | Test Method |
|---|---|---|
| Tensile Strength | 4900 MPa | ISO 10618 |
| Tensile Modulus | 250 GPa | ISO 10618 |
| Tensile Strain | 2 % | ISO 10618 |
| Density | 1.79 g/cm$^3$ | ISO 10119 |
| Linear Density | 800 g/1000 m | ISO 1889 |

## 2.1.3. Nanosilica

Silica (Silicon oxide, $SiO_2$) nanoparticles (or nanosilicas) with a primary particle size of 15-20 nm manufactured by Nanostructured & Amorphous Materials Inc.-USA was used as nano-reinforcement in epoxy resin systems. The properties of silicon oxide provided from the manufacturer is given at Table 2.5. The TEM image and X-ray diffraction pattern of silicon oxide particles were provided by the manufacturer are given in Figure 2.1 and Figure 2.2, respectively. The purchased silica nanoparticles were dispersed in distilled water for 2 minutes using a probe type ultrasonic processer and then particle size measurements were performed using the laser diffraction method (Malvern Mastersizer 2000). The particle size distribution of these particles is given in Figure 2.3. The volumetric weighted mean D[4,3] was measured as 98 nm and 50% of cumulative mass d(0,5) was measured as 93 nm. Also the SEM pictures of those dispersed particles are shown Figure 2.5 and Figure 2.6, clusters due to agglomeration between particles and it is not possible to measure particle size from these images. When the silicon oxide particles were dispersed in isopropyl alcohol, clusters of silicon oxide particles were broken in fair amount and particle size of particles are decreased to 25-40 nm.

**Table 2.5** General properties of silicon oxide provided from manufacturer.

| Properties | Value | Test Method |
|---|---|---|
| Purity | 99.5 % | ICP |
| Average Particle Size | 15-20 nm | TEM |
| Specific Surface Area | ~640 $m^2/g$ | BET |
| Morphology | Spherical, Porous | TEM |
| Bulk Density | 0.10 $g/cm^3$ | Measuring by weight and volume |
| True Density | 2.2-2.6 $g/cm^3$ | Measuring by weight and volume |

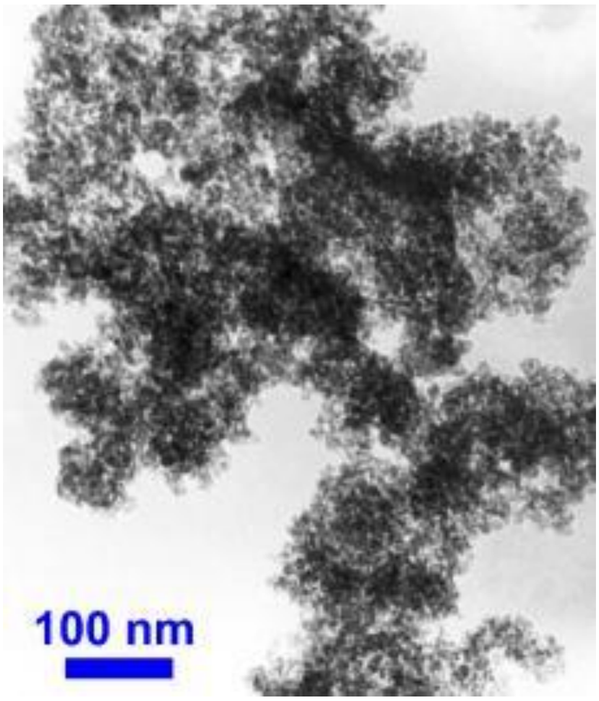

**Figure 2.1** TEM image of silicon oxide provided from manufacturer.

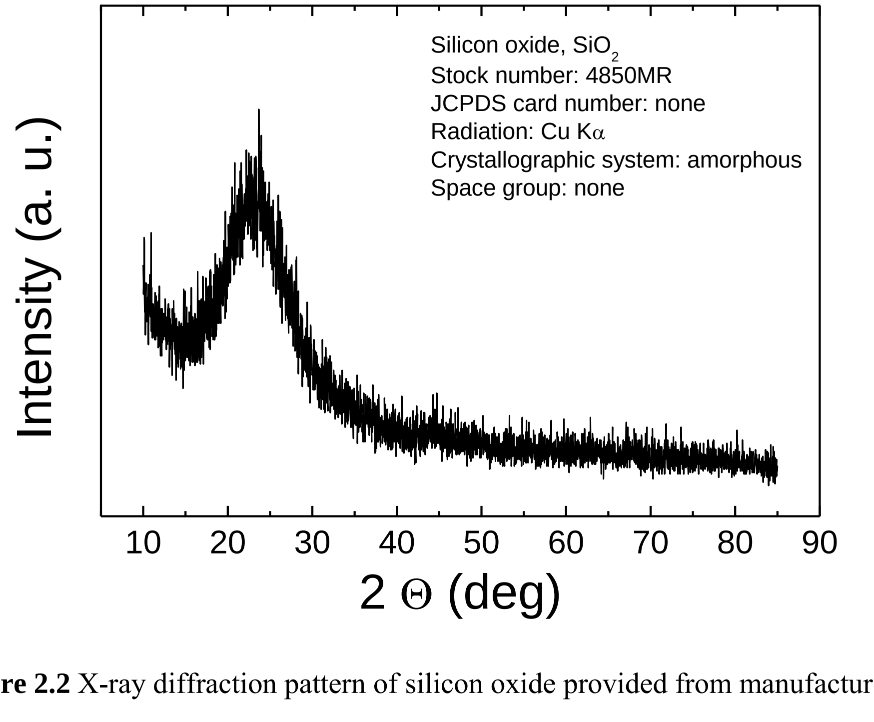

**Figure 2.2** X-ray diffraction pattern of silicon oxide provided from manufacturer.

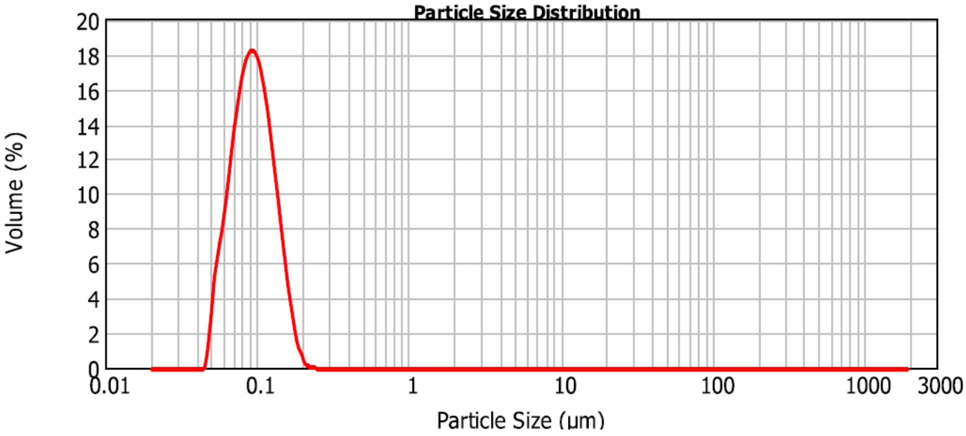

**Figure 2.3** Particle size distribution of silicon oxide which was dispersed at water for 2 minutes with probe type ultrasonic processer.

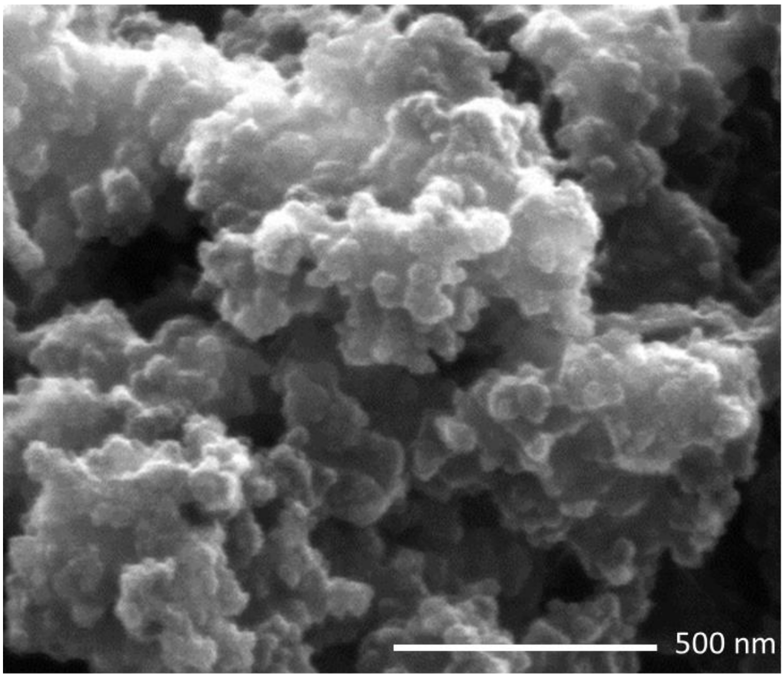

**Figure 2.4** SEM image of silicon oxide particles as purchased.

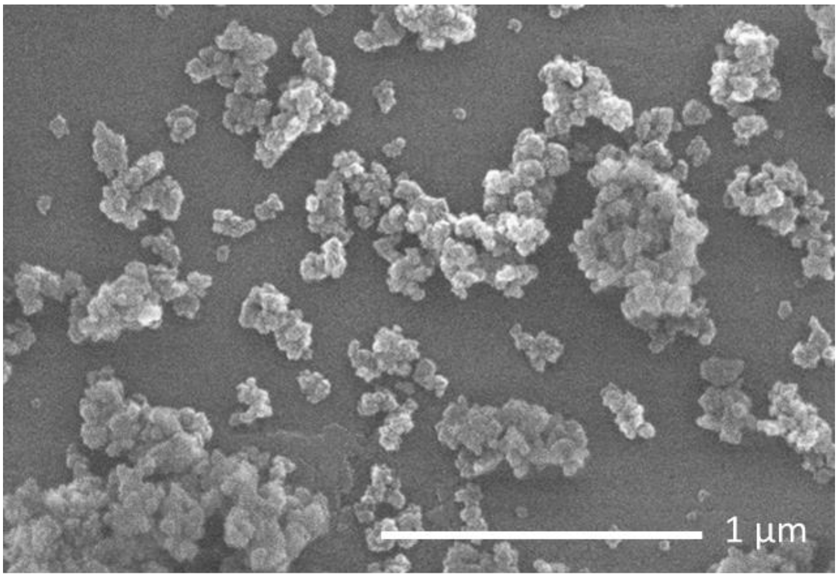

**Figure 2.5** SEM image of silicon oxide particles at 100000X magnification (dispersed at isopropyl alcohol for 20 minutes with probe type ultrasonic processer).

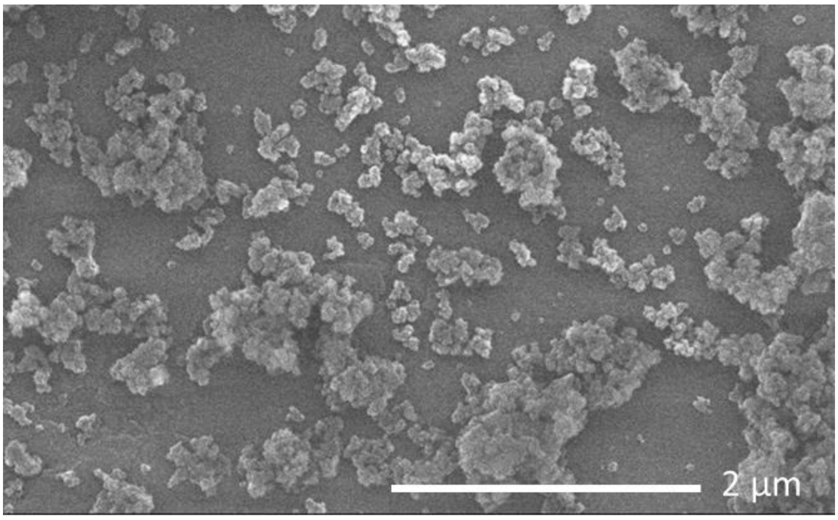

**Figure 2.6** SEM image of silicon oxide particles at 500000X magnification (dispersed at isopropyl alcohol for 20 minutes with probe type ultrasonic processer).

## 2.2. Experimental Methods for Production of Nanosilica Filled Epoxy Composites

### 2.2.1. Dispersion Process

The nanosilica particles were dispersed in the Part A component (Bisphenol A-Epoxy) of the resin system using a probe (horn) type ultrasonic device (BSP-1200 ultrasonic processer, Sonomechanics). The schematic illustration of the ultrasonic processor with a power of 1200 Watt is given in Figure 2.7. The tip diameter of the processor was 35 mm the amplitude of the processor can be up to 100 microns. The horn was immersed into the resin and nanoparticle mixture slightly above its nodal point, where a groove or flange is located. The container and transducer were cooled with a chiller for preventing heat generation during the dispersion process.

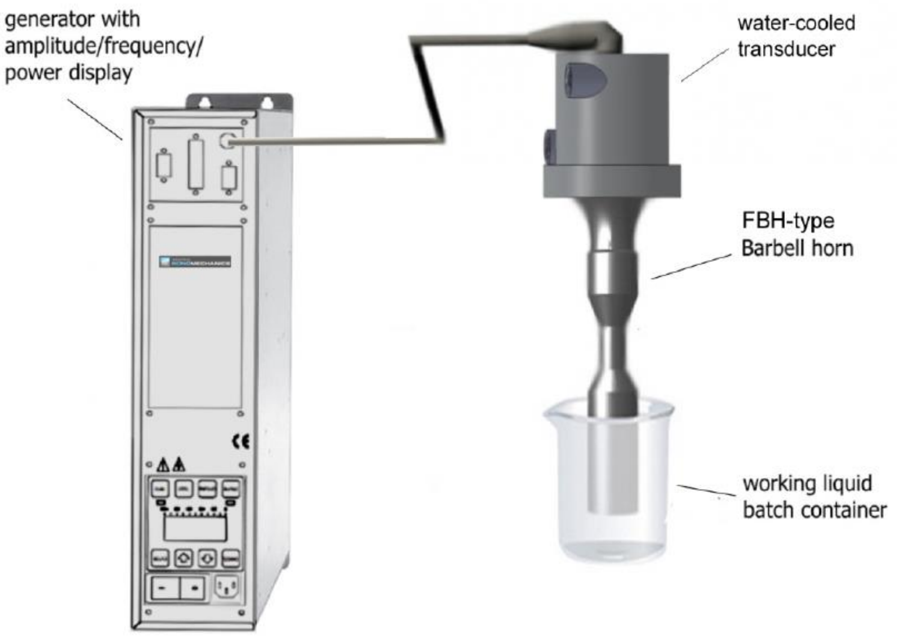

**Figure 2.7** Schematic illustration of the ultrasonic processor used in this study.

In this study, three different weight percentage of nanosilica in epoxy resin mixture was studied as 0.5 wt%, 1.0 wt%, 2.0 wt%. After calculation of ratios as decided, epoxy resin Part A component and nanosilica particles were weighted in balance. The ultrasonication process was set to 80% amplitude with between 19000-20000 Hz. The ultrasonic processor was repeated at 20 stages which were taken time for 60 seconds for each stage. The applied energy was between 800-960 Watt. The double wall steel container which is connected to chiller was used for cooling mixture. After each stage temperature of mixture was measured and allowed to cool 60 $^{\circ}$C. The height between probe tip and container bottom was set as 20 mm in each process and the height of the probe in container kept constant with controlling it with remote control. The process parameters applied at each process stage is given in Table 2.6 which is same for applied 3 different loading rates of nanosilica in epoxy. The ultrasonic dispersion processer picture is given in Figure 2.8 with related accessories used at dispersion process. Epoxy-Part A and nanosilica mixture dispersion process picture is given in Figure 2.9. The following characterization tests were performed according to process parameters which are given at Table 2.6.

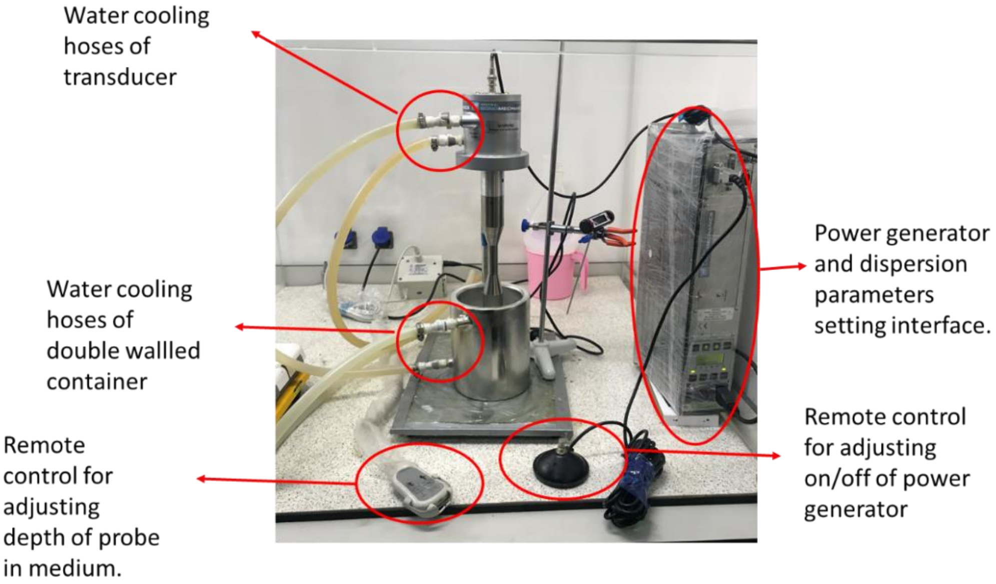

**Figure 2.8** The dispersion setup and related accessories.

**Table 2.6** Process parameters applied at each stage during ultrasonic dispersion.

| **Stage Number** | **Process Parameters**<br>A: Amplitude, %<br>P: Power, Watt<br>F: Operating Frequency, Hz | **Temperature of Mixture after Dispersion, ˚C** | **Time for cooling to 60 ˚C, seconds** |
|---|---|---|---|
| 1 | A: 80, P: 950-958, F: 20000 | 12 | - |
| 2 | A: 80, P: 950-956, F: 20000 | 27 | - |
| 3 | A: 80, P: 947-955, F: 20000 | 35 | - |
| 4 | A: 80, P: 945-958, F: 20000 | 47 | - |
| 5 | A: 80, P: 944-954, F: 20000 | 50 | - |
| 6 | A: 80, P: 944-952, F: 20000 | 57 | - |
| 7 | A: 80, P: 940-953, F: 20000 | 72 | 90 |
| 8 | A: 80, P: 942-950, F: 20000 | 70 | 100 |
| 9 | A: 80, P: 937-945, F: 20000 | 75 | 115 |
| 10 | A: 80, P: 925-932, F: 20000 | 72 | 125 |
| 11 | A: 80, P: 927-933, F: 20000 | 75 | 130 |
| 12 | A: 80, P: 920-928, F: 20000 | 72 | 140 |
| 13 | A: 80, P: 915-924, F: 20000 | 73 | 150 |
| 14 | A: 80, P: 910-917, F: 20000 | 75 | 160 |
| 15 | A: 80, P: 909-917, F: 20000 | 75 | 160 |
| 16 | A: 80, P: 909-915, F: 20000 | 77 | 200 |
| 17 | A: 80, P: 905-912, F: 20000 | 75 | 200 |
| 18 | A: 80, P: 906-912, F: 20000 | 76 | 200 |
| 19 | A: 80, P: 905-911, F: 20000 | 75 | 250 |
| 20 | A: 80, P: 901-908, F: 20000 | 74 | 250 |

**Figure 2.9** Epoxy-Part A and nanosilica dispersion at ultrasonic processor.

### 2.2.2. Nanosilica Filled Epoxy Test Coupon Manufacturing

The dog bone shaped test coupons were manufactured for tensile tests with using open metallic tool which has cavities according to ISO 527 standard test method which is given in Figure 2.10. The equal amount of resin mixture was poured into the mold cavities with using injector. During this process paid attention to the bubble formation. After mold cavities were filled with resin mixture, they were cured at 4 hours 95 $^{\circ}$C and 4 hours 125 $^{\circ}$C with 3 °C/minute heating and cooling rate cycle in oven. The broken tensile test specimens were also used for other characterization tests such as Differential Scanning Calorimetry (DSC).

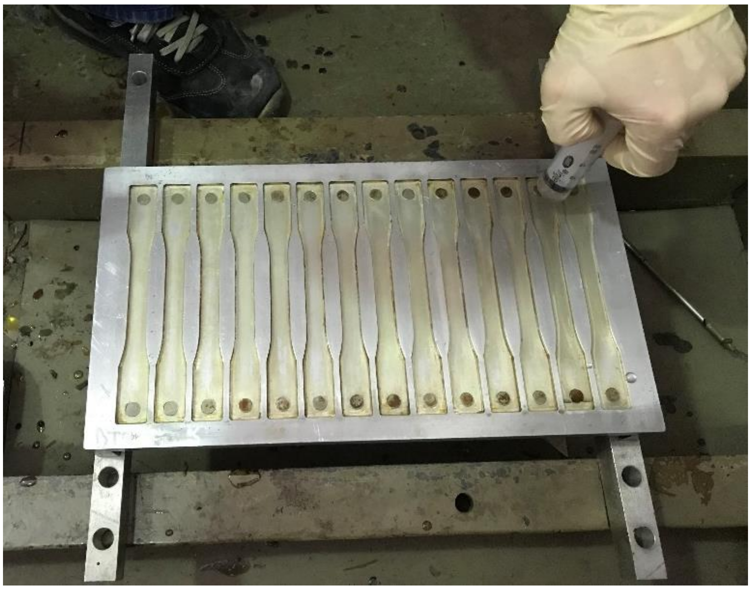

**Figure 2.10** Tensile test coupon manufacturing tool.

### 2.2.3. Characterization Tests for Nanosilica Filled Epoxy

#### 2.2.3.1. Rheological Characterization of Nanosilica Filled Epoxy

Viscosity measurements were done for 0.5 wt%, 1.0 wt%, 2.0 wt% loading rates in epoxy resin system. These measurements were performed with Brookfield Viscometer according to ISO 2555 standard at 30 °C, 40 °C and 50 °C bath temperature for 2 hours duration. During viscosity measurements 75 rpm applied as the speed of spindle.

#### 2.2.3.2. Mechanical Characterization of Nanosilica Filled Epoxy

Tensile tests were performed using dog bone specimens which were manufactured according dimensions stated at ISO 527 standard. At least 5 specimens were tested for each epoxy-silica composite. Before tensile testing, the grip sections of dog bone specimens were rubbed with an emery paper as shown in Figure 2.11.

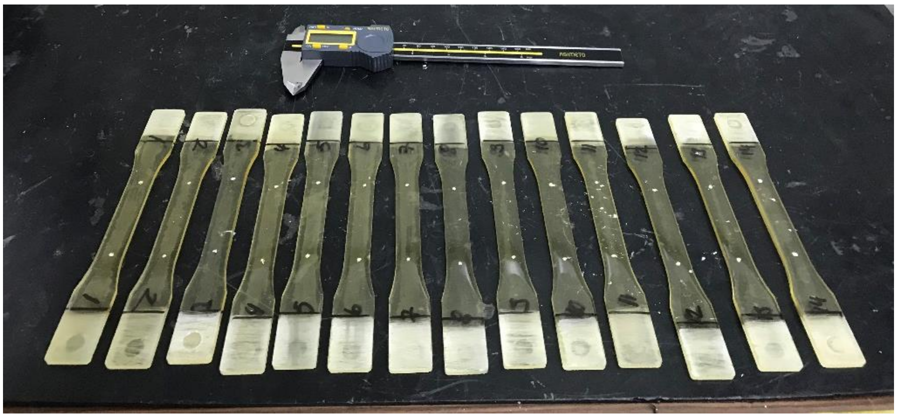

**Figure 2.11** Dog bone specimens for tensile tests.

### 2.2.3.3. Thermal Characterization of Nanosilica Filled Epoxy

Thermal analysis of the neat and nanosilica filled epoxy samples were carried out by a DSC (Q200, TA instruments) to determine the glass transition temperatures of the samples. DSC measurements were performed by loading 20-30 mg of samples into $Al_2O_3$ crucibles and heated from room temperature to 180 ˚C with a heating rate of 10 ˚C/min. The measurements were performed under a high purity helium atmosphere.

### 2.2.3.4. Morphological Characterization of Nanosilica Filled Epoxy

The fracture surfaces of tensile test coupons were used for SEM analysis. The fracture surfaces of neat, 1.0 wt% and 2.0 wt% nanosilica filled epoxy batches were analyzed. The microstructural information obtained from SEM images was used to elucidate the influences of nanosilica addition on the damage mechanisms of the nanosilica filled epoxy composites.

## 2.3. Experimental Methods for Production of Nanosilica Filled Carbon Fiber Reinforced Epoxy Composites

Filament winding process was used to manufacture the test plates of carbon fiber reinforced epoxy composites. The filament winding machine is Mc Clean Anderson brand with 4 axis CNC control. The machine has a tensioner unit for applying tension to fibers during the filament winding process. As shown in Figure 2.12, the tensioned fibers passed through drum type resin bath for wetting purpose of dry fibers, and then wetted fibers were placed on filament winding test plate tool according to program was set on the machine computer. “ISO 1268-5 Fibre-reinforced plastics-Methods of producing test plates-Part 5: Filament winding” international standard was followed for the filament winding process [33]. After completing the filament winding process on the test plate tool, the curing process was done. Then, the cured test panels were cut into the test coupon dimensions according to the related test standard. As a result, physical, thermal and mechanical characterization test coupons were manufactured from the test plates of both neat and nanosilica filled resin systems.

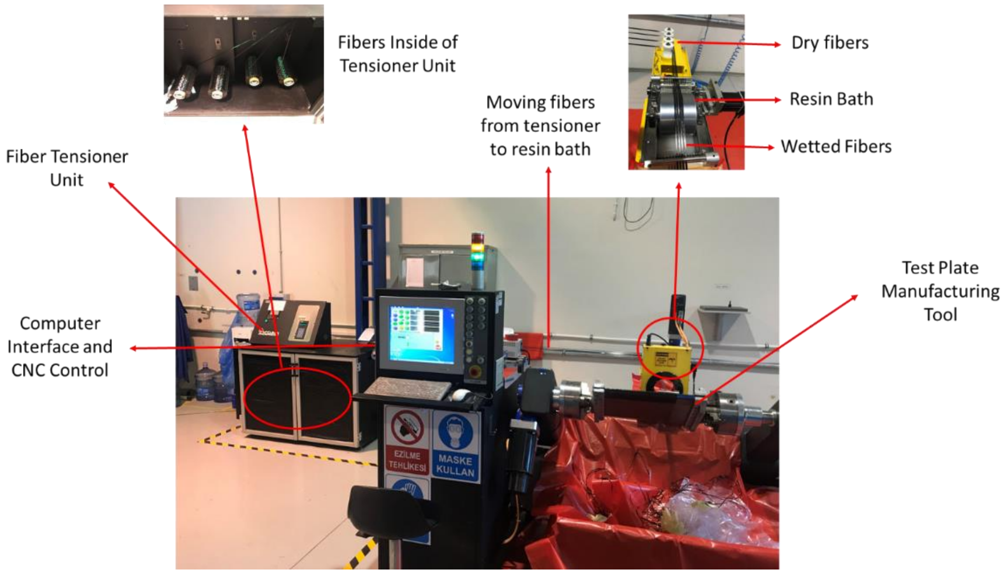

**Figure 2.12** Filament winding machine.

### 2.3.1. Tooling of Filament Winding Process

The tooling of test plate manufacturing in filament winding process was designed according to ISO 1268-5 standard. There are three sections of the tooling which are shaft, filament wound section, and closing plates. The shaft and filament wound sections of tools are made of steel and the outer closing plates are made of aluminum. The purpose of using aluminum is the advantage of high thermal conductivity of aluminum during the curing process of epoxy composites. The left and right shaft sections were used for loading of tooling to filament winding machine from both headstock as shown in Figure 2.13. After filament winding process on the test plate manufacturing tool, the closing plates were assembled for getting the flat surfaces on the outer surfaces of test plates as shown in Figure 2.14.

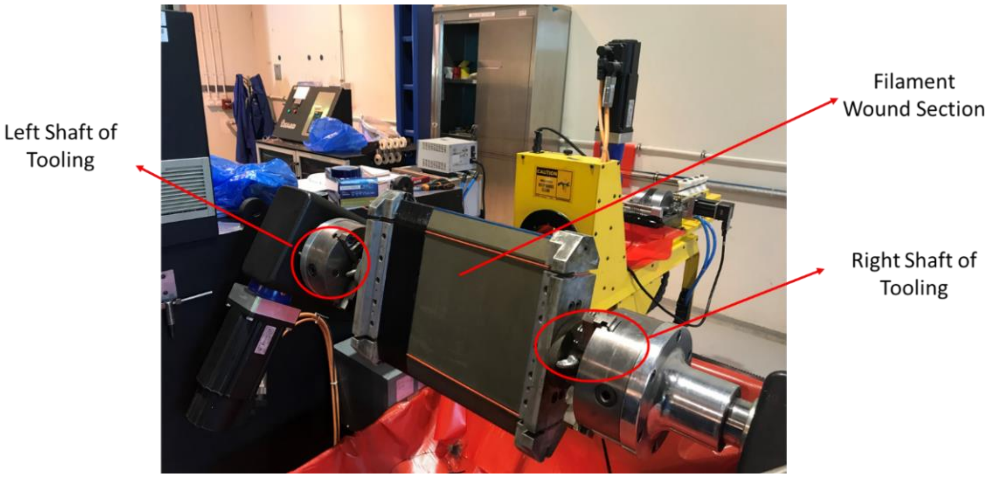

**Figure 2.13** The sections of test plate manufacturing tooling of filament winding process.

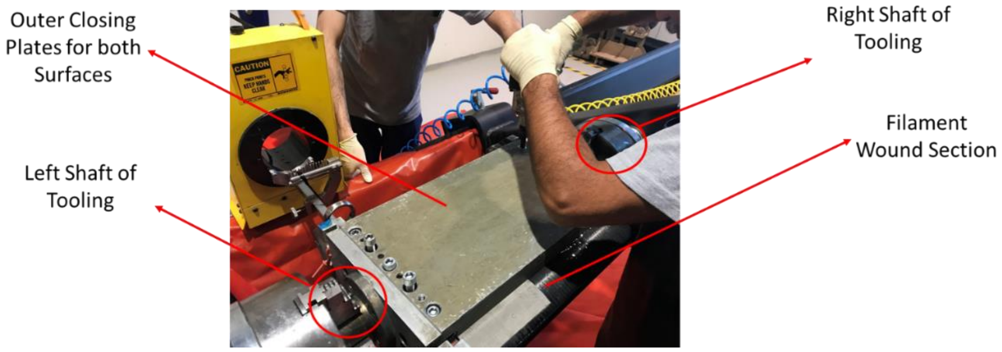

**Figure 2.14** The outer closing plates for both surfaces of test plate manufacturing tooling.

### 2.3.2. Process Parameters of Filament Winding

During the filament winding process, the drum type resin bath (Figure 2.15) at 30 °C with 4 bobbins of carbon filament were used. Unidirectional [0°] test plates were manufactured using the wetted carbon fibers which were winded at fiber longitudinal [0°] axis. During the winding process, 1 kg tension was applied to each carbon fiber for providing compaction at the mandrel during the filament winding process. Test plates with 3 mm thickness were manufactured by 6 layers of winding on the tooling. The manufactured test plates were cut into the suitable dimensions for analyses of density, fiber weight ratio, tensile test, mode I interlaminar fracture toughness energy, mode II interlaminar fracture toughness energy, and DMA tests.

The 12 μm thick film was placed on the mid-plane of filament wound layers for creating intended crack/defect inside the test coupons of fracture toughness, as shown in Figure 2.16. After finishing 6 layers of 0° winding on test plate tooling, the side plates were closed (Figure 2.14) and screwed for getting compaction on fibers and flat finish surfaces of composite test plates. The same parameters were applied for neat and nanosilica filled epoxy used filament winding processes.

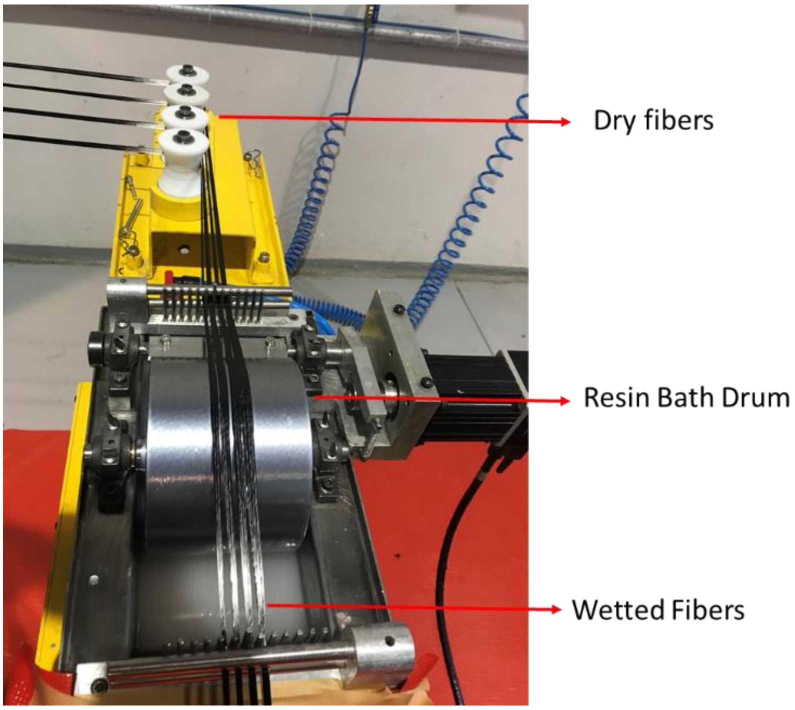

**Figure 2.15** Resin bath sections of filament winding machine.

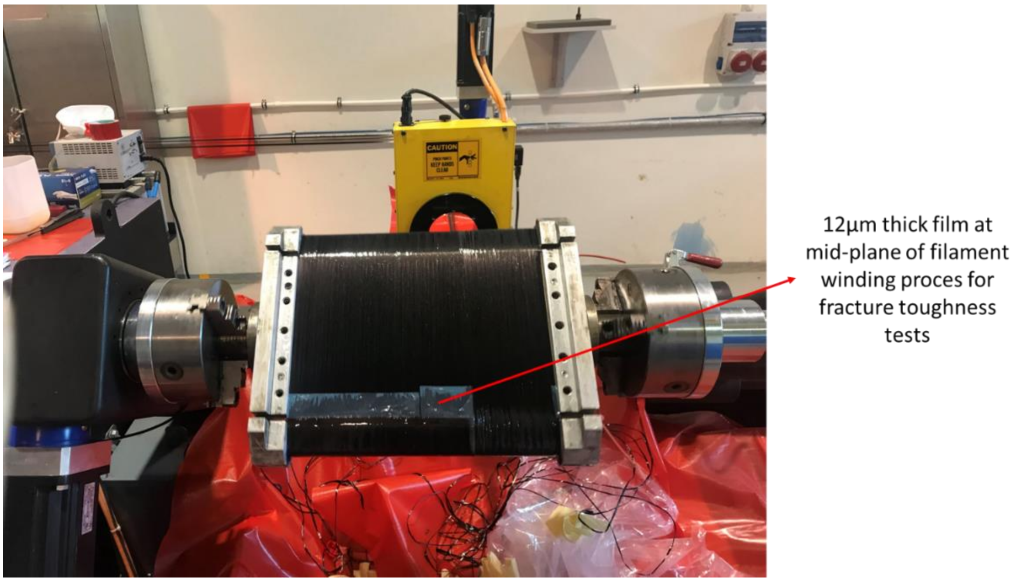

**Figure 2.16** Film placement for fracture toughness test coupons during filament winding process.

### 2.3.3. Curing

The manufactured test plates were cured in a curing oven with controlled heating and cooling rates. The applied curing cycle was 4 hours 95 °C and 4 hours 125 °C with 3 °C/min. heating and cooling rates. The curing oven was calibrated and each process cycle was controlled from the oven control panel.

### 2.3.4. Manufacturing of Test Coupons

The test coupons were cut from the manufactured composite test plates according to related test standards. The test coupons cutting processes were done by a CNC controlled composite coupon cutting machine as shown in Figure 2.18. During the cutting process, a water cooling system was used for preventing heat formation in the test coupons.

The tabbing was applied to unidirectional [0°] test coupons for preventing slippage from the grip sections of the universal testing machine during the tensile tests as shown in. As a tab material, glass a fiber reinforced epoxy composite was used and the adhesion surfaces of tab and test plates were rubbed with a grinding paper as shown in Figure 2.17. The paste type epoxy adhesive was used for bonding the tab material to the test plates. After curing of adhesive, the test plates were sliced to required dimensions (Figure 2.19) using the coupon cutting machine as shown in Figure 2.18.

For mode I interlaminar fracture toughness energy tests, aluminum blocks were manufactured for gripping the test specimens to the universal testing machine. The aluminum blocks were bonded to the up and down surfaces of the test coupons using an epoxy adhesive (Figure 2.20). Other test specimens were cut into the required dimensions without any additional process as shown in Figure 2.21.

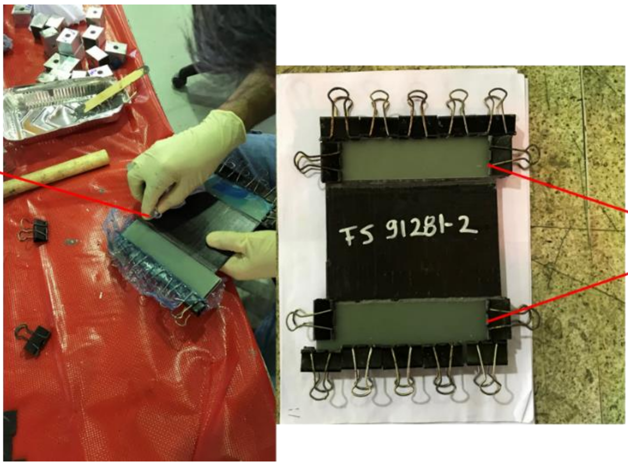

Cleaning of adhesive used for bonding tab material to test coupons

Tabbing of 0° tensile test coupons

**Figure 2.17** Tabbing of 0$^{\circ}$ direction (longitudinal direction) tests tensile test plate.

**Figure 2.18** Composite test coupon cutting machine.

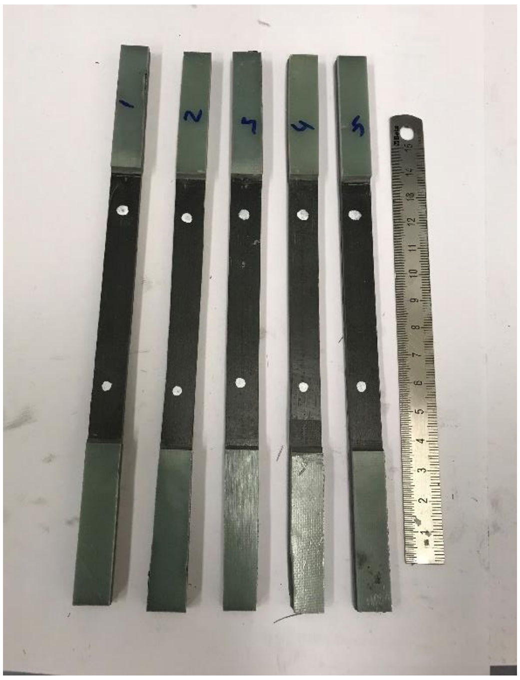

**Figure 2.19** Unidirectional (longitudinal direction) tensile test coupons.

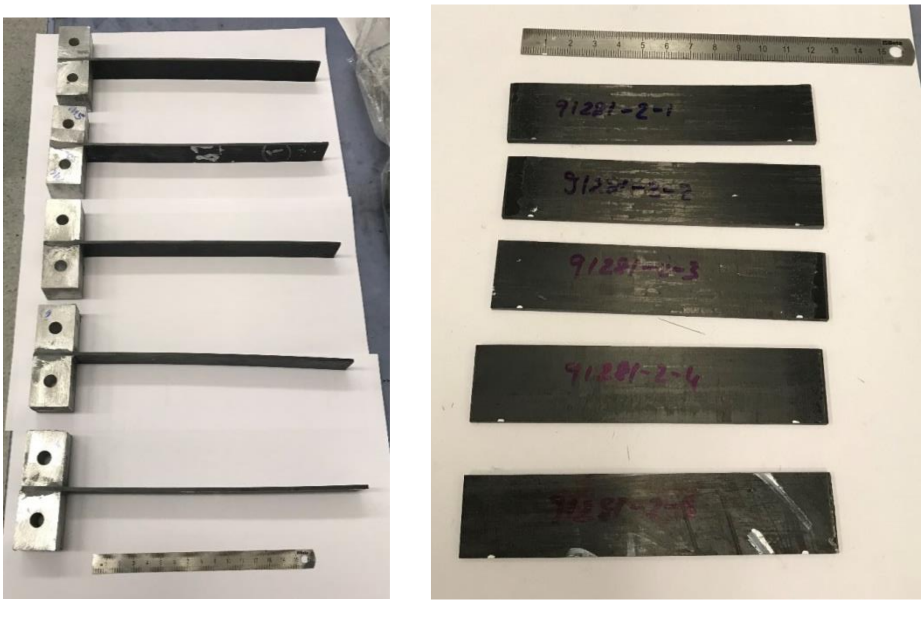

**Figure 2.20** Mode I (left) and mode II (right) interlaminar fracture toughness energy test coupons.

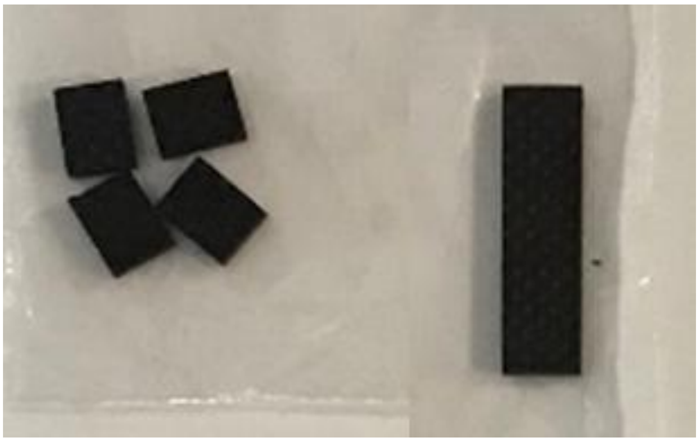

**Figure 2.21** Physical characterization (left) and DMA (right) test coupons.

### 2.3.5. Characterization Tests of Nanosilica Filled Carbon Fiber Reinforced Epoxy Composites

#### 2.3.5.1. Physical Characterization of Nanosilica Filled Carbon Fiber Reinforced Epoxy Composites

The density measurements of the samples were done according to the Archimedes principle by following ASTM D792 for the fiber reinforced neat and nanosilica filled epoxy test samples. Rectangular prisms with dimensions of 10 mm x 10 mm x 3 mm were produced for the density measurements. After the density tests, the fiber weight ratio tests were performed with the same density test coupons which were dried at 40 °C for an hour. The fiber weight ratio of test coupons were calculated according to Equation 2.1 and matrix digestion approach based on ASTM D3171-Procedure B. The fiber volume ratio of test coupons was calculated via Equation 2.2. For void content calculations, ASTM D2734 and Equation 2.4 were used. The theoretical density of composites was calculated according to Equation 2.3. The fiber volume ratios were used to normalize the mechanical test results for each batch.

$$W_r = \frac{M_f}{M_i} \times 100$$

**Equation 2.1**

Where:

| | |
|---|---|
| $W_r$ | Reinforcement content by weight, % |
| $M_i$ | Initial mass of the specimen, gram |
| $M_f$ | Final mass of the specimen after digestion or combustion, gram |

Reinforcement content, volume percent

$$V_r = \frac{M_f}{M_i} \times 100 \times \frac{p_c}{p_r}$$

**Equation 2.2**

Where:

| | |
|---|---|
| $V_r$ | Reinforcement content by volume, % |
| $p_r$ | Density of the reinforcement, gram/cm$^3$ |
| $p_c$ | Density of the composite specimen, gram/cm$^3$ |

$$T_d = \frac{100}{(\frac{R}{D}+\frac{r}{d})}$$

**Equation 2.3**

Where:

| | |
|---|---|
| $T_d$ | Theoretical composite density |
| R | Resin in composite, weight % |
| D | Density of resin |
| r | Reinforcement in composite, weight % |
| d | Density of reinforcement |

$$V = \frac{100(T_d - M_d)}{T_d}$$

**Equation 2.4**

Where:

| | |
|---|---|
| V | Void content, volume % |
| $T_d$ | Theoretical composite density |
| $M_d$ | Measured composite density |

#### 2.3.5.2. Mechanical Characterization of Nanosilica Filled Carbon Fiber Reinforced Epoxy Composites

Unidirectional (or longitudinal direction) [$0^\circ$] tensile test, mode I and mode II interlaminar fracture toughness energy tests were performed for investigating mechanical properties of fiber reinforced neat and nanosilica filled epoxy composites. For those mechanical tests, Instron brand universal testing machine was used with the necessary apparatus.

For unidirectional tensile tests, ASTM D3039 test method was followed for determining tensile behavior of the manufactured test coupons. During the tensile testing, a video extensometer was used for measuring elongation values of the test coupons, so that the modulus of test samples can be calculated accurately. Test specimens were loaded to test machine grips from the tabbed sections of coupons and test speed was set as 2 mm/min. After failures had occurred, failure mode analysis was done according to ASTM D3039 standard.

Interlaminar fracture toughness energy, $G_{IC}$, of manufactured test coupons from unidirectional test plates was determined using the mode-I fracture toughness test based on DIN EN 6033:2016-02. According to this test method, the interlaminar fracture toughness energy is the energy per unit plate width which is necessary to produce a unit crack growth at an interlaminar crack between two plies of a laminate by applying a peel force to the crack plane. Initial cracks of the test coupons (25 mm in length) were created during the test plate manufacturing stage and aluminum blocks were bonded to up and down surfaces of open ends of the test coupon. The blocks were used for gripping the test specimens to the universal testing machine. The specimens were loaded with a cross-head speed of 10 mm/min until a total crack length of about 100 mm was reached. After completing the test, load against cross head displacement curves were obtained (see Figure 2.22). The interlaminar fracture toughness energy ($G_{IC}$) values were calculated by using Equation 2.5.

$$G_{IC} = \frac{A}{a \times w} \times 10^6$$ **Equation 2.5**

Where:

| | |
|---|---|
| $G_{IC}$ | is the fracture toughness energy, in J/m$^2$ |
| A | is the energy to achieve the total propagated crack length, in J<br>(integration of the area of the load-cross head displacement graph) |
| A | is the propagated crack length, in mm<br>(final crack length minus initial crack length) |
| W | is the width of the specimen, in mm |

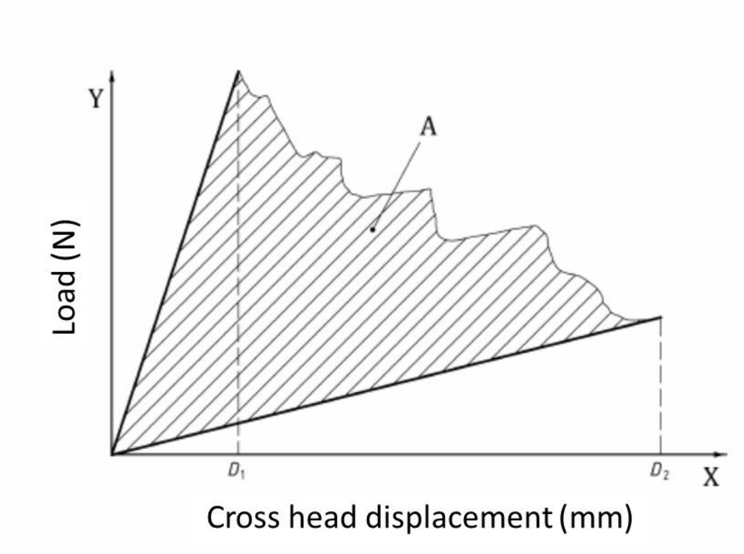

| | |
|---|---|
| $D_1$ | Cross head displacement at initial crack length |
| $D_2$ | Cross head displacement at final crack length |
| A | Calculated energy |

**Figure 2.22** Load cross head displacement curve of mode-1 interlaminar fracture toughness energy test [21].

Mode-II interlaminar fracture toughness energy, $G_{IIC}$, of the manufactured test coupons were determined according to DIN EN 6034:2016-02. For this test method, the interlaminar fracture toughness energy is the energy per unit plate width which is necessary to produce an unit crack growth at an interlaminar crack between two plies of a laminate by applying shear forces at the crack tip introduced by flexural test. A precracked test specimen (40 mm in length) was placed at a three point bending test fixture for this test method. The picture of the designed test fixture is shown in Figure 2.23. The test specimens were positioned on the test fixture according to the position of the precrack which was created during the filament winding process. A cross head speed of 1 mm/min was applied to the test specimens and load-displacement curves were obtained. The interlaminar fracture toughness energy of specimens were calculated according to Equation 2.6.

$$G_{IIC} = \frac{9 \times P \times a^2 \times d \times 1000}{2 \text{ x } w(\frac{1}{4L^3} + 3 a^3)}$$

**Equation 2.6**

Where:

| | |
|---|---|
| $G_{IIC}$ | is the fracture toughness energy, in J/m$^2$ |
| $D$ | is the crosshead displacement at crack delamination onset, in mm |
| $P$ | is the critical load to start the crack, in N |
| $A$ | is the initial crack length, in mm |
| $W$ | is the width of the specimen, in mm |
| $L$ | is the span length, in mm |

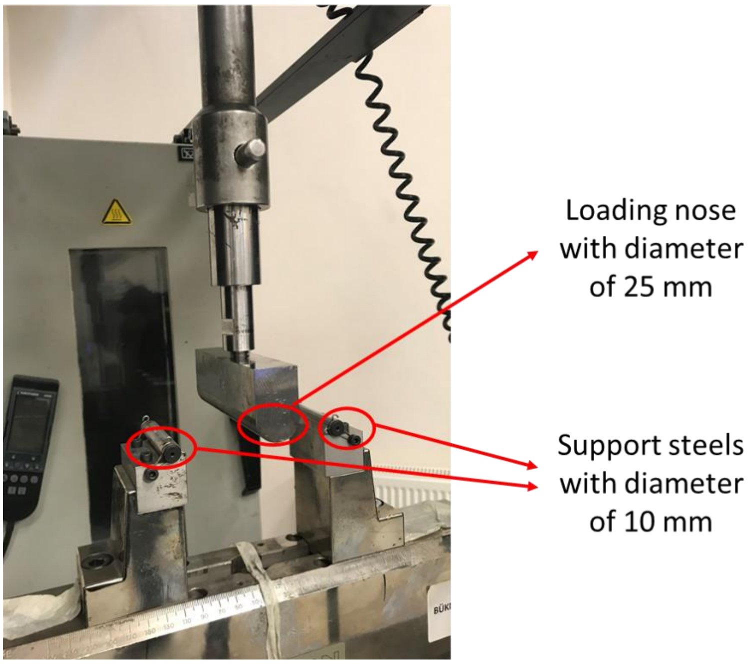

**Figure 2.23** Test fixture for mode II interlaminar fracture toughness energy tests.

All mechanical characterization test results were normalized according to 55% fiber volume fraction which is a typical volume fraction for the filament wound composites, so that true comparisons between batches can be possible. The normalization was fulfilled based on explained normalization theory formula given in Equation 2.7 [34].

$$\text{Normalized Value} = \text{Test Value} \times \frac{FV_{normalizing}}{FV_{specimen}} \qquad \textbf{Equation 2.7}$$

Where:

| | |
|---|---|
| $FV_{normalizing}$ | Normalization value of fiber volume fraction |
| $FV_{specimen}$ | Specimen fiber volume fraction |

#### 2.3.5.3. Thermal Characterization of Nanosilica Filled Carbon Fiber Reinforced Composites

For understanding thermal effects of nanosilica addition in epoxy composites, DMA tests were carried out for the carbon fiber reinforced test coupons using a rheometer (Ares 6A, TA Instruments). For those tests, a torsion rectangular apparatus was used and ASTM D7028 standard test method was followed. The test parameters for the DMA tests were 5 °C/min heating rate, 1 Hz frequency and 0.01% strain amplitude. Test coupon dimensions with length of 50 mm, a width of 12.5 mm, and a thickness of 3 mm were used. The coupons were tested at fiber longitudinal direction [0°]. The glass transition temperatures of test coupons were evaluated using DMA thermograms.

#### 2.3.5.4. Morphological Characterization of Nanosilica Filled Carbon Fiber Reinfoced Composites

The fracture surfaces of tensile, mode I and mode II interlaminar fracture toughness energy coupons were used for SEM analysis. The fracture surfaces of neat, 1.0 wt% and 2.0 wt% nanosilica filled epoxy batches were analyzed. EDX analyses was done to specific areas in SEM images for elementary analysis. With the SEM analyses, toughening mechanisms and defects in nanosilica filled carbon fiber reinforced epoxy composites were investigated and correlated with mechanical characterization test results.

# CHAPTER 3

# RESULTS & DISCUSSION

## 3.1. Effects of Nanosilica on Epoxy Properties

### 3.1.1. Viscosity Measurements

The viscosity measurements were carried out for the neat epoxy and nanosilica filled (0.5 wt%, 1.0 wt%, and 2.0 wt%) epoxy uncured resin systems.

The viscosities of the neat epoxy resin system (reference) as a function of time at 30 °C, 40 °C and 50 °C are shown in Figure 3.1. The initial viscosity of the neat epoxy resin system is low at 50 °C, when compared with the viscosity values at 30 °C and 40 °C. The highest viscosity values were obtained at 50 °C and 2 hours. An epoxy resin system with a high viscosity is not wanted since the wetting of carbon fibers during filament winding process may not be efficient.

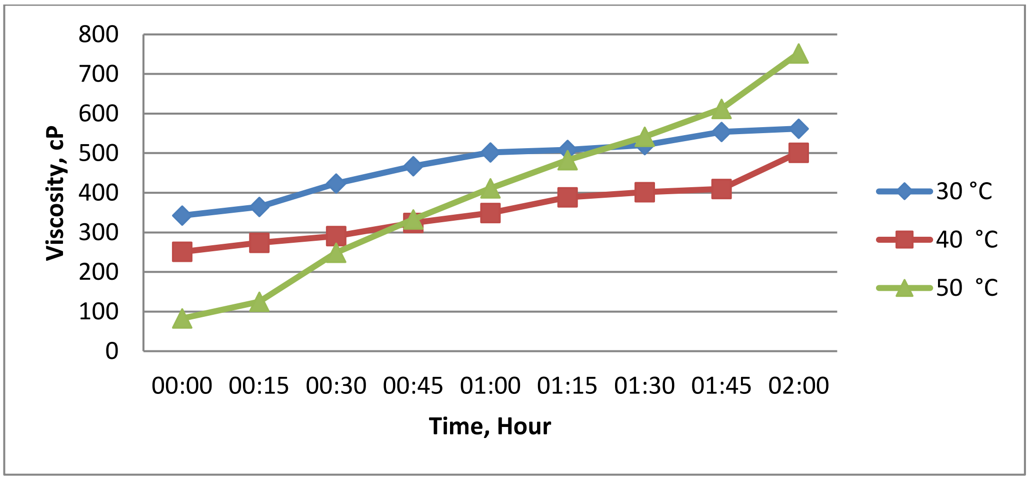

**Figure 3.1** Viscosities of the neat epoxy resin system as a function of time at 30 °C, 40 °C, and 50 °C.

The viscosities of the epoxy resin system with 0.5 wt% nanosilica loading as a function of time at 30 °C, 40 °C and 50 °C are shown in Figure 3.2. The dispersion process was applied according to given steps and parameters given in Table 2.6 for this loading rate. As can be seen from Figure 3.2, the initial viscosity of epoxy resin system is low at 50 °C when compared with those of the resin systems at 30 °C and 40 °C. After 2 hours, the viscosities of the resins systems at 30 °C and 50 °C were around 900 cP. The viscosity values obtained ranging between 600-800 cP could be regarded as suitable viscosities for filament winding processes.

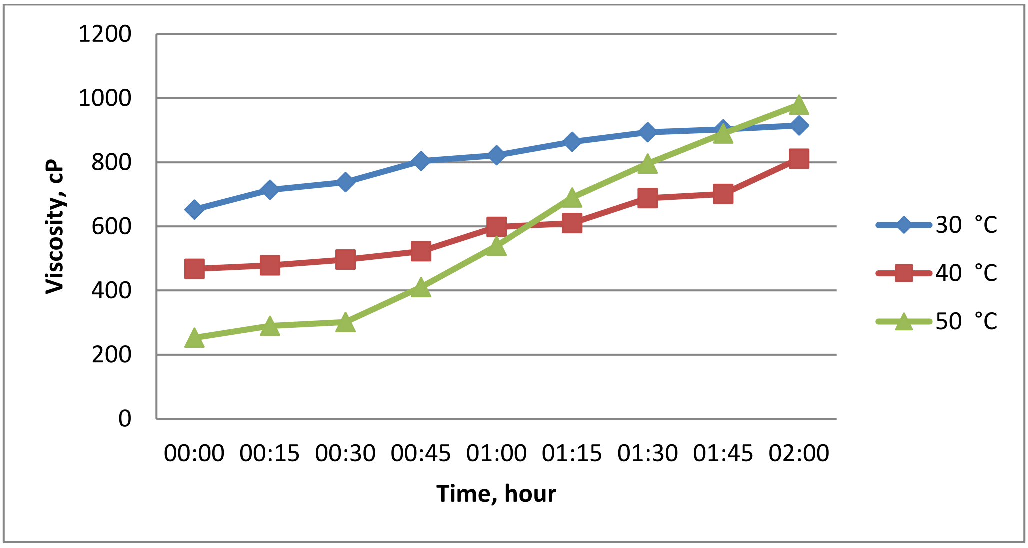

**Figure 3.2** Viscosities of the epoxy resin system epoxy resin system with 0.5 wt% nanosilica loading as a function of time at 30 °C, 40 °C, and 50 °C.

The viscosities of the epoxy resin system with 1.0 wt% nanosilica loading as a function of time at 30 °C, 40 °C and 50 °C are shown in Figure 3.3. The dispersion process was applied according to given steps and parameters in Table 2.6. The initial viscosity values at 30 °C and 40 °C were 752 cP and 639 cP, respectively. After 1 hour, the viscosities of the resin system at 30 °C and 40 °C reached around 900 cP, which can not be regarded as a suitable viscosity for a filament winding process due to the risk of gelation. Based on the results of viscosity measurements, the temperature of 50 °C would be the most suitable temperature for the filament winding process for the resin system containing 1.0 wt% nanosilica. However, the viscosities of the resin system at 50 °C for longer times became similar or higher than those of the resin system at 30 and 40 °C, suggesting that the winding process should be completed around 1 hour.

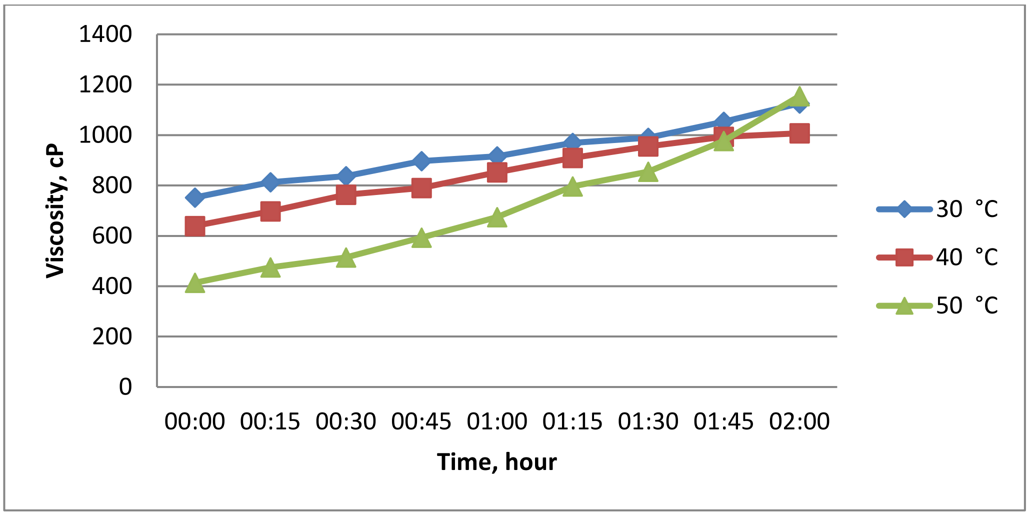

**Figure 3.3** Viscosities of the epoxy resin system with 1.0 wt% nanosilica loading as a function of time at 30 °C, 40 °C and 50 °C.

Finally, the viscosities of the epoxy resin system with 2.0 wt% nanosilica loading as a function of time at 30 °C, 40 °C and 50 °C are shown in Figure 3.4. The dispersion process was applied according to the parameters given in Table 2.6. The initial viscosity values of the resin system at 30 °C is very high for filament winding processes when compared with the viscosity values for the resin systems at 40 °C and 50 °C. After 75 minutes, it was not possible to make measurement due to gel like behavior of mixtures for all temperatures. For 2.0 wt% nanosilica loading rate, the most applicable viscosity was obtained at 30 °C. However, the viscosity at 30 °C caused gelation problem after 30 minutes due to high viscosity observed as shown in Figure 3.4.

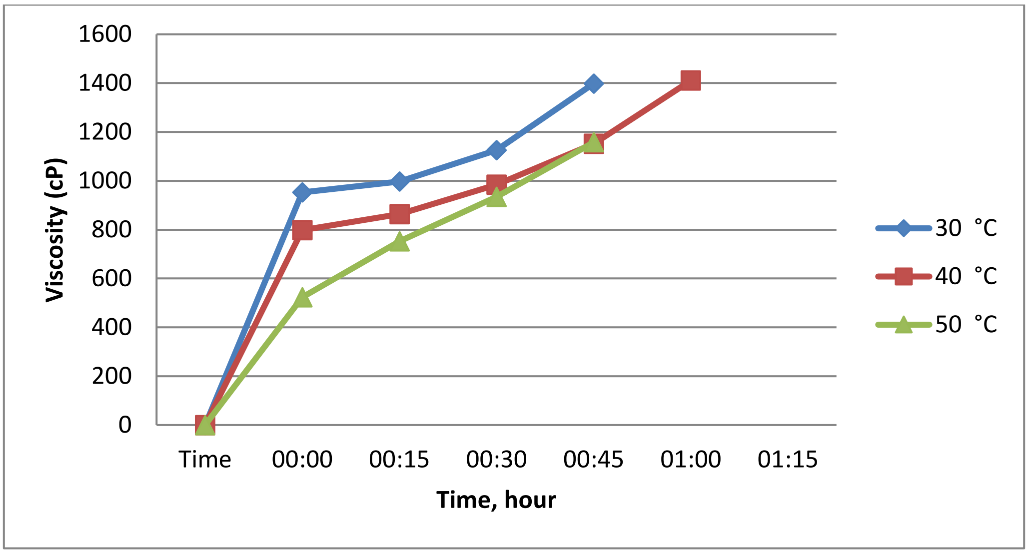

**Figure 3.4** Viscosities of the epoxy-nanosilica resin with 2.0 wt% silica loading results at 30 °C, 40 °C and 50 °C as a function of time.

To sum up, with the addition of nanosilica particles to the epoxy resin system, the viscosities of the epoxy resin containing nanosilicas increased comparing to that of the neat epoxy. With the increasing in temperature, the viscosities of the epoxy resins decreased initially, however, they increased considerably at longer times due to acceleration of cross linking of the resins at higher temperatures. High viscosities (> 1000 cP) for the resin systems are not preferred for the filament winding process. In literature, Sprenger *et al.* [35] commented that filler addition to epoxy resin systems have a negative impact on the viscosity of the resin, which prevents their use in some applications. Hackett *et al.* [36] stated that resin must flow during curing process of nanoparticle filled composites to allow air to be removed from the laminate and to fully wet out all of the fibers. As a consequently, for this thesis, the resin bath temperature of 40 °C was seemed the most suitable temperature for controlling viscosity of nanosilica filled resin system during fiber reinforced composite manufacturing in filament winding process.

### 3.1.2. DSC Tests

DSC analyses were conducted to investigate the thermal behaviour of all cured epoxy and nanosilica filled epoxy specimens. These analyses were performed in order to determine the glass transition temperatures ($T_g$) of specimens. In this study, dispersion of nanosilica particles were done with ultrasonic processor. In addition to this, for understanding effeciency of ultrasonication, also manuel mixing for 5 minutes was applied for preparing nanocomposites with 1.0 wt% nanosilica. The calculation of $T_g$ values from DSC thermograms are represented in Table 3.1 and typical DSC thermograms was given in Figure 3.5 and thermograms of all batches are given in Appendix-A.

**Table 3.1** Calculated $T_g$ values from DSC thermograms.

| n-Silica Loading Rate at Epoxy (wt%) | Mixing Method | $T_g$ °C |
|---|---|---|
| **Reference** | | 110.23 |
| **0.5 wt%** | Ultrasonication | 118.67 |
| **1.0 wt%** | Ultrasonication | 122.8 |
| **2.0 wt%** | Ultrasonication | 123.63 |
| **1.0 wt%** | Manuel Mixing | 119.08 |

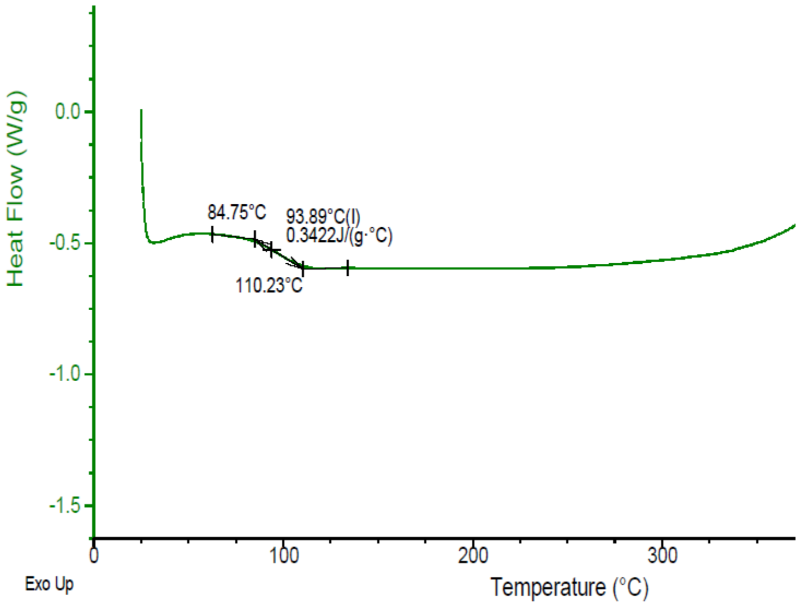

**Figure 3.5** DSC thermogram of the cured neat epoxy.

As can be seen from Table 3.1, the glass transition temperatures of the epoxy resin system increased when nanosilica particles were added to the epoxy resin. As the particle size of nanoparticles decreases, the interfacial area between the nanoparticle and the polymer matrix increases dramatically. It is possible that increasing the interfacial area can influence the polymer chain mobility and, therefore, change the $T_g$ of the epoxy nanosilica composites.

### 3.1.3. Tensile Tests

Tensile tests were conducted to investigate the tensile properties (tensile strength and modulus) of cured epoxy and nanosilica filled epoxy specimens. Tensile test strength and modulus averages, standard deviations, coefficient of variation (COV) values were given in Table 3.2 and Table 3.3. Percent change of nanosilica filled epoxy coupons with comparing neat epoxy tensile strength and modulus values are given in these tables.

**Table 3.2** Tensile strength values of the neat epoxy and the nanosilica filled epoxy samples without carbon fiber reinforcement.

| Tensile Strength, MPa | | | | | |
|---|---|---|---|---|---|
| **Batch Name** | **Reference** | **0.5 wt%** | **1.0 wt%** | **2.0 wt%** | **1.0 wt% manuel mixed** |
| **Average** | 65.98 | 74.96 | 63.98 | 59.66 | 50.3 |
| **Standard Dev.** | 3.45 | 2.87 | 4.44 | 2.15 | 10.44 |
| **COV, %** | 5.22 | 3.83 | 6.93 | 3.61 | 20.76 |
| **Change, %** | | **13.61** | **-3.03** | **-9.58** | **-23.76** |

**Table 3.3** Tensile modulus values of the neat epoxy and the nanosilica filled epoxy samples without carbon reinforcement.

| Tensile Modulus, GPa | | | | | |
|---|---|---|---|---|---|
| **Batch Name** | **Reference** | **0.5 wt%** | **1.0 wt%** | **2.0 wt%** | **1.0 wt% manuel mixed** |
| **Average** | 3.09 | 3.06 | 3.11 | 3.16 | 3.06 |
| **Standard Dev.** | 0.10 | 0.15 | 0.08 | 0.08 | 0.17 |
| **COV, %** | 3.20 | 5.02 | 2.59 | 2.66 | 5.61 |
| **Change, %** | | **-0.93** | **0.78** | **2.33** | **-1. 04** |

When the epoxy resin was filled wth 0.5 wt%, the tensile strength of the nanosilica filled epoxy samples was increased about 13.61%. For the other samples, reduction in the tensile strength values were observed. The modulus values were remained unchanged. For strain measurements, a video extensometer was used. Failure modes of the test coupons are given in Figure 3.6. At tensile tests, failures on the gauge section was evaluated as an acceptable test, and most of failures were occurred at the gauge section of test coupons. It was observed that if the test coupon had bubbles on the surface, the failures took place at the bubble zones of the coupons. Tensile test results were depended on the quality of test coupons, therefore, the samples should be nearly defect free. Chen *et al.* [38] was studied the influences of nanosilica particle with a size of 12 nm on the properties of epoxy resins. The added 1.25, 5, 10, and 20 wt% nanosilica and disperse them using an ultrasonic processer. The tensile modulus and strength of their samples showed a monotonic increase up to 20 wt% and 10 wt%, respectively. The author commented that the brittle behaviour of nanosilica particles decreased tensile strength at higher loadings and similar behaviour was observed in this thesis studies.

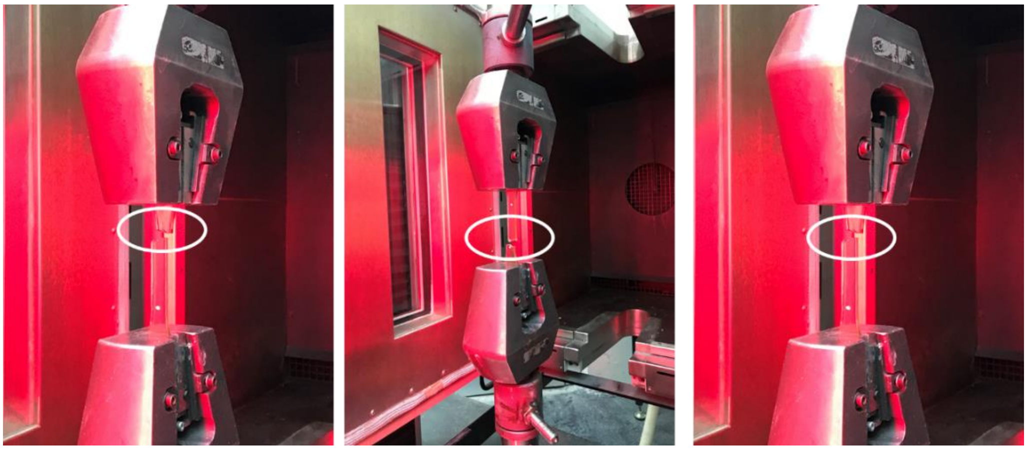

**Figure 3.6** Failure of tensile test coupons during tension tests.

### 3.1.4. Fracture Surface Analyses of Tensile Test Coupons by SEM

The fracture surfaces of the tensile test coupons were prepared for SEM analyses. The SEM pictures for the fracture surfaces of the neat, 1.0 wt% and 2.0 wt% nanosilica filled epoxy batches are shown in Figure 3.7, Figure 3.8, and Figure 3.9. and these pictures were compared to understand influences of nanosilica particles on the damage mechanisms of the epoxy. EDX (Energy Dispersive X-Ray) analyses were done for elemental characterization of the samples.

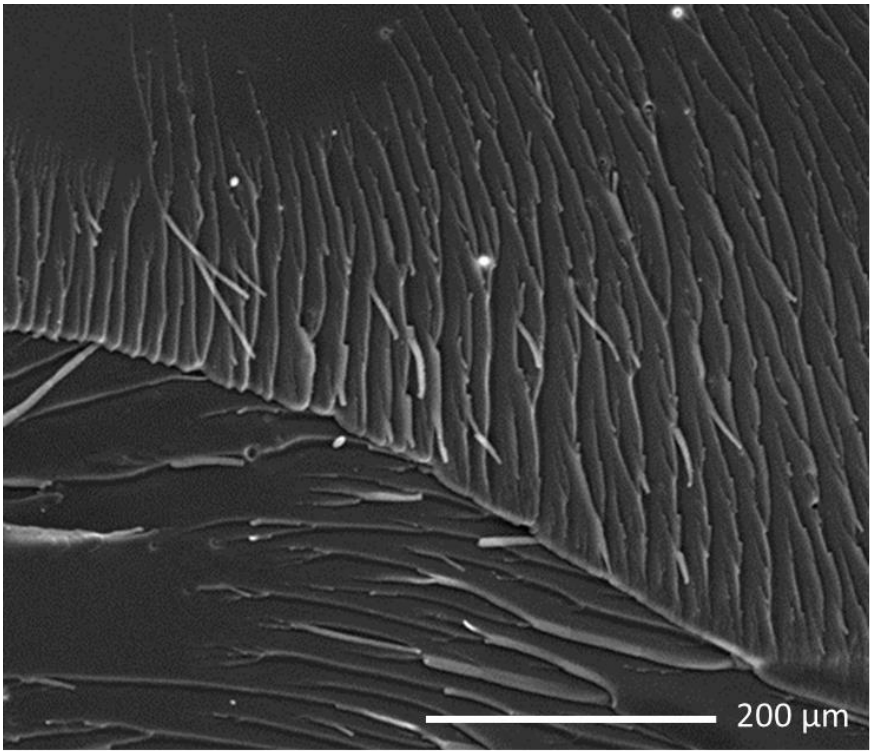

**Figure 3.7** SEM picture for the fracture surface of the neat epoxy tensile test coupon.

As seen in Figure 3.7, the facture surface of the neat epoxy tensile test coupons show a stepped and brittle surface behaviour.

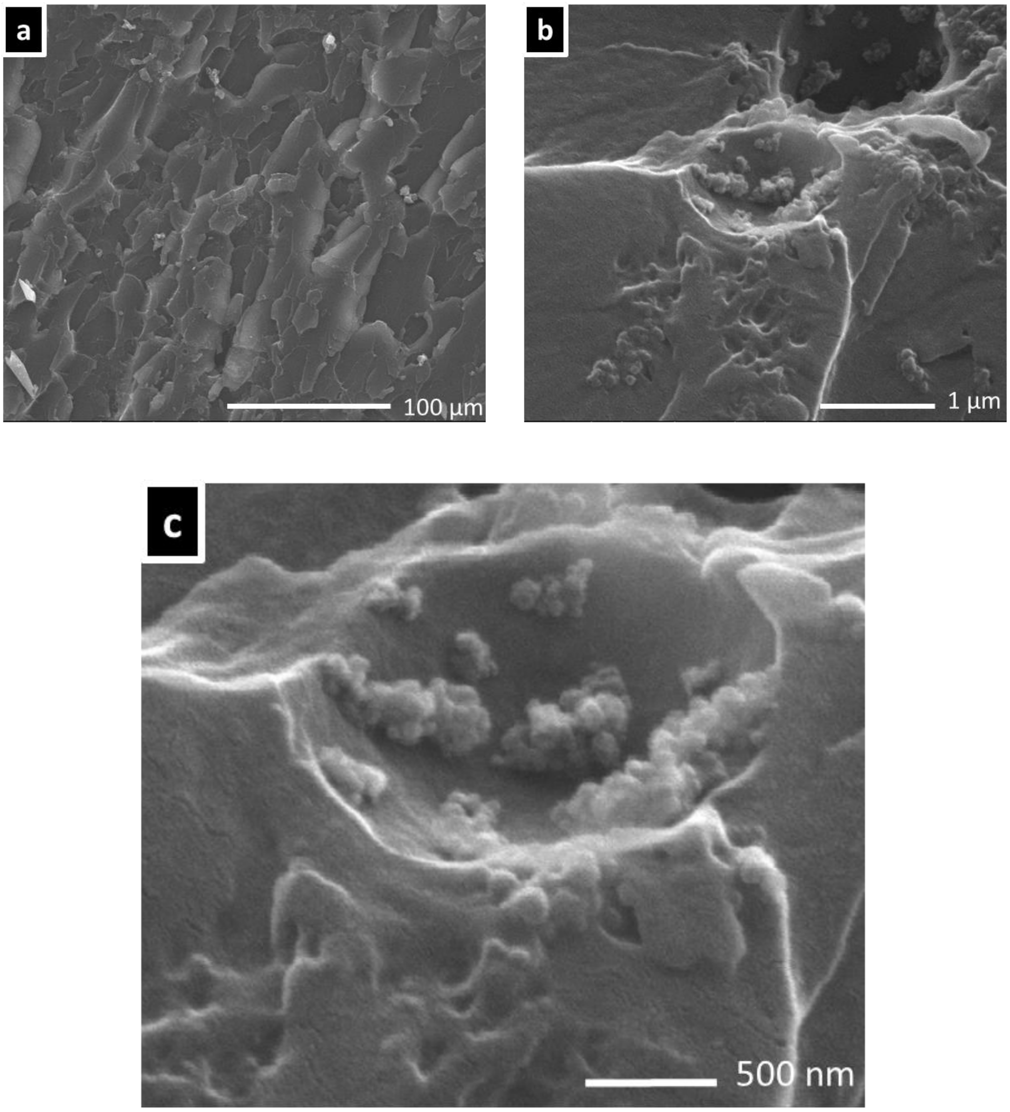

**Figure 3.8** SEM pictures for the fracture surfaces of 1.0 wt% nanosilica filled epoxy tensile test coupon a) 1000x b) 100000x c) 200000x magnifications.

As can be seen in Figure 3.8, the SEM fracture surface of 1.0 wt% nanosilica filled epoxy tensile test coupon has the appearance of a fish surface (large fish scale). At higher magnifications, it is seen that there are circular voids on the fracture surfaces. It is observed that some of the nanosilica agglomerates fill these voids (cavities).

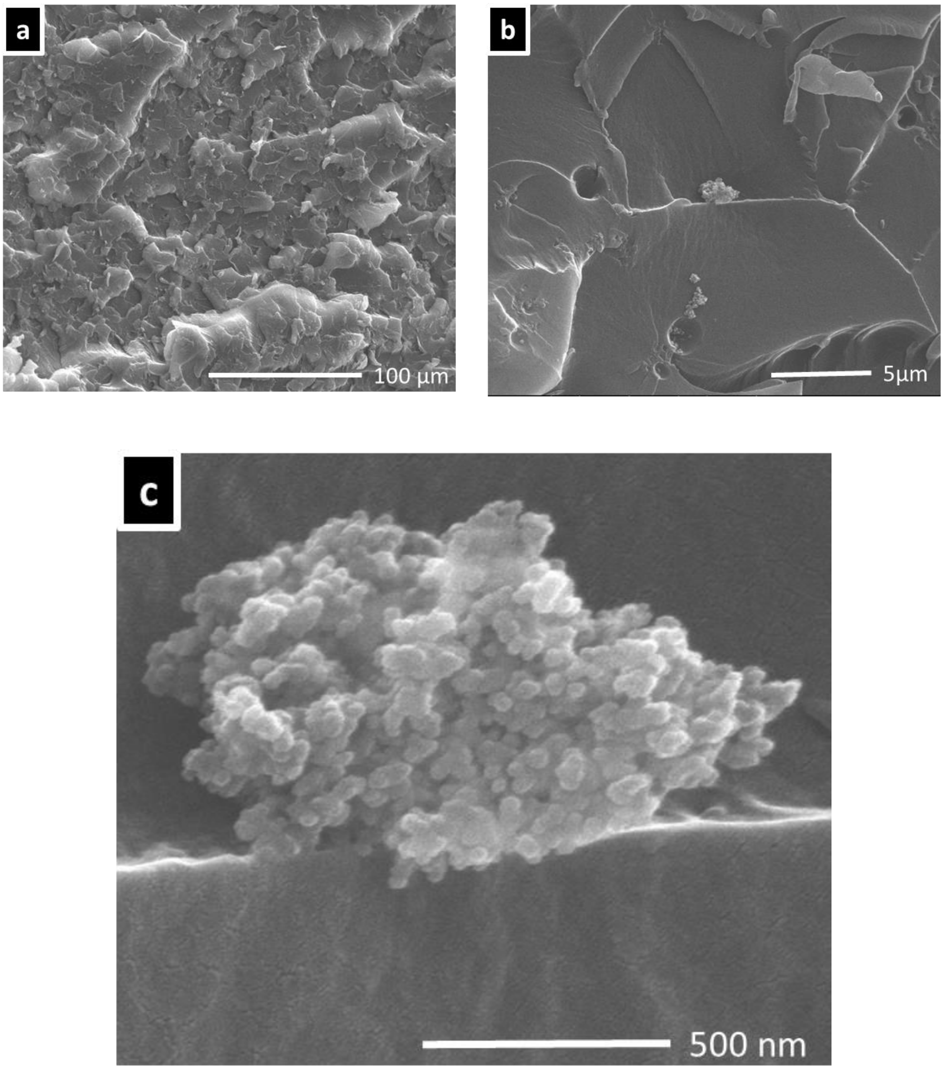

**Figure 3.9** SEM fracture surface analyses of 2.0 wt% nanosilica filled epoxy tensile test coupon a) 1000x b) 100000x c) 200000 x magnifications.

The size of fish scales in the fracture surface of the 2.0 wt% nanosilica filled epoxy (Figure 3.9-a) became smaller, but the number of fish scales increased compared with the fish scales observed in 1.0 wt% nanosilica filled epoxy fracture surface (Figure 3.8-a). Large nanosilica agglomerates are observed in the microstructure of 2.0 wt% nanosilica filled epoxy.

When 2.0 wt% nanosilica filled epoxy fracture surface is examined in detail as shown in Figure 3.10, it is observed that there are many voids in the structure as shown by red circles in Figure 3.10-a. The EDX analysis of the rectangular region on the fracture surface proved to be silica, as shown in Figure 3.10-b.

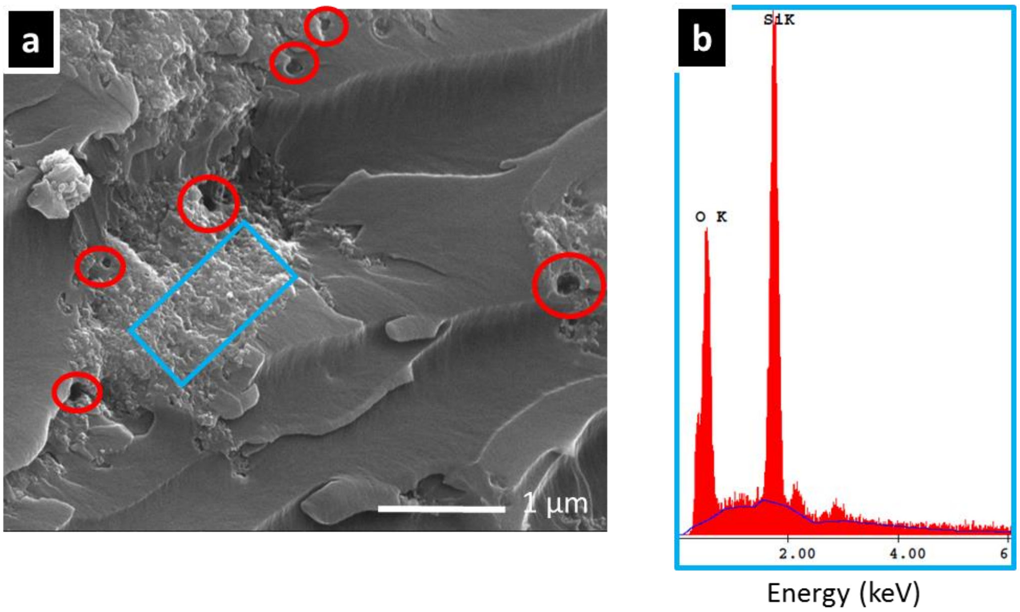

**Figure 3.10** SEM fracture surface image of 2.0 wt% nanosilica filled epoxy tensile test coupon a) void formation areas b) EDX analysis of the blue coloured region in the picture a.

Zamanian *et al.* [39] studied fracture toughness properties of epoxy resins containing nanosilica particles with average sizes of 12 nm, 20 nm and 40 nm. They conduct SEM analyses to elucidate debonding and any subsequent plastic void growth in the polymer. The authors comment that the nanoparticles were well dispersed in the epoxy matrix, but there were the presence of small agglomerates ranging between 20 and 100 nm and it was stated that the shear forces, applied during the mixing and dispersion processes, were not efficient enough to break the agglomerates.

In SEM images, the author stated that the surfaces of the neat epoxy had glassy and smooth appearance and the addition of nanosilicas to cross-linked polymers can lead to various mechanisms such as crack path deflection, crack pinning, plastic deformation and plastic void growth. The plastic void growth of the epoxy matrix, initiated by debonding of the nanoparticles. Matrix–particle debonding is essential in the matrix plastic void growth mechanism, which is a significant part of the matrix plastic deformation in nanosililica filled epoxy materials. The plastic void growth was observed in the samples produced in this study (see Figure 3.10). The size of the voids observed in this study much bigger due to the existence of larger agglomerates.

Tian *et al.* [40] studied stress transfer mechanism of nanosilica filled epoxy composites. It is explained that nanoparticles can effectively suppress the formation and propagation of micro-cracks in the matrix. As mentioned before, voids appear between nanosilica and matrix and resulting in larger surface area which consumes substantial deformation energy with the help of toughening effect of nanosilica. Finally, nanosilica can act as interlocking pins within the inter-phase and create a higher friction between fiber and matrix which is good for fracture toughness properties. In this thesis, the similar interlocking behaviour of nanosilica particles was observed at fracture toughness tests of carbon fiber reinforced nanocomposites which was explained in Heading 3.2.

## 3.2. Effects of Nanosilica on Carbon Fiber Reinforced Epoxy Composites

### 3.2.1. Density, Fiber Weight Ratio and Void Content Tests

To conduct characterization tests for the carbon fiber reinforced epoxy composites, four specimens from each seven different manufacturing batches were prepared. Density, fiber content by wt% and vol%, theoretical density and void content results for the nanosilica added carbon fiber reinforced epoxy composites were given in Table 3.4.

**Table 3.4** Physical characterization test results.

| **Fiber Reinforced Nanocomposite Batch Name** | **Density, g/cm$^3$** | **Reinforcement Amount , weight %** | **Theoretical Density, g/cm$^3$** | **Void Content, Volume %** |
|---|---|---|---|---|
| **Reference** | 1.482 | 64.70 | 1.50 | 0.94 |
| **0.5 wt% Nanosilica, 1st Batch** | 1.474 | 63.70 | 1.49 | 1.02 |
| **0.5 wt% Nanosilica, 2nd Batch** | 1.467 | 63.40 | 1.49 | 1.35 |
| **1.0 wt% Nanosilica** | 1.457 | 64.50 | 1.49 | 2.52 |
| **2.0 wt% Nanosilica, 1st Batch** | 1.449 | 61.50 | 1.47 | 1.71 |
| **2.0 wt% Nanosilica, 2nd Batch** | 1.445 | 60.50 | 1.47 | 1.53 |
| **1.0 wt% Nanosilica Manuel Mixed** | 1.454 | 62.40 | 1.48 | 1.77 |

As can be seen in Table 3.4, small variations in the density and fiber content values were observed for the specimens, which can be acceptable for the filament winding process due to the nature of process. The reason of the observed small differences may be due to different resin wetting and flow behaviour of nanosilicas in the epoxy resin. Furthermore, since the filament winding process is not totally an automatic process and there are some operator dependent processing step variations which may be another reason for the physical property differences. As the nanosilica content was increased in the epoxy resin, the void content of the fiber reinforced epoxy composite increased because the flowability of the resin was reduced with the addition of nanosilicas.

### 3.2.2. Tensile Tests

Tensile test results for unidirectional carbon fiber reinforced neat and nanosilica filled epoxy test coupons are given in Table 3.5 and 3.6. At least five specimen were tested and their averages, standard deviations and coefficient of variations (COV) values were given. The pictures of the unidirectional carbon fiber reinforced epoxy composites before and after the tensile test are shown in Figure 3.11. Failure mode of test coupons could be descirbed as explosive which is defined at ASTM D3039 and it was observed that the same damage mechanism was observed for neat and nanosilica filled epoxy resin used composites as shown at Figure 3.12.

**Table 3.5** Tensile strength values for the neat carbon fiber reinforced epoxy (reference) and the nanosilica added composites.

| Tensile Strength, MPa | | | | | |
|---|---|---|---|---|---|
| **Batch Name** | **Reference** | **0.5 wt%, 1st Batch** | **1.0 wt%** | **2.0 wt%, 1st Batch** | **1.0 wt% manuel mixed** |
| **Average** | 1279.96 | 1306.25 | 1258.35 | 1176.74 | 1185.93 |
| **Standard Dev.** | 66.77 | 54.47 | 70.05 | 122.39 | 212.41 |
| **COV, %** | 5.22 | 4.17 | 5.57 | 10.40 | 17.91 |
| **Change, %** | | **2.05** | **-1.69** | **-8.06** | **-7.35** |

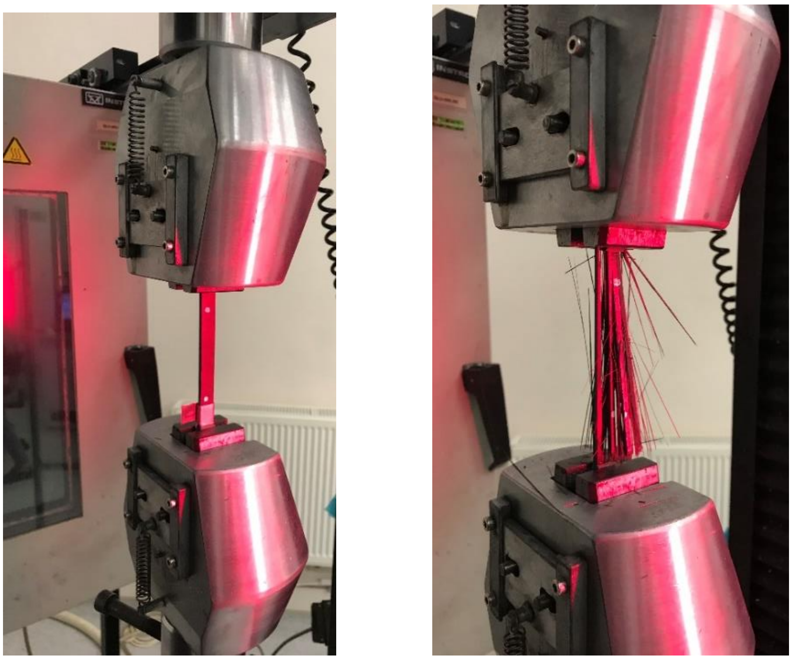

**Figure 3.11** Pictures of the test coupons before (left) and after (right) the tensile test for 0.5 wt% nanosilica filled carbon fiber reinforced epoxy nanocomposites.

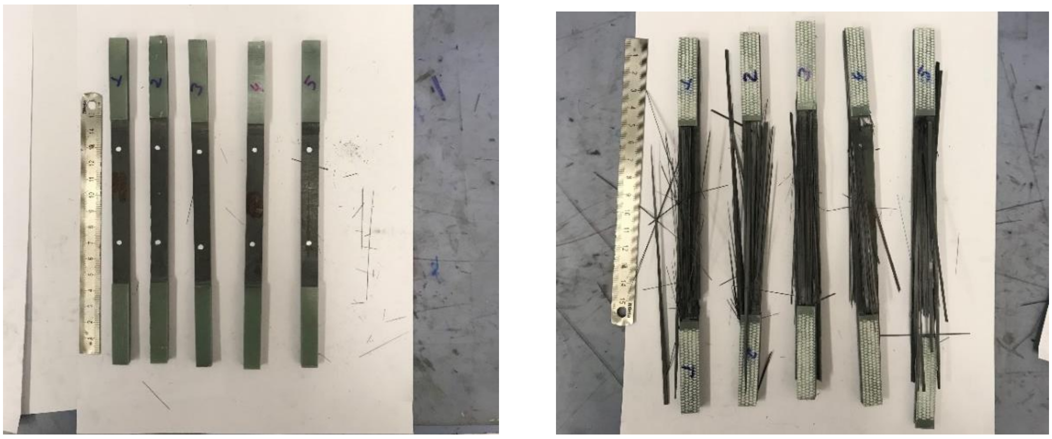

**Figure 3.12** Pictures of the test coupons before (left) and after (right) the tensile test for 1.0 wt% nanosilica filled carbon fiber reinforced epoxy nanocomposites.

When 0.5 wt% nanosilica was added to the carbon fiber reinforced epoxy resin, the tensile strength increased compared to the reference specimen. The tensile strength of the specimens containing 2.0 wt% nanosilica and 1.0 wt% nanosilica (manuel mixed) reduced compared with the reference ones.

**Table 3.6** Tensile modulus values for the neat carbon fiber reinforced epoxy (reference) and the nanosilica added epoxy composites.

| **Tensile Modulus, GPa** | | | | | |
|---|---|---|---|---|---|
| **Batch Name** | **Reference** | **0.5 wt%, 1st Batch** | **1.0 wt%** | **2.0 wt%, 1st Batch** | **1.0 wt% Manuel Mixed** |
| **Average** | 119.92 | 117.62 | 117.38 | 117.71 | 117.34 |
| **Standard Dev.** | 1.52 | 3.09 | 3.68 | 12.05 | 13.42 |
| **COV, %** | 1.27 | 2.62 | 3.14 | 10.24 | 11.43 |
| **Change, %** | | **-1.91** | **-2.11** | **-1.84** | **-2.15** |

No significant change was observed for the tensile modulus values for the carbon reinforced epoxy composites (neat and nanosilica added), suggesting that the addition of nanosilica did not influence the modulus of the carbon fiber reinforced epoxy composites. Uddin *et al.* [39] studied influences of nanosilica particle (20 nm average size) addition on the properties of the glass fiber reinforced epoxy composites prepared using a Vacuum Assisted Resin Transfer Molding (VARTM) process. When 15 wt% nanosilica was added to the glass fiber reinforced epoxy composites, 11% increase on longitudinal tensile strength and almost no change on the modulus values were observed for the glass fiber reinforced epoxy composites.

### 3.2.3. Mode I Interlaminar Fracture Toughness Energy Tests

Mode I interlaminar fracture toughness energy, $G_{IC}$, of the neat carbon fiber reinforced epoxy (reference) and the nanosilica filled composites are given in Table 3.7. At least five specimens were tested. Pictures of mode I interlaminar fracture toughness energy test are shown in Figure 3.13 and Figure 3.14.

**Table 3.7** Mode I interlaminar fracture toughness energy values for the neat carbon fiber reinforced epoxy (reference) and the nanosilica added composites.

| $G_{IC}$,J/m$^2$ | | | | | | |
|---|---|---|---|---|---|---|
| **Batch Name** | **Reference** | **0.5 wt%** | **1.0 wt%** | **2.0 wt%, 1st Batch** | **2.0 wt% 2nd Batch** | **1.0 wt% manuel mixed** |
| **Average** | 339.80 | 434.43 | 604.83 | 711.53 | 727.36 | 387.14 |
| **Standard Dev.** | 19.52 | 56.80 | 21.62 | 32.19 | 25.43 | 125.33 |
| **COV, %** | 5.75 | 13.07 | 3.58 | 4.52 | 3.50 | 32.37 |
| **Change, %** | | **24.52** | **73.37** | **103.95** | **108.49** | **10.97** |

**Figure 3.13** Pictures of mode I fracture toughness energy test coupons before loading (left) and after initiation of crack growth starting from the tip of the pre-crack.

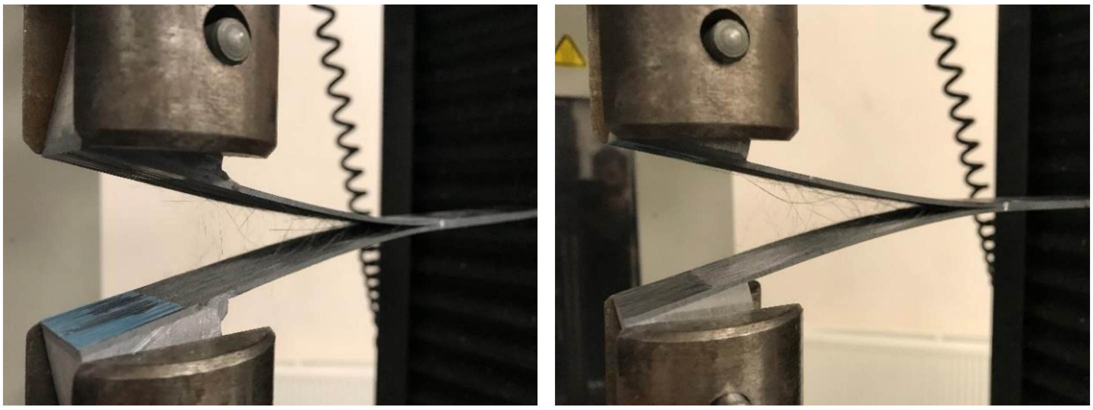

**Figure 3.14** Pictures of mode I fracture toughness energy test coupon just before reaching total crack length of about 100 mm.

This test related with the energy necessary for causing crack growth at interlaminar region (starting from the precrack region) of the fiber reinforced composites. Addition of nanosilica to the epoxy resin composite increased resistance to crack propagation, as a result, mode I fracture toughness energy values of the epoxy composites increased. With the increasing of nanosilica content, $G_{IC}$ values of the epoxy composites also increased. The highest $G_{IC}$ values were obtained for 2.0 wt% nanosilica added epoxy composites. To test reproducibility of the results, another batch of epoxy composite, containing 2.0 wt% nanosilica, was produced and tested. As can be seen in Table 3.7, the $G_{IC}$ values of 2.0 wt% nanosilica batches were similar, suggesting that the $G_{IC}$ measurements were reproducible. The lowest increment was obtained for the samples prepared by manuel mixing due to the fact that uniform distribution of nanosilicas within the epoxy matrix was not possible by the manuel mixing method. This observation was also supported by the high COV values of the manuel mixed batch. During the measurements, fiber fuzzes were appeared at the midplane of the test coupons as shown in Figure 3.16 due to the bonding of fibers between layers.

Tang *et al.* [41] studied mode I fracture toughness properties of carbon fiber reinforced epoxy containing 10.0 wt% and 20.0 wt% nanosilica. The Vacuum Assisted Resin Infusion Moulding (VARIM) process was used to prepare composite specimens and ASTM D5528-1 standard method was used for the mode I fracture toughness tests. In their study, about 92% and 179% improvements were achieved on the mode I fracture toughness energy values for those epoxy composites when 10.0 wt% and 20.0 wt% nanosilica added to the epoxy matrix, respectively. They stated that the strength of matrix-fiber interfacial bonding dominate the mode I interlaminar fracture behaviour. The fracture surfaces of the nanosilica added epoxy test coupons were rougher than those of the neat epoxy test coupons, suggesting that the fiber-matrix interface improved with the addition of nanosilica. In this study, the nanosilica content more than 2.0 wt% was not possible because the viscosities of the epoxy resin mixtures increased to high values which was not suitable for the filament winding process.

### 3.2.4. Mode II Interlaminar Fracture Toughness Energy Tests

Mode II interlaminar fracture toughness energy values, $G_{IIC}$, of the neat carbon fiber reinforced epoxy (reference) and the nanosilica added epoxy composites were given in Table 3.8. Mode II interlaminar fracture toughness energy values were calculated from the load against the cross head displacement curves. The picture of the fixture used for the measurements is shown in Figure 3.15. At least 5 specimens were tested.

**Table 3.8** Mode II interlaminar fracture toughness energy values of the neat carbon fiber reinforced epoxy (reference) and the nanosilica added epoxy composites.

| $G_{IIC}$, J/m$^2$ | | | | | | |
|---|---|---|---|---|---|---|
| **Batch Name** | **Reference** | **0.5 wt% 1st Batch** | **0.5 wt% 2nd Batch** | **1.0 wt%** | **2.0 wt%** | **1.0 wt% Manuel Mixed** |
| **Average** | 613.14 | 739.62 | 746.70 | 659.74 | 499.17 | 346.80 |
| **Standard Dev.** | 67.81 | 38.30 | 32.84 | 14.48 | 49.99 | 105.25 |
| **COV, %** | 11.06 | 5.18 | 4.40 | 2.19 | 10.01 | 30.35 |
| **Change, %** | | **20.63** | **21.78** | **7.60** | **-18.59** | **-43.44** |

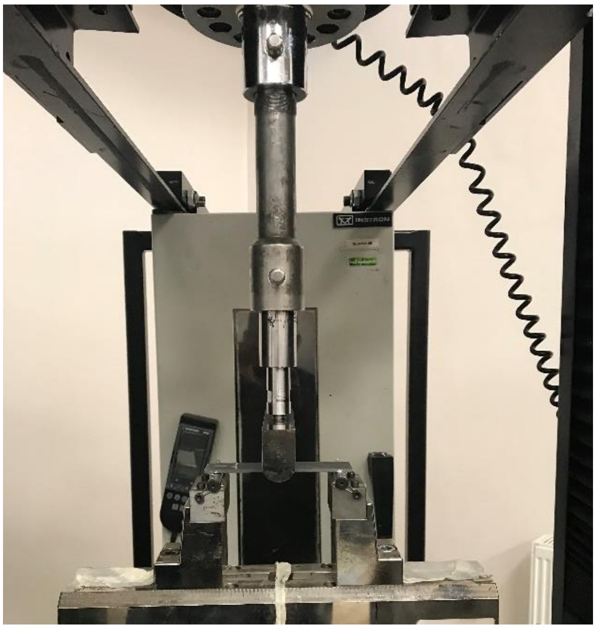

**Figure 3.15** Test fixture for mode II interlaminar fracture toughness energy measurements.

**Figure 3.16** Crack propagation from mid-plane and cross section appearance of mode II interlaminar fracture toughness energy test coupons during test.

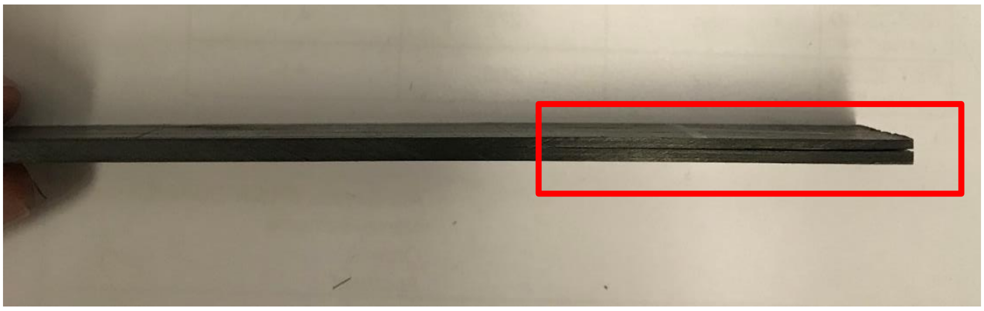

**Figure 3.17** Crack created at the end of mode II interlaminar fracture toughness energy test.

In the mode II inter-laminar fracture toughness energy test, shear forces were created at the crack tip of the pre-cracked test coupons when the samples were subjected to a flexural test (3 point bending test). The side appearance of a damaged test coupon is given in Figure 3.16 and Figure 3.17. The $G_{IIC}$ of the fiber reinforced test coupons was increased with the addition of nanosilica. The maximum increment was obtained when 0.5 wt% nanosilica was added. In order to test reproducibility of this batch, a new batch of 0.5 wt% nanosilica added fiber reinforced test coupons was produced and subsequently they were tested. As seen in Table 3.8, the $G_{IIC}$ values of the two batches were similar, suggesting that the dispersion and filament winding processes for the 0.5 wt% nanosilica added fiber reinforced test coupons were reproducible. With the increasing of nanosilica addition, the $G_{IIC}$ values decreased. The lowest GIIC values and highest COV values were obtained for the manuel mixed test coupons containing 1.0 wt% nanosilica. The similar behaviour was also observed for the mode I fracture toughness energy tests. It can be commented that nonuniform distribution of nanosilica particles in the fiber reinforced epoxy resins prepared using the manuel mixing method caused drop in both the mode I and mode II interlaminar fracture toughness energy test values with high COV values.

Tang *et al.* [41] studied the mode II interlaminar fracture toughness energy properties of carbon fiber reinforced epoxy with 10 wt% and 20 wt% loading rates of nanosilica. In their study, they observed decrease with the increasing loading rate of nanosilica in carbon fiber reinforced composites. The fracture surfaces of nanosilica were analyzed using a SEM and they stated that the zipper like pattern, which was observed in the neat epoxy resin, was not observed or amount of those patterns was reduced. They commented that even though the tensile strength of the nanosilica added epoxy resins increased, the mode II fracture toughness energy values decreased, suggesting that the actual failure mechanism for the test coupons was by means of shearing.

### 3.2.5. DMA Tests

The glass transition temperatures ($T_g$) of the carbon fiber reinforced resin composites (the neat and nanosilica added) are given in Table 3.9. The $T_g$ values were calculated from the onset of storage modulus and the maximum of tangent delta curves of the DMA thermograms. Since ASTM D7028 standard states that the glass transition temperature must be determined using the storage modulus extrapolation analysis, the influence of nanosilica addition on the $T_g$ in terms of the percent change, was determined based on the onset value of storage modulus (E’). A typical DMA thermogram is given in Figure 3.18 and the DMA thermograms of all batches are given in Appendix-B.

**Table 3.9** The glass transition temperatures of the epoxy composites determined from the DMA thermograms.

| **Batch Name** | **$T_g$ at Storage Modulus, °C** | **$T_g$ at Tan delta, °C** | **Change at Storage Modulus, %** |
|---|---|---|---|
| **Reference** | 107.74 | 122.52 | |
| **0.5 wt%** | 107.24 | 124.66 | -0.47 |
| **1.0 wt%** | 105.58 | 120.33 | -1.57 |
| **2.0 wt%** | 110.16 | 124.66 | 4.16 |
| **1.0 wt% manuel mixed** | 115.6 | 129 | 4.71 |

As can be seen in Table 3.9, no significant changes on the $T_g$ values for the epoxy composites were observed which may be due to no change in phsyical and chemical structure of neat epoxy resin system with addition of nanosilica.

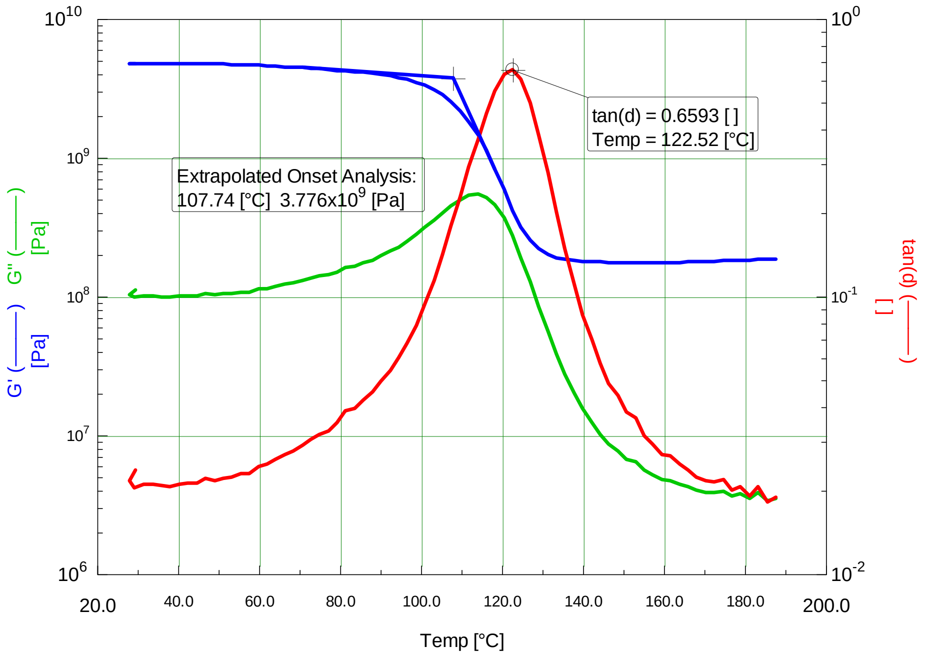

**Figure 3.18** Typical DMA thermogram of neat epoxy with carbon fiber reinforcement.

### 3.2.6. Fracture Surface Analyses of Fiber Reinforced Nanosilica Filled Composites by SEM

#### 3.2.6.1. SEM Analyses of Unidirectional Tensile Test Coupons

The fracture surfaces of the tensile test coupons were prepared for SEM analyses. The neat and 0.5 wt% nanosilica filled carbon fiber reinforced epoxy test coupons fracture surfaces are shown in Figure 3.19 and Figure 3.20.

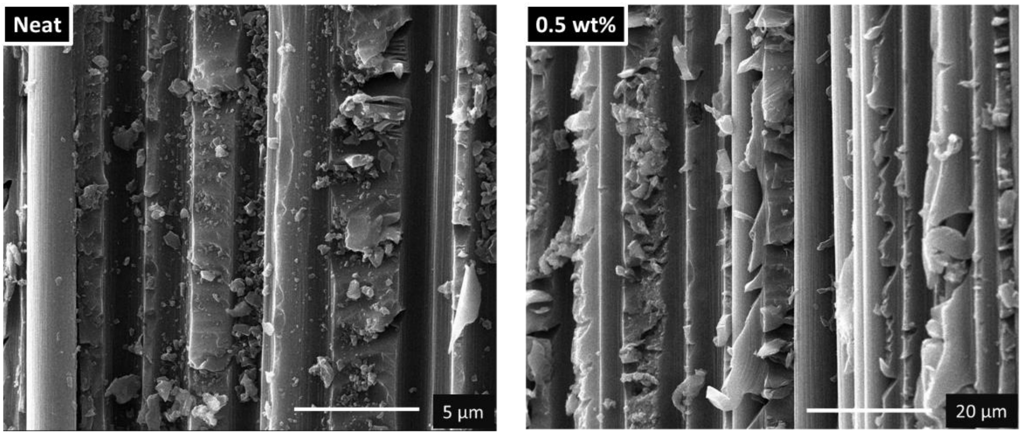

**Figure 3.19** The SEM images of the fracture surfaces of the neat (left) and 0.5 wt% nanosilica filled (right) carbon fiber reinforced epoxy test coupons at 5000X.

The fracture behaviour of the neat and nanosilica filled epoxy resin matrices was different from each. There are many small particles of the epoxy matrix on the fracture surface of the neat carbon fiber reinforced epoxy test coupon due to brittle nature of fracture. The fracture surface of 0.5 wt% nanosilica filled carbon fiber reinforced epoxy composites showed sharp edged features of the epoxy matrix. Less fiber debonding was observed for the nanosilica added composite. However, the observed microstructural differences for the test coupons did not influence the mechanical properties of these test coupons.

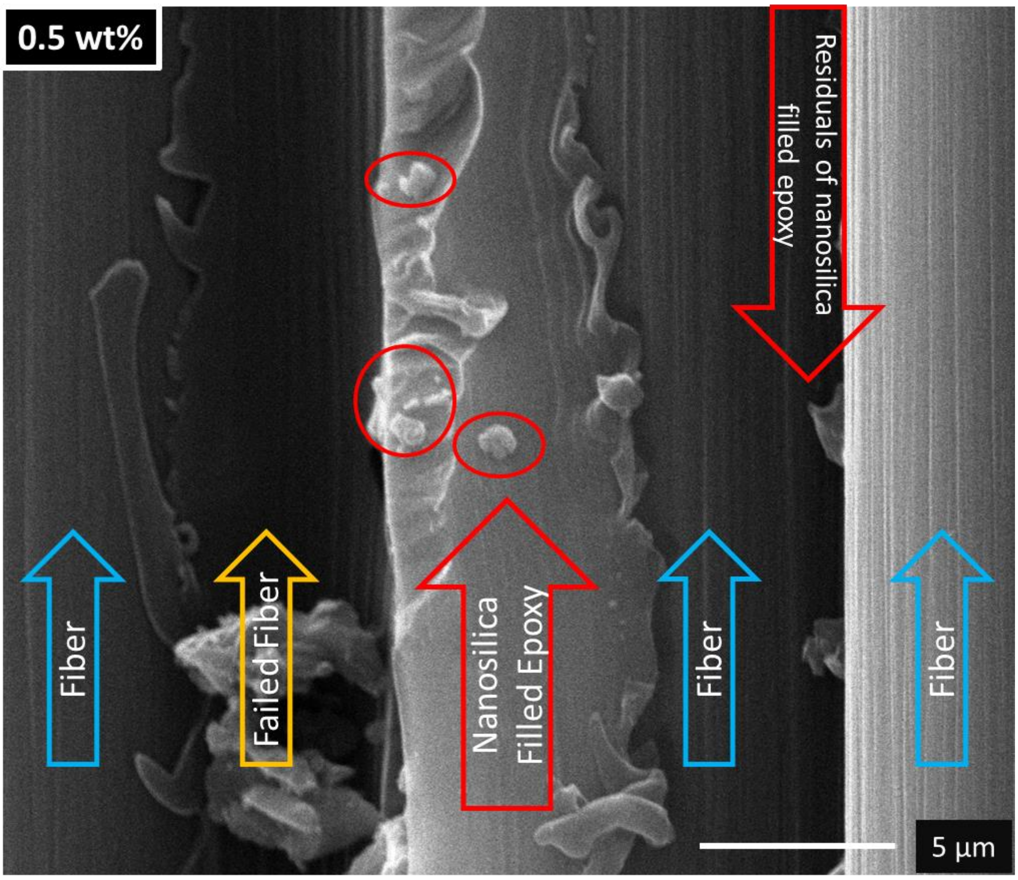

**Figure 3.20** SEM image at 20000x for the fracture surface of 0.5 wt% nanosilica filled carbon fiber reinforced epoxy composite unidirectional tensile test coupons.

SEM image of 0.5 wt% nanosilica filled carbon fiber reinforced epoxy composite at 20000x magnification is given in Figure 3.20. There are some nanosilica agglomerates with an approximate size of 500 nm in the fractured surface of the nanosilica filled epoxy composite as shown with red circles in Figure 3.20. There are some residuals of the epoxy containing nanosilica particles, which is referred to as nanosilica filled epoxy, on the surface of carbon fibers.

SEM image of 1.0 wt% nanosilica filled carbon fiber reinforced epoxy composite unidirectional tensile test coupons is shown in Figure 3.21. No debonding between the nanosilica filled epoxy and carbon fibers was observed. Nanosilica agglomerates were observed on the fracture surface of the nanosilica filled epoxy matrix and shown with the green rectangle. As can be seen from the SEM image that many nanosilica agglomerates were attached to the surfaces of carbon fibers. The EDX analysis of the nanosilica agglomerate indicated with the yellow circle was performed, and results shown in Figure 3.21-b. The silica peak in the EDX, confirm that presence of the nanosilica agglomerates.

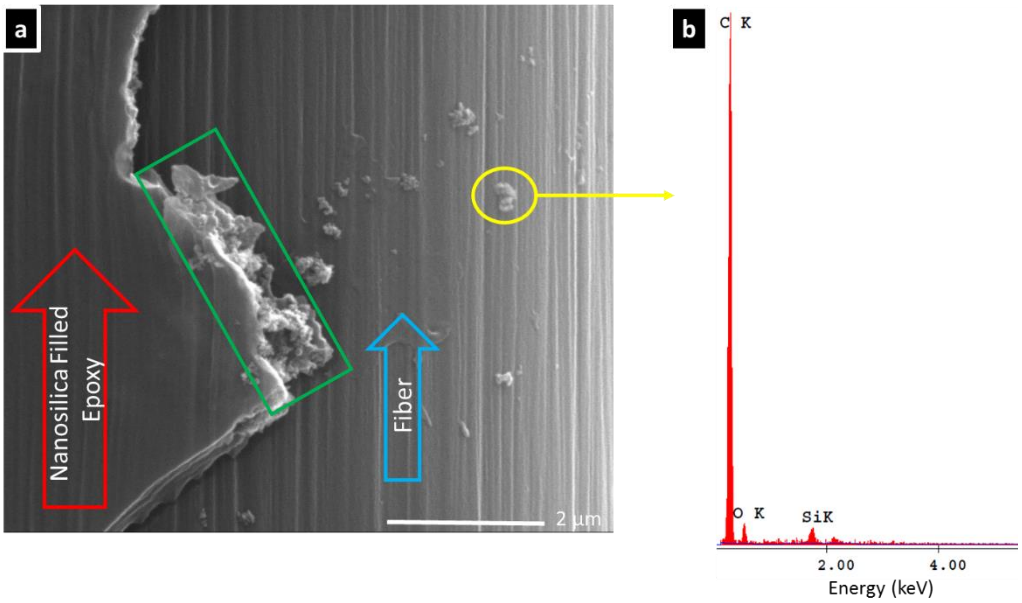

**Figure 3.21** SEM fracture surface analyses of 1.0 wt% nanosilica filled carbon fiber reinforced epoxy composite unidirectional tensile test coupons a) fiber-nanosilica filled epoxy resin interface b) EDX analyses of yellow coloured region at picture a.

Vashisth *et al.* [42] studied the effects of nanosilica addition for the carbon reinforced epoxy composite tubes produced using a filament wounding process. They used commercially available epoxy resin–nanosilica mixture commercially designated as 3M 4833, which consists of mainly bis-F-epoxide and 37.0 wt% surface-functionalized nanosilica particles with an average particle size of 142 nm. The SEM images for the fracture surface of tensile test coupons obtained from the carbon reinforced epoxy composite tubes. They reported that the tensile modulus of the nanosilica reinforced composites increased 37.0% with respect to neat resin used test tubes.

The longitudinal tensile strength of carbon fiber reinforced epoxy composites is expected to be increased when the epoxy resin is filled with nanosilica particles due to the crack arresting property of nanosilica particles. Tensile strength of the fiber reinforced composites containing 0.5 wt% nanosilica particles was increased by 2%. and the tensile strength values of the composites was decreased when the content of nanosilica particles was increased beyond 0.5 wt%. As the longitudinal tensile strength of the composites in fiber direction is highly depend on the properties of fiber, the resin modification should not have strong influence on the tensile properties of the composite.

#### 3.2.6.2. SEM Analyses of Mode I Interlaminar Fracture Toughness Energy Test Coupons

The midplane propagated precrack surfaces of the mode I fracture toughness energy test coupons were prepared for SEM analyses. SEM images for the neat, 0.5 wt%, 1.0 wt%, 2.0 wt% nanosilica and 1.0 wt% manuel mixed nanosilica filled carbon fiber reinforced epoxy composites coupons are shown in Figure 3.22.

0.5 wt% nanosilica added test coupons matrix regions had epoxy resin regions with sharp edged featured, the same features were also observed for the carbon fiber reinforced longitudinal tensile test coupons containing 0.5 wt% nanosilica. The appearance of these features decreased with the increasing of nanosilica content. At 2.0 wt% nanosilica content, the cracks follow tortuous path which was not observed for the neat and other samples containing 0.5 and 1.0 wt% nanosilica. Highest mode I fracture toughness energy values observed for the test coupons containing 2.0 wt% nanosilica may also be due to the tortuous path created with nanosilica addition to the epoxy resin matrix.

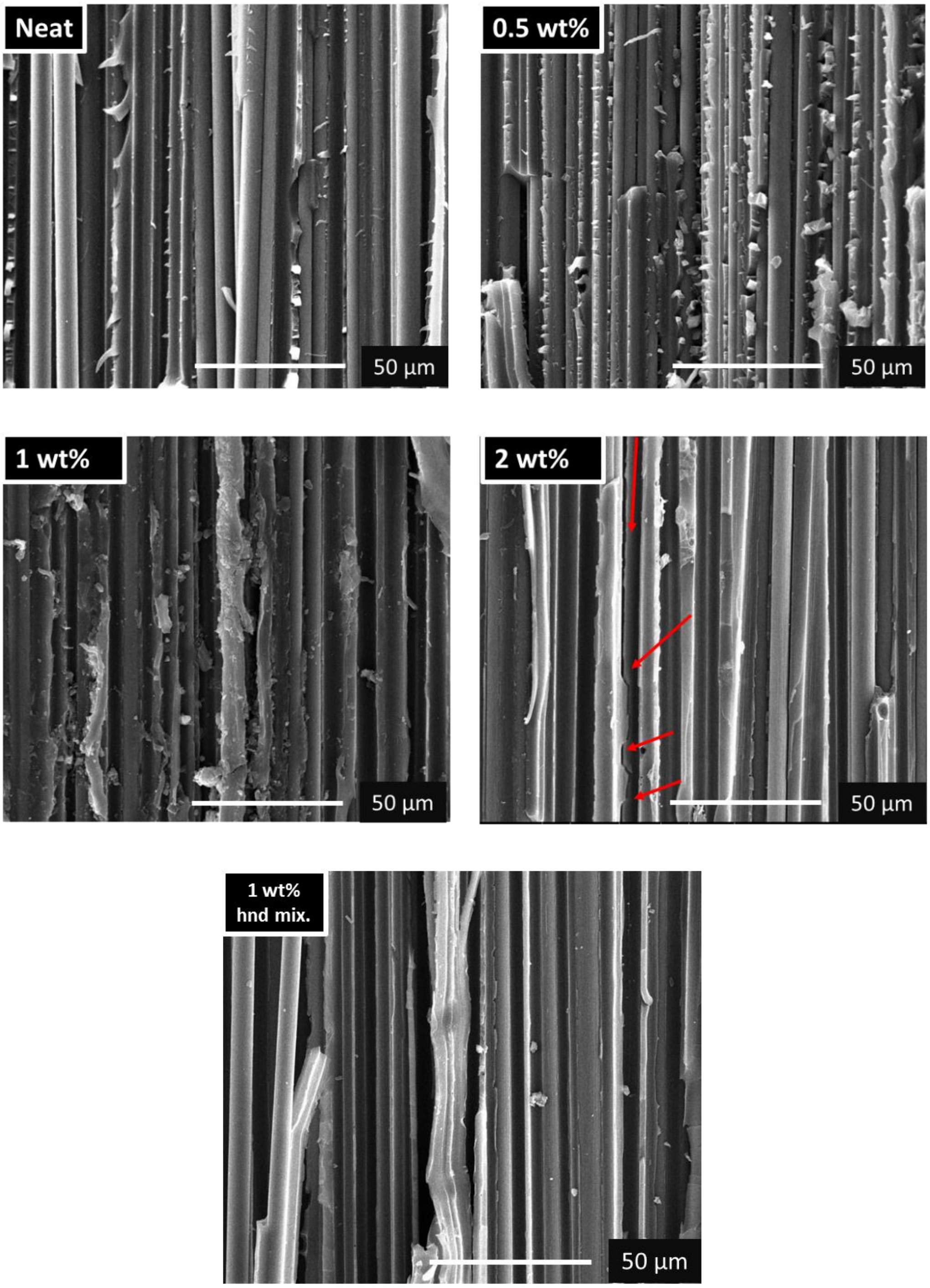

**Figure 3.22** SEM fracture surface analyses of neat, 0.5 wt%, 1.0 wt%, 2.0 wt% and 1.0 wt% manuel mixed nanosilica filled carbon fiber reinforced epoxy composites mode I interlaminar fracture toughness energy test coupons at 2000X magnification.

SEM images of the fracture surfaces of 2.0 wt% nanosilica filled carbon fiber reinforced epoxy composites mode I interlaminar fracture toughness energy test coupons at 20000x magnification are given in Figure 3.23. Nanosilica agglomerates were seen on the fracture surfaces of the test coupons indicated with a red rectangular and circle. These regions may behave as obstacles for crack propagation; as a result, they may increase the toughness energy of the samples.

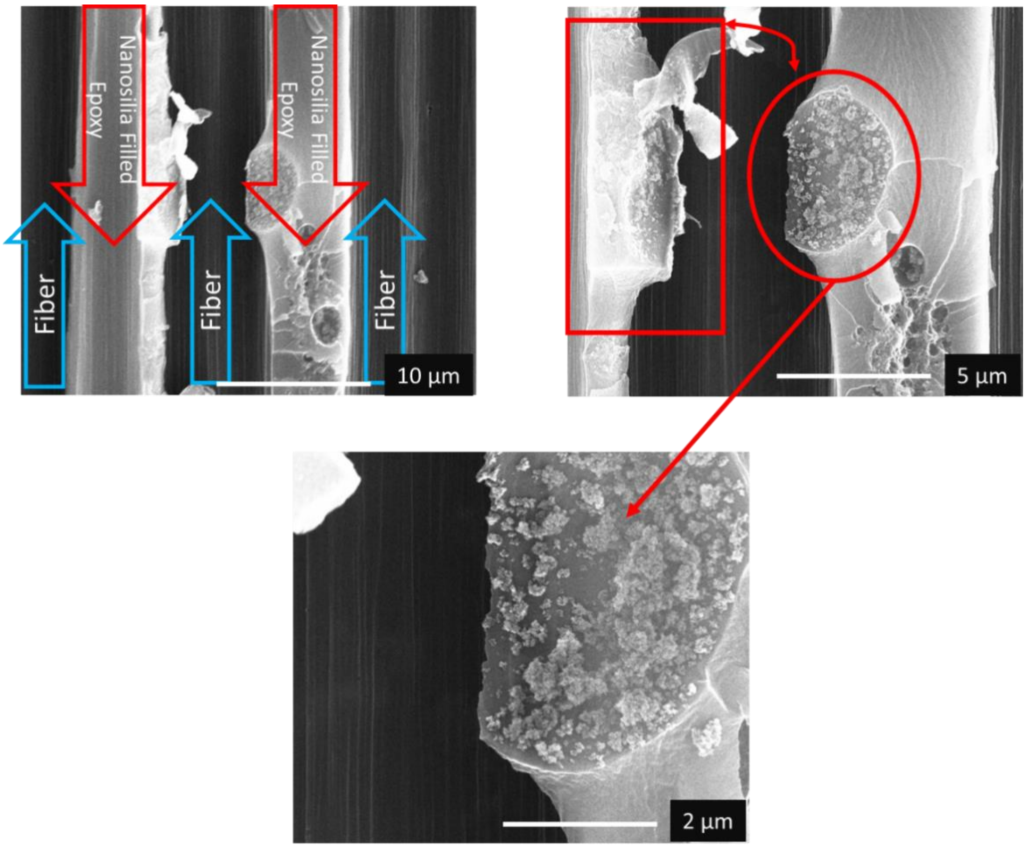

**Figure 3.23** SEM fracture surface analyses of 2.0 wt% nanosilica filled carbon fiber reinforced epoxy composites mode I interlaminar fracture toughness energy test coupons.

Carolan *et al.* [43] studied fracture behaviour of carbon fiber reinforced polymer (CFRP) composites with an epoxy resin cured with anhydride hardener containing silica nanoparticles. Double cantilever beam (mode I fracture toughness) tests were done to test coupons which had been manufactured by vacuum infusion process. Nanosilica particles predispersed in a hardener with a content of 40.0 wt% were purchased from Evonik GMBH. Those predispersed particles were mixed with an epoxy resin, and then the mixture was used in the process. Mode I fracture tests were conducted according to BS-ISO 15024 (2001 test method). The addition of nanosilica did not significantly influence the toughness energy of the nanosilica filled CFRP composites. When the fracture surfaces of mode I interlaminar fracture toughness energy tests coupons were analysed in SEM, it is observed that nanosilica particles were well dispersed within the CFRP and debonding of carbon fiber from the surrounding matrix. The authors also stated that the surfaces of the carbon fibers were very clean, indicating that the level of adhesion between the carbon fibers and the matrix was quite poor.

Similar materials and processes used by Carolan *et al.* [43] were also used by Tang *et al.* [41] study. They prepared CFRP composite samples containing 10.0 and 20.0 wt% nanosilica. SEM images reported by Tang et al. for the mode I interlaminar fracture surfaces of CFRP laminates in the initial region of crack growth. The fracture surface of the neat epoxy matrix looks glossy and exhibits brittle behavior and the surface of nanosilica filled epoxy matrix looks rougher compared to that of the neat matrix. They stated that stronger interfaces between fibres and epoxy matrix were observed when the epoxy matrix filled with nanosilica particles, as a result, the mode I fracture toughness energy of the samples containing nanosilica particles were improved. Different results reported in literature, our results for the mode I fracture toughness energy agrees with those of Tang *et al.* [41].

#### 3.2.6.3. SEM Analyses of Mode II Interlaminar Fracture Toughness Energy Test Coupons

The midplane propagated precrack surfaces of the mode II fracture toughness energy test coupons were prepared for SEM analyses, and SEM images for the neat and nanosilica filled samples (0.5 wt% and 1.0 wt%) are shown in Figure 3.24 and Figure 3.25.

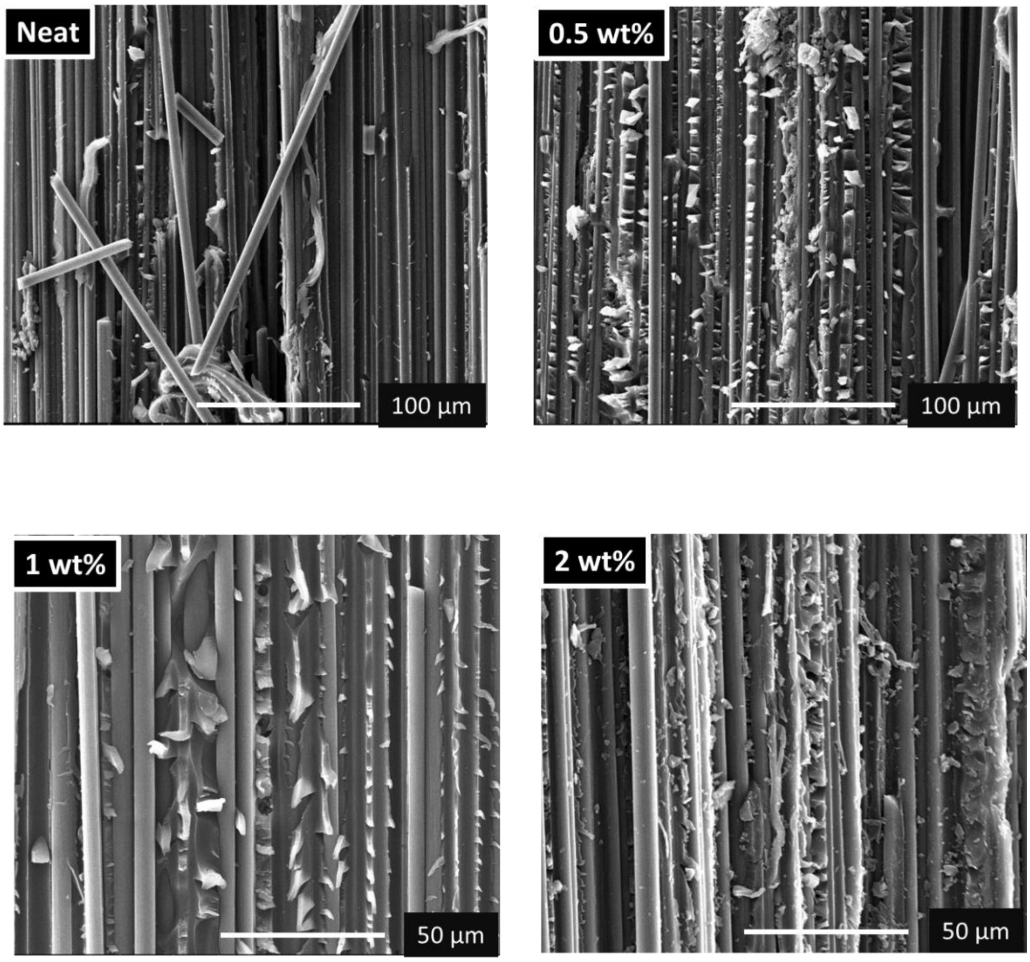

**Figure 3.24** SEM fracture surface analyses of neat (top-left), 0.5 wt% nanosilica filled carbon fiber reinforced epoxy composite (top-right), 1.0 wt% nanosilica filled carbon fiber reinforced epoxy composite (bottom-left), 2.0 wt% nanosilica filled carbon fiber reinforced epoxy composite (bottom-right) mode II interlaminar fracture toughness energy test coupons.

The midplane propagated precrack surfaces of the neat test coupons are different from the nanosilica added test coupons. Many sharp edged epoxy matrix features attached to the surfaces of the fibres were observed for the test coupons containing nanosilica particles. This observation suggest that stronger fiber-epoxy interface achieved when nanosilica added to the epoxy matrix.

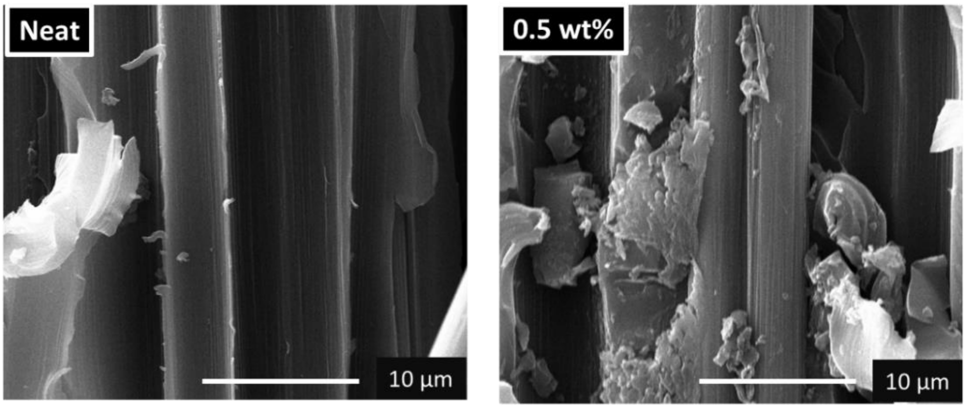

**Figure 3.25** SEM fracture surface analyses of neat (left) and 0.5 wt% nanosilica filled carbon fiber reinforced epoxy composite (right) mode II interlaminar fracture toughness energy test coupons at 10000X.

When the midplane propagated precrack surfaces of the test coupons were examined at 10000x magnification, it can be seen that the epoxy resin and fibers appears to be two discrete phases (features) for the neat test coupons suggesting that weaker fiber – matrix interfaces were obtained for the neat test coupons.

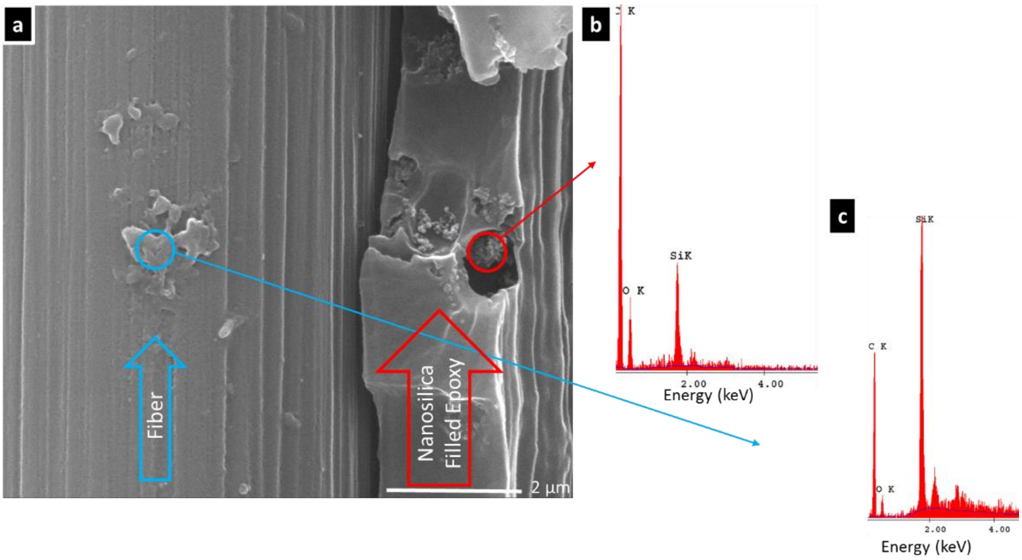

**Figure 3.26** SEM fracture surface analyses of 0.5 wt% nanosilica filled carbon fiber reinforced epoxy composite mode II interlaminar fracture toughness energy test coupons a) fiber-resin interface b) EDX analyses of red coloured region at picture a c) EDX analyses of red coloured region at picture a.

The fracture surface of 0.5 wt% nanosilica filled carbon fiber reinforced epoxy mode II fracture toughness energy test coupon was analyzed at SEM as shown at Figure 3.26. In both fiber and nanosilica filled epoxy resin fracture surfaces have nanosilica particles and these particles availability were analyzed with EDX as shown in Figure 3.26-b and Figure 3.26-c. Since carbon fiber and nanosilica filled epoxy resin has good interface properties, it may cause to increase in mode II fracture toughness energy. Nanosilica particles were located in the fracture surface of nanosilica filled epoxy resin especially in voids which may formed during fracture. Some nanosilica particles which were located on the carbon fiber surface showed good adhesion properties of nanosilica particles to carbon fiber as seen in Figure 3.26-a.

Both fiber and nanosilica filled epoxy resin fracture surfaces have nanosilica particles as evidenced by EDX analyses (see Figure 3.26-b and Figure 3.26-c). Since the carbon fiber and nanosilica filled epoxy resin has good interfacial properties, which may cause improvement in the mode II interlaminar fracture toughness energy values for these samples. The results obtained in this study agrees with those of Tang *et al.*[41]. The test coupons containing 2.0 wt% nanosilica did not exhibit improvement on the mode II fracture toughness energy values, this may be due to sample preparation problems such as inefficient mixing and dispersion of nanosilica particles.

# CHAPTER 4

# CONCLUSIONS

In this thesis, the effects of nanosilica particle addition (0.5, 1.0, and 2.0 wt%) to the epoxy resin and the carbon fiber reinforced epoxy composites were investigated. An ultrasonic processor was used to disperse nanosilica particles in the epoxy resin. To test the effectiveness of the ultrasonic processor for dispersing nanosilicas in the epoxy resin matrix, the conventional manuel mixing method was also used to disperse the nanosilicas. The nanosilica added epoxy resins were used to produce carbon fiber reinforced composites using the filament winding process. The flat filament wound fiber reinforced test coupons were used for physical characterization, mode I and mode II interlaminar fracture toughness energy, tensile and DMA tests. The fracture surfaces of the test coupons were examined by using a SEM.

## 4.1. Effects of Nanosilica on Epoxy Properties

- The viscosity of the nanosilica added epoxy resins increased and the gelling time of the nanosilica added epoxy resins decreased with the increasing of nanosilica content. The bath temperature of 40 °C for the epoxy resin was selected as the optimum temperature for the filament winding process for all epoxy resin mixtures in this thesis.
- The tensile strength improvement (about 13.6%) was only realized for the epoxy resin containing 0.5 wt% nanosilica dispersed using the ultrasonic processer. No significant changes were observed on the tensile modulus values of the epoxy resins.
- With the increasing of nanosilica content (1.0 and 2.0 wt%) in the epoxy resin, tensile strengths of nanosilica added epoxy composites decreased. The worst

tensile strength reduction (23.75 %) was observed for the epoxy sample containing 1.0 wt% nanosilica dispersed using the manuel mixing method.

- The SEM analyses was performed on the fracture surfaces of tensile test coupons and fish like structures were observed for the nanosilica added epoxy test coupons.
- When the SEM images taken at high magnifications were investigated, circular cavities (voids) were observed on the fracture surfaces of the epoxy samples and there were nanosilica agglomerates in those cavities as confirmed by EDX analysis. These voids in the nanosilica added epoxies might be formed during the curing cycle or the tensile testing.
- As the nanosilica content was increased in the epoxy resin, bigger agglomerates were observed in the SEM images. Those large agglomerates may be the reason for the reduction on the tensile strengths of the nanosilica filled epoxy.

## 4.2. Effects of Nanosilica Filled Epoxy on Filament Wound Carbon Fiber Reinforced Epoxy Composites

- Only small changes were observed on the physical properties (fiber weight ratio, density and void content) of the carbon fiber reinforced epoxy composites, which can be related to the viscosity variations for the nanosilica filled epoxy resin. The viscosity of the epoxy resin influence the fiber wetting behavior and cause changes on the physical properties of nanosilica filled carbon fiber epoxy composites.
- The tensile strength improvement was also only realized for the carbon fiber reinforced epoxy composite containing 0.5 wt% nanosilica. The damage mechanism for the carbon fiber reinforced nanosilica added epoxy composites was similar to that of the nanosilica added epoxy resins. No significant changes

were observed in the tensile modulus values of nanosilica filled carbon fiber reinforced epoxy composites.

- The mode I interlaminar fracture toughness energy tests pointed out that with the increasing of nanosilica content in the carbon fiber reinforced epoxy composites, the mode I fracture toughness energy values were increased due to toughening effects of nanosilica particles. The maximum increment of 108% was obtained when 2.0 wt% nanosilica was added. Another batch of the carbon fiber reinforced epoxy composites containing 2.0 wt% nanosilica was prepared in order to show whether the results were reproducible or not. Both batches showed similar fracture toughness energy values.
- The mode II interlaminar fracture toughness energy values of the fiber reinforced epoxy composites were increased 20.6% and 7.6% with the 0.5 wt% and 1.0 wt% nanosilica addition, respectively. Another batch containing 0.5 wt% nanosilica was prepared and tested. Both batches showed similar mode II interlaminar fracture toughness energy values.
- Using DMA method, effects of nanosilica addition on the glass transition temperature of the carbon fiber reinforced epoxy composites were investigated. No significant changes on the $T_g$ values were observed since no changes on the chemical structure of epoxy was expected.
- The dispersion of nanosilica in the epoxy resin matrix using the ultrasonication method was more efficient compared to the manuel mixing method since the mechanical properties of the samples (tensile strength, mode I and mode II interlaminar fracture toughness energy) prepared using the manuel mixing technique reduced considerably.
- The effective toughening mechanisms for nanosilica filled epoxy and their carbon fiber composites were evaluated as the crack deflection and the void growth. Some defects such as fiber-matrix debonding and fiber pull out were not observed in the nanosilica filled test coupons. Most of the nanosilica particles appeared as agglomerates in the epoxy matrix suggesting that the

dispersion of the nanosilica particles in the epoxy resin was not fully achieved using the ultrasonication technique.

## 4.3. Overall Structural Evaluation of Nanosilica Filled Epoxy in Filament Wound Composites

- The nanosilica filled epoxy resin can be considered as an effective approach for improving the mechanical properties (tensile strength, mode I and mode II interlaminar fracture toughness) of the filament wound epoxy composites.
- Nanosilica filled epoxy resins can be integrated to the conventional filament winding process to manufacture parts such as pressure vessels, pipes, sporting goods.
- Despite the high loading rates of nanosilica such as 5, 10, 15 wt% were studied in literature, the aim of this study was to improve structural properties of carbon fiber reinforced composites by adding small amount of nanosilica particles. So that low cost manufacturing can be achieved.

## 4.4. Future Study Suggestions

- Effects of nanosilica particles with surface functionalization such as silane coupling agents and utilization of dispersion agents may be studied for further studies.
- Particles with different sizes (larger than 20 nm) can be studied since small nanosilica particles tend to agglomerate severely in epoxy matrix and hard to disperse them.
- Different dispersion techniques can be studied to disperse nanosilica particles in epoxy such as three roll mixer, microfluidization or high shear mechanical mixer.

- It is easy to study with batches with small amount of volumes, but it is necessary to develop effective dispersion methods for high volume batches.

- Even though reproducibility was tested for some batches, it would have been better to test the reproducibility for all batches.

# REFERENCES

[1] T.-C. Huang, J.-M. Yeh, and C.-Y. Lai, “Polymer nanocomposite coatings,” *Adv. Polym. Nanocomposites*, pp. 605–638, Jan. 2012.

[2] N. Karak, “Chapter 1-Fundamentals of Nanomaterials and Polymer Nanocomposites,” *Nanomaterials and Polymer Nanocomposites*, pp. 1-45, 2019.

[3] E. I. Akpan, X. Shen, B. Wetzel, and K. Friedrich, “Design and Synthesis of Polymer Nanocomposites,” in *Polymer Composites with Functionalized Nanoparticles*, Elsevier, 2019, pp. 47–83.

[4] ASM International. Handbook Committee., *ASM handbook-Volume21, Composites*. .

[5] S. Pandita *et al.*, “Clean wet-filament winding – Part 1: design concept and simulations,” *J. Compos. Mater.*, vol. 47, no. 3, pp. 379–390, Feb. 2013.

[6] S. T. Peters, *Composite Filament Winding*. ASM International, 2011.

[7] A. Asadi and K. Kalaitzidou, *Process-Structure-Property Relationship in Polymer Nanocomposites*. Elsevier Inc., 2018.

[8] T. Hielscher, “Ultrasonic Production of Nano-Size Dispersions and Emulsions,” Aug. 2007.

[9] “Three Roll Mill,” *ROSS*. [Online]. Available: https://www.mixers.com/products/three-roll-mill/. [Accessed: 07-Jul-2019].

[10] “Standard Test Methods for Density and Specific Gravity (Relative Density) of Plastics by Displacement,” *ASTM D792*, vol. 08.01, 2013.

[11] “Standard Test Methods for Constituent Content of Composite Materials,” *ASTM D3171*, vol. 15.03, 2015.

[12] “Standard Test Method for Ignition Loss of Cured Reinforced Resins,” *ASTM D2584*, vol. 08.01, 2018.

[13] “Standard Test Methods for Void Content of Reinforced Plastics,” *ASTM D2734*, vol. 06.01, 2016.

[14] “Standard Test Method for Assignment of the Glass Transition Temperatures by Differential Scanning Calorimetry,” *ASTM E1356*, vol. 14.05, 2014.

[15] “Standard Test Method for Glass Transition Temperature of Polymer Matrix Composites by Dynamic Mechanical Analysis (DMA),” *ASTM D7028*, vol. 15.03, 2015.

[16] “Standard Test Method for Linear Thermal Expansion of Solid Materials by Thermomechanical Analysis,” *ASTM E831*, vol. 14.05, 2019.

[17] “Standard Test Method for Tensile Properties of Polymer Matrix Composite Materials,” *ASTM D3039*, 2017.

[18] “Standard Test Method for Mode I Interlaminar Fracture Toughness of Unidirectional Fiber-Reinforced Polymer Matrix Composites 1,” *ASTM D5528*, 2001.

[19] C. E. de Normalisation, “DIN EN 6033- Aerospace series - Carbon fibre reinforced plastics - Test method - Determination of interlaminar fracture toughness energy - Mode I - $G_{IC}$.” 2016.

[20] “Standard Test Method for Determination of the Mode II Interlaminar Fracture Toughness of Unidirectional Fiber-Reinforced Polymer Matrix Composites ,” *ASTM D7905*, 2001.

[21] C. E. de Normalisation, “DIN EN 6034- Aerospace series - Carbon fibre reinforced plastics - Test method - Determination of interlaminar fracture toughness energy -$G_{IIC}$ Mode II ” 2013.

[22] K. E. Jackson, "Sub-Ply Level Scaling Approach Investigated for Grahite-Epoxy Composite Beam-Columns," in *American Society for Composites, Eighth Proceedings*, 1993, p. 229.

[23] U. S. D. of T. Federal A. Administration, "Composite Aircraft Structure-Advisory Circular," 2010.

[24] M. Conradi, "Nanosilica-Reinforced Polymer Composites Nanosilica-Reinforced Polymer Composites" *Mater Technol.,* vol. 47, pp. 285-293, 2013.

[25] K. L. Thunhorst, A. M. Hine, P. Sedgwick, M. R. Huehn, and D. P. Goetz, "Nanosilica Concentration Effect on Epoxy Resins and Filament-Wound Composite Overwrapped Pressure Vessels," SAMPE 2011, pp. 23-26, 2011.

[26] Z.-Q. Yu, S.-L. You, and H. Baier, "Effect of organosilane coupling agents on microstructure and properties of nanosilica/epoxy composites," *Polym. Compos.*, vol. 33, no. 9, pp. 1516–1524, Sep. 2012.

[27] P. Panse, A. Anand, V. Murkute, A. Ecka, R. Harshe, and M. Joshi, "Mechanical properties of hybrid structural composites reinforced with nanosilica," *Polym. Compos.*, vol. 37, no. 4, pp. 1216–1222, Apr. 2016.

[28] Y. Zhu, C. E. Bakis, and J. H. Adair, "Effects of carbon nanofiller functionalization and distribution on interlaminar fracture toughness of multi-scale reinforced polymer composites," *Carbon N. Y.*, vol. 50, no. 3, pp. 1316–1331, Mar. 2012.

[29] W. Han, Y. Yu, L. Fang, M. R. Johnston, S. Z. Qiao, and Y. Tang, "Functionalised silica/epoxy nanocomposites with enhanced fracture toughness for large-scale applications," *J. Compos. Mater.*, vol. 49, no. 12, pp. 1439–1447, May 2015.

[30] M. T. Demirci, N. Tarakçıoğlu, A. Avcı, A. Akdemir, and İ. Demirci, “Fracture toughness (Mode I) characterization of SiO2 nanoparticle filled basalt/epoxy filament wound composite ring with split-disk test method,” *Compos. Part B Eng.*, vol. 119, pp. 114–124, 2017.

[31] T. H. Hsieh, A. J. Kinloch, K. Masania, A. C. Taylor, and S. Sprenger, “The mechanisms and mechanics of the toughening of epoxy polymers modified with silica nanoparticles,” *Polymer (Guildf).*, vol. 51, no. 26, pp. 6284–6294, 2010.

[32] C. Chen, R. S. Justice, D. W. Schaefer, and J. W. Baur, “Highly dispersed nanosilica-epoxy resins with enhanced mechanical properties,” *Polymer (Guildf).*, vol. 49, no. 17, pp. 3805–3815, 2008.

[33] “ISO 1268-5 Fibre-reinforced plastics — Methods of producing test plates,” *ISO*, vol. 2001, no. Part 5: Filament Winding, 2001.

[34] US Department of Defense, “Composite Materials Handbook Volume 1: Polymer Matrix Composites - Guidelines for Characterisation of Structural Materials,” *Compos. Mater. Handb. Ser.*, vol. 1, no. June, pp. 1–586, 2002.

[35] S. Sprenger, “Epoxy Resin Composites with Surface-Modified Silicon Dioxide Nanoparticles: A Review,” *J. Appl. Polym. Sci*, vol. 130, pp. 1421–1428, 2013.

[36] S. C. Hackett, J.M. Nelson, Hine A.M., and Sedgwick P, “The Effect of Nanosilica Concentration on the Enhancement of Epoxy Matrix Resins for Prepreg Composites,” 2010.

[37] Y. Sun, Z. Zhang, K.-S. Moon, and C. P. Wong, “Glass Transition and Relaxation Behavior of Epoxy Nanocomposites,” *J Polym Sci Part B Polym Phys*, vol. 42, pp. 3849–3858, 2004.

[38] C. Chen, R. S. Justice, D. W. Schaefer, and J. W. Baur, “Highly dispersed nanosilica-epoxy resins with enhanced mechanical properties,” *Polymer (Guildf).*, vol. 49, no. 17, pp. 3805–3815, Aug. 2008.

[39] M. Zamanian, M. Mortezaei, B. Salehnia, and J. E. Jam, “Fracture toughness of epoxy polymer modified with nanosilica particles: Particle size effect,” *Eng. Fract. Mech.*, vol. 97, no. 1, pp. 193–206, 2013.

[40] Y. Tian, H. Zhang, and Z. Zhang, “Influence of nanoparticles on the interfacial properties of fiber-reinforced-epoxy composites,” *Compos. Part A Appl. Sci. Manuf.*, vol. 98, pp. 1–8, Jul. 2017.

[41] Y. Tang, L. Ye, D. Zhang, and S. Deng, “Characterization of transverse tensile, interlaminar shear and interlaminate fracture in CF/EP laminates with 10 wt% and 20 wt% silica nanoparticles in matrix resins,” *Compos. Part A Appl. Sci. Manuf.*, vol. 42, no. 12, pp. 1943–1950, Dec. 2011.

[42] A. Vashisth and C. E. Bakis, “Multiscale Characterization and Modeling of Nanosilica-Reinforced Filament Wound Carbon/Epoxy Composite,” *Mater. Perform. Charact.*, vol. 8, no. 1, p. 20180108, 2019.

[43] D. Carolan, A. J. Kinloch, A. Ivankovic, S. Sprenger, and A. C. Taylor, “Mechanical and fracture performance of carbon fibre reinforced composites with nanoparticle modified matrices,” in *Procedia Structural Integrity*, 2016, vol. 2, pp. 96–103.

# APPENDICES

## A. DSC Thermograms

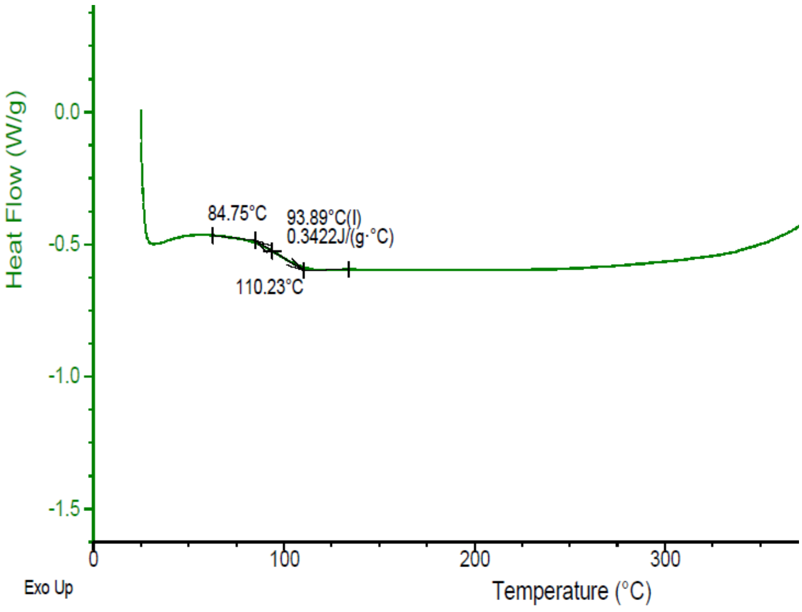

**Figure A-1** DSC thermogram of neat cured epoxy.

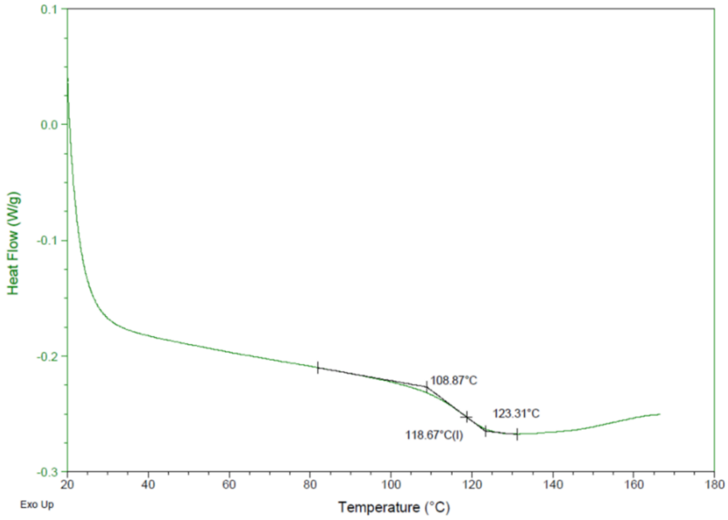

**Figure A-2** DSC thermogram of 0.5 wt% nanosilica filled cured epoxy composite.

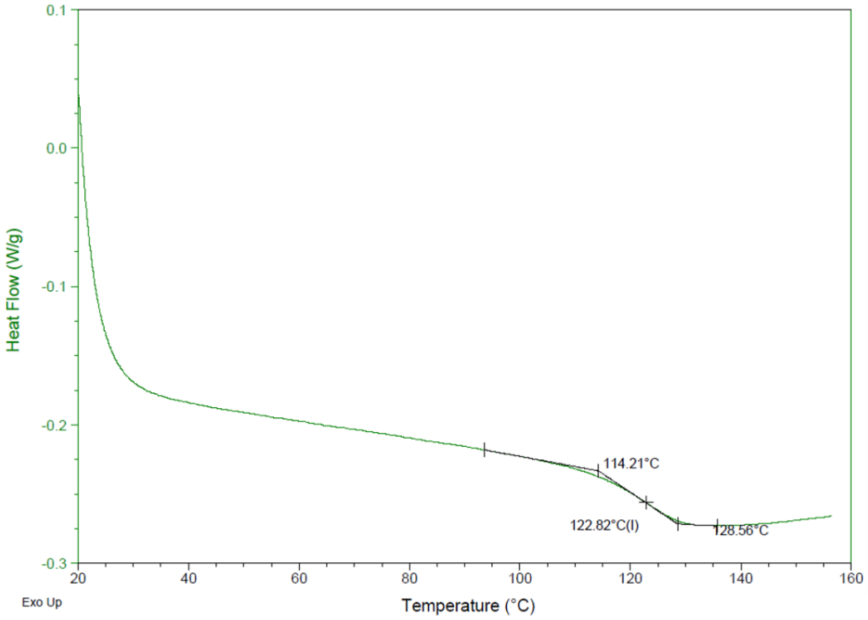

**Figure A-3** DSC thermogram of 1.0 wt% nanosilica filled cured epoxy composite.

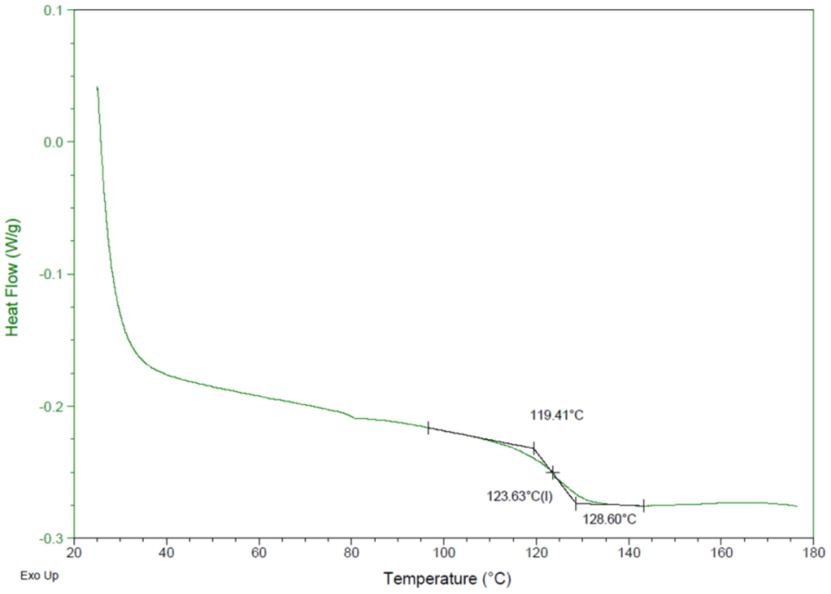

**Figure A-4** DSC thermogram of 2.0 wt% nanosilica filled cured epoxy composite.

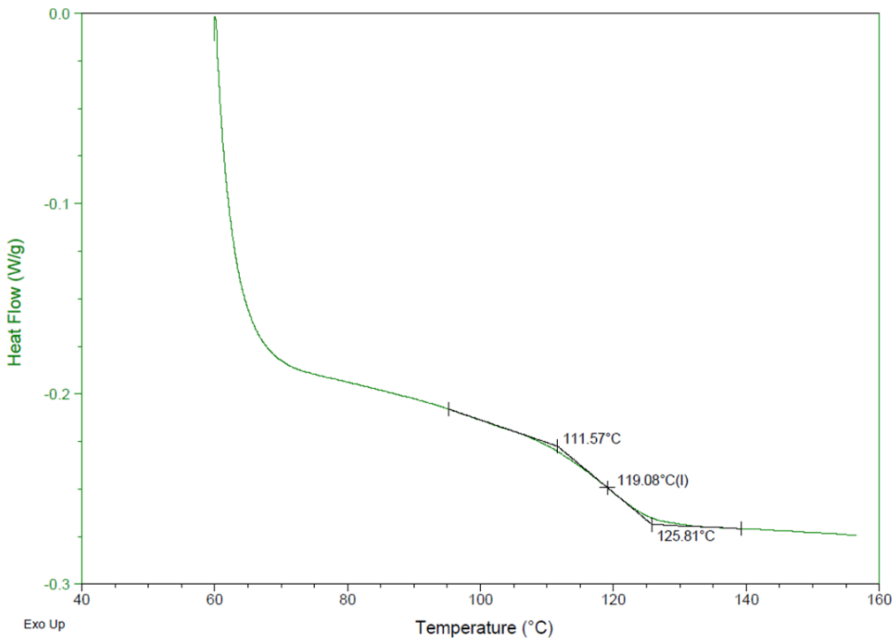

**Figure A-5** DSC thermogram of manuel mixed 1.0 wt% nanosilica filled cured epoxy composite.

## B. DMA Thermograms

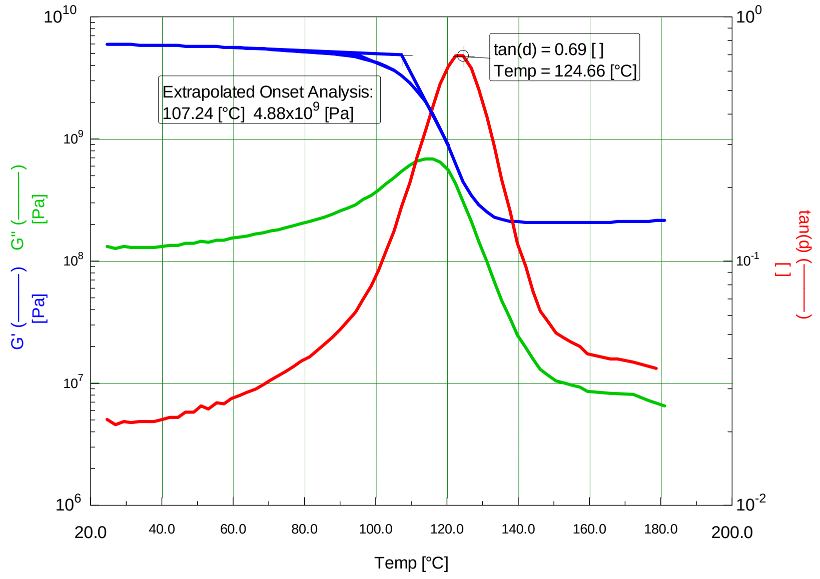

**Figure B-1** DMA thermogram of neat epoxy composite with carbon fiber reinforcement.

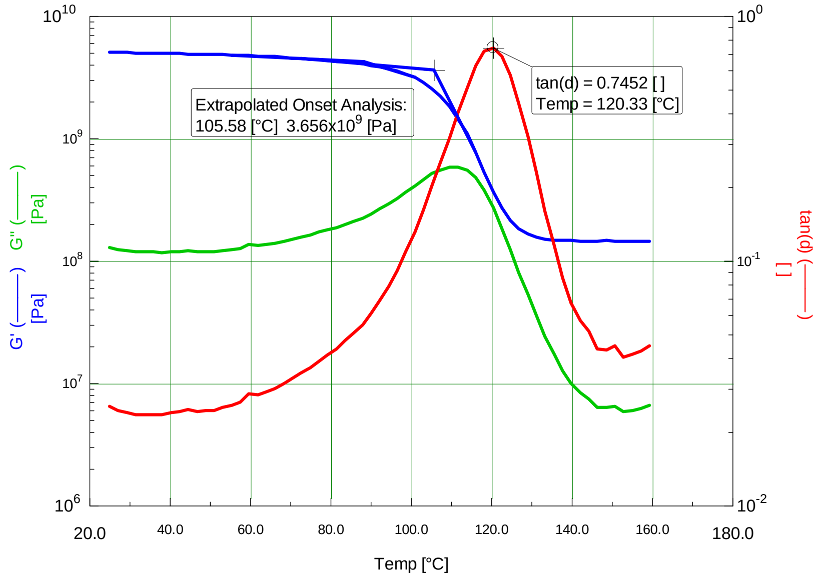

**Figure B-2** DMA thermogram of 0.5 wt% nanosilica filled epoxy composite with carbon fiber reinforcement.

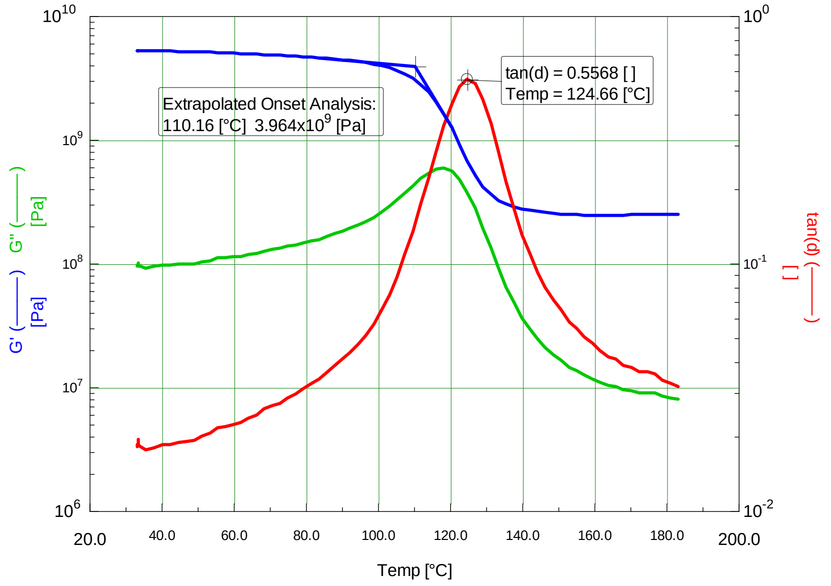

**Figure B-3** DMA thermogram of 2.0 wt% nanosilica filled epoxy composite with carbon fiber reinforcement.

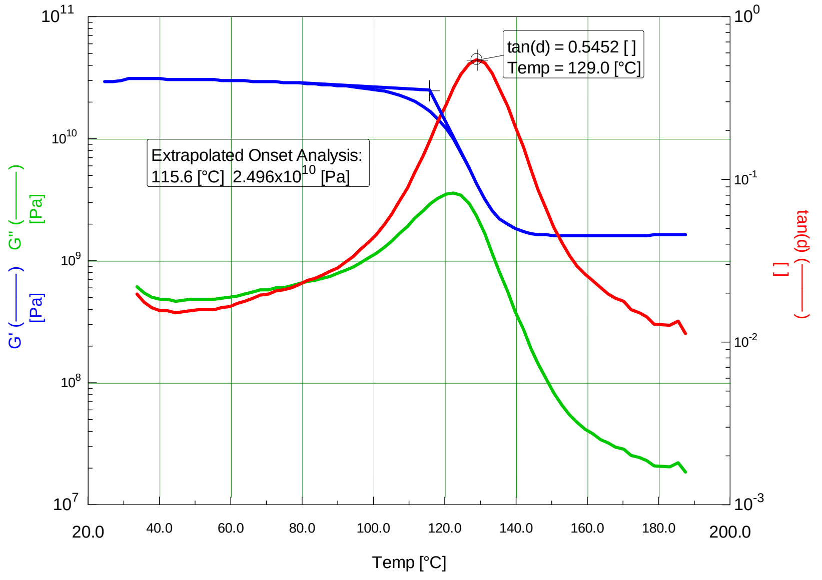

**Figure B-4** DMA thermogram of 1.0 wt% manuel mixed nanosilica filled epoxy with carbon fiber reinforcement.

## C. Stress-Strain Curves

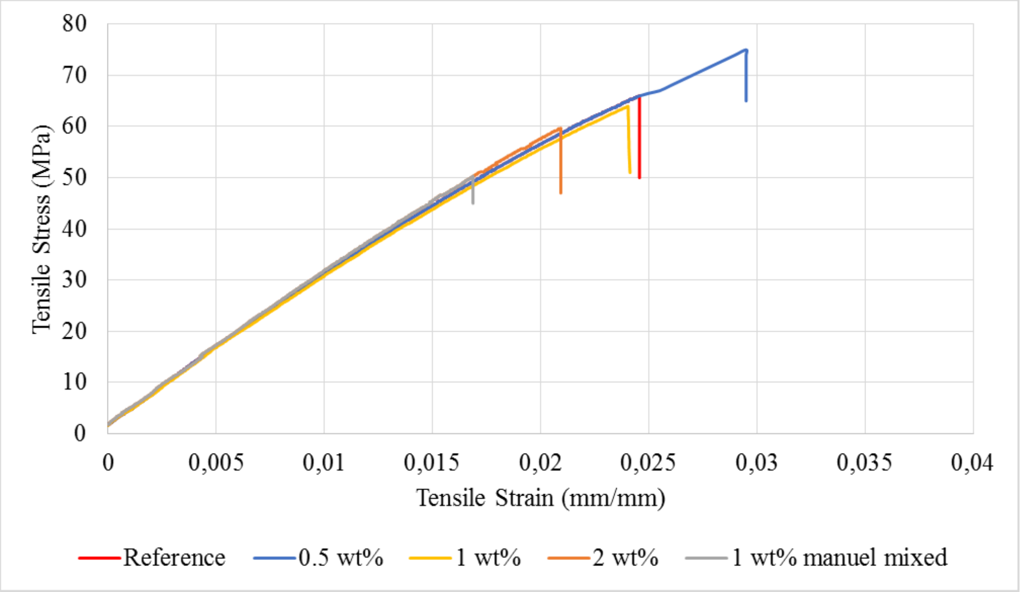

**Figure C-1** Stress-strain curve of the neat epoxy and the nanosilica filled epoxy samples without carbon fiber reinforcement.

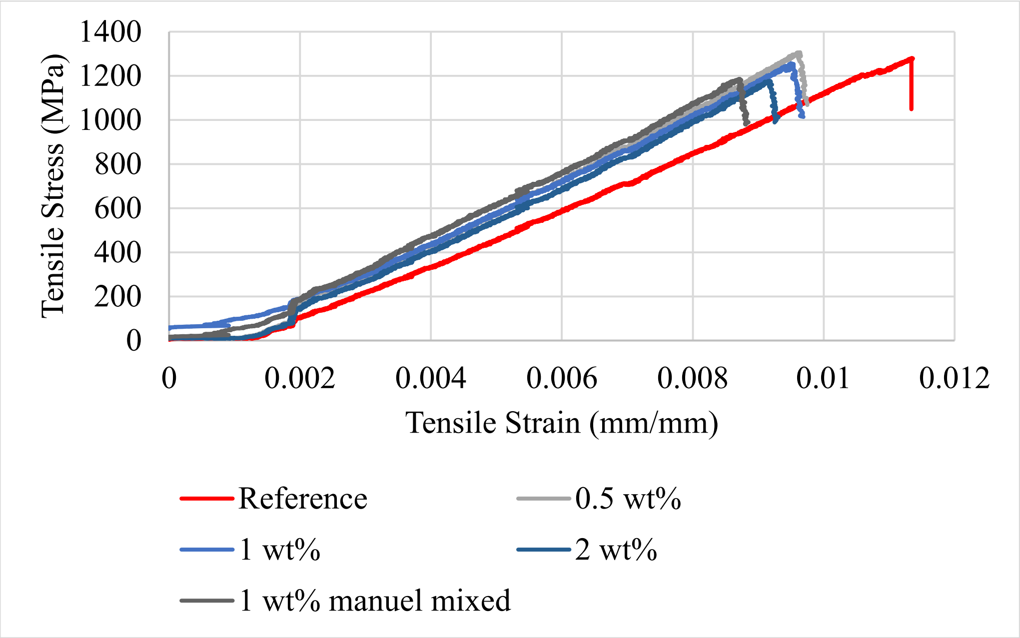

**Figure C-1** Stress-strain curve of the neat epoxy and the nanosilica filled epoxy samples with carbon fiber reinforcement.